



AJSTTD



Vol. 29, No. 2, December 2012
ISSN 0217-5460

A Journal of the ASEAN Committee on
Science & Technology



ASEAN
JOURNAL ON
SCIENCE &
TECHNOLOGY FOR
DEVELOPMENT

ABOUT THE ASEAN JOURNAL ON SCIENCE AND TECHNOLOGY FOR DEVELOPMENT

The ASEAN Journal on Science and Technology for Development is a refereed Journal of the ASEAN Committee on Science and Technology (ASEAN COST). It reports on science and technology policies and programmes, and research activities undertaken by COST in support of social and economic development of the ASEAN member countries.

The coverage is focused but not limited to, the main areas of activity of ASEAN COST, namely, Biotechnology, Non-Conventional Energy Research, Materials Science and Technology, Marine Sciences, Meteorology and Geophysics, Food Science and Technology, Microelectronics and Information Technology, Space Applications, and Science and Technology Policy, Infrastructure and Resources Development.

ABOUT THE ASEAN COMMITTEE ON SCIENCE AND TECHNOLOGY

The ASEAN Committee on Science and Technology was established to strengthen and enhance the capability of ASEAN in science and technology so that it can promote economic development and help achieve a high quality of life for its people. Its terms and reference are:

- To generate and promote development of scientific and technological expertise and manpower in the ASEAN region;
- To facilitate and accelerate the transfer of scientific and technological development among ASEAN countries and from more advanced regions of the world to the ASEAN region;
- To provide support and assistance in the development and application of research discoveries and technological practices of endogenous origin for the common good, and in the more effective use of natural resources available in the ASEAN region and in general; and
- To provide scientific and technological support towards the implementation of existing and future ASEAN projects.

Information on the activities of ASEAN COST can be obtained at its website <http://www.asnet.org>

DISCLAIMER

While every effort is made to see that no inaccurate or misleading data, opinion or statement appears in the Journal, articles and advertisements in the Journal are the sole responsibility of the contributor or advertiser concerned. They do not necessarily represent the views of the Editors, the Editorial Board nor the Editorial Advisory Committee. The Editors, the Editorial Board and the Editorial Advisory Committee and their respective employees, officers and agents accept no responsibility or liability whatsoever for the consequences of any inaccurate or misleading data, opinion or statement.

© Copyright 2013: ASEAN Committee on Science and Technology

No part of this publication may be reproduced, stored in a retrieval system or transmitted in any form of by any means, without permission in writing from the copyright holder.

Editorial Board

Editor-in-Chief

Emeritus Prof Md Ikram Mohd Said
*School of Chemical Sciences and Food Technology,
Faculty of Science and Technology, Universiti Kebangsaan Malaysia*

Editorial Board Members

Malaysia

Dr Ahmad Ibrahim
*Chief Executive Officer,
Academy of Sciences Malaysia*

Prof Abdul Halim Shaari
Faculty of Science, Universiti Putra Malaysia

Prof Thong Kwai Lin
*Institute of Biological Science, Faculty of
Science/UMBIO Cluster, Institute of Graduate
Studies, University of Malaya*

Assoc. Prof Mohd Fadzil Mohd Idris
*Higher Education Leadership Academy,
Ministry of Higher Education*

Brunei Darussalam

Rosita Abdullah
*Senior Special Duties Officer,
Ministry of Development*

Assoc. Prof Zohrah Sulaiman
*Deputy Vice-Chancellor,
Universiti Brunei Darussalam*

Myanmar

Dr Zaw Min Aung
*Director General, Department of Technical and
Vocational Education,
Ministry of Science and Technology*

Philippines

Dr Carol M. Yorobe
*Undersecretary for Regional Operations,
Department of Science and Technology*

Singapore

Assoc. Prof Ong Sim Heng
*Department of Electrical and Computer
Engineering, National University of Singapore*

Assoc. Prof Tan Tin Wee
*Department of Biochemistry,
National University of Singapore*

Thailand

Prof Narongrit Sombatsompop
*School of Energy, Environment and Materials,
King Mongkut's University of Technology,
Thonburi*

Prof Prida Wibulswas
President, Shinawatra University

Cambodia

Pal Des
Vice-Rector, Royal University of Phnom Penh

Indonesia

Dr Warsito Purwo Taruno
*Minister, Special Advisor for Research and
Cooperation*

Lao PDR

Kongsaysy Phommaxay
*Acting Director General,
Cabinet Office of the Ministry of Science
and Technology*

Keonakhone Saysuliane
*Acting Director General,
Department of Information Technology*

Vietnam

Dr Mai Ha
*Director General,
Ministry of Science and Technology*

Editorial Advisory Panel

Brunei Darussalam

Eddie Sunny
*Deputy Permanent Secretary,
Ministry of Development*

Myanmar

Dr Ko Ko Oo
*National COST Chairman,
Deputy Minister, Ministry of Science and
Technology*

Cambodia

Dr Om Romny
Director, Institute of Technology of Cambodia

Philippines

Dr Graciano P. Yumul
*Undersecretary for R&D,
Department of Science and Technology*

Indonesia

Prof Syamsa Ardisasmita, DEA
*Deputy Minister for Science and Technology
Network, National COST Chairman*

Lao PDR

Dr Maydom Chanthanasinh
*Deputy Minister, Ministry of Science and
Technology, National COST Chairman*

Singapore

Prof Low Teck Seng
*National COST Chairman,
Managing Director, Agency for Science,
Technology and Research*

Thailand

Assoc. Prof Weerapong Pairsuwan
*Deputy Permanent Secretary,
Ministry of Science and Technology*

Malaysia

Dr Madinah Mohamad
*National COST Chairman,
Secretary General, Ministry of Science,
Technology and Innovation*

Vietnam

Dr Le Dinh Tien
*Deputy Minister for Science and Technology,
National COST Chairman*

Editor/Technical Editor/Executive Editor

Kanesan Solomalai
Academy of Sciences Malaysia

Dr Mohaida Mohin
Higher Education Leadership Academy, Malaysia

Nooni Ezdiani Yasin
Academy of Sciences Malaysia

Production Manager

Kamariah Mohd Saidin
Universiti Putra Malaysia

Publisher

Universiti Putra Malaysia Press

Contents

ASEAN J. Sc. Technol. Dev.
Volume 29(2), 2012

Performance of Jatropha Oil-based Biodiesel Fuel in a Single-cylinder Four-Stroke Diesel Engine	77
H. H. Win	
Developing a Generalized Combined Model for Gas-liquid Two-phase Flow Pressure Drop in Elbow Bends	88
N. Z. Aung and T. Yuwono	
Ethanol Production in Yeasts Isolated from Fermented Kitchen Waste	99
S. Wong, S. K. Wong and J. S. Bujang	
Chemical Composition of Leaf and Seed Oils of <i>Dryobalanops aromatica</i> Gaertn. (Dipterocarpaceae)	105
A. S. Kamariah, T. Ozek, B. Demirci and K. H. C. Baser	
Evaluation of Mixture Viscosity Models in the Prediction of Two-phase Flow Pressure Drops	115
N. Z. Aung and T. Yuwono	
Utilization of Agricultural Wastes in the Manufacture of Composite Boards	129
P. M. Macatangay, E. C. Magundayao and C. A. M. Rosales	

Performance of Jatropha Oil-based Biodiesel Fuel in a Single-cylinder Four-Stroke Diesel Engine

H. H. WIN

Studies on alternative fuels have been active in Myanmar because the rapid mechanization of the agricultural sector demands higher diesel consumption. Jatropha oil-based biodiesel is one of the potential alternatives because of the relative ease of growing and producing this plant. In this study, both the experimental and theoretical analyses of Jatropha oil-based B20 biodiesel were performed and compared with conventional diesel. First, B20 was prepared by the base-catalyzed transesterification of the oil and its properties were measured. Second, separate performance tests were conducted on diesel and the biodiesel fuel using a LEYER-16 diesel engine. The speed range of interest was between 1000 r.p.m and 2000 r.p.m. Third, performance simulations were done in MATLAB using an algorithm written based on the theory of the engine operating cycle and air/fuel compositions. Both experimental and simulation results show that there were no significant differences in the brake power and thermal efficiency of the engine between using diesel and the B20 diesel. However, fuel consumption when using B20 was slightly higher than that of diesel. This difference was marginal and it can be concluded that engine performance characteristics are the same for both diesel and B20 suggesting that B20 has great potential to be used as a substitute for diesel.

Key words: Jatropha biodiesel; B20 biodiesel; alternative fuel; diesel engine performance; biofuel; experimental and theoretical analyses

The agriculture sector in Myanmar is completely dependent on diesel for its motive power. Increased farm mechanization in agriculture has also further increased the use of diesel fuel. As diesel is relatively expensive, the search for alternative fuels has been active in Myanmar. Many alternative fuels like biogas, methanol, ethanol and vegetable oils have been evaluated as a partial or complete substitute for diesel. Vegetable oils can be used directly in a diesel engine as a fuel, because their calorific value is almost equal to that of diesel. Therefore, several studies and research groups in Myanmar have focused attention on the technologies to produce, collect and extract vegetable oil from different oil seeds such as Jatropha.

Jatropha oil is non-edible oil and has a comparable cetane number to diesel; hence no major modification in the diesel engine is necessary when it is used. Moreover, it is relatively safe to store, handle and transport Jatropha oil because its initial flash point (110°C) is higher than that of diesel (50°C). Therefore, compared with edible vegetable oils, Jatropha oil is an ideal alternative fuel to diesel. To promote the use of Jatropha oil, Myanmar is speeding up the growing of the Jatropha plant. Several studies and research on biodiesel have also been conducted by several government organizations in Myanmar, such as the Ministry of Industry 1, the Ministry of Industry 2, and the Department of Farm

Machinery of the Ministry of Science and Technology (Kywe & Oo 2009).

The objective of this study is to investigate the performance of a biodiesel blend (B20) and compare it with that of diesel in a conventional diesel engine through experimental and theoretical studies. Performance tests were conducted using a single-cylinder, four-stroke diesel engine. This study will provide answers as to whether biodiesel could be used as an alternative to diesel and provide the guidelines for converting the diesel engine to a biodiesel engine.

MATERIALS AND METHODS

Biodiesel Fuel

Biodiesel blend B20 (80% diesel, 20% Jatropha biodiesel) was prepared by base-catalyzed

transesterification. The transesterification process with methanol consisted of two steps: (i) esterification of the fatty acids of crude Jatropha oil (8.8% of FFA) into refined Jatropha oil and (ii) transesterification of neutral glycerides mixture into methyl ester by adding methanol and KOH as catalysts through washing and filtration (*Figure 1*). The esterification process was carried out at 75°C to 100°C in a standard atmosphere. In the transesterification process, methanol was used to deactivate lipase enzymes and this took 12 h to 15 h. Finally, pure biodiesel was obtained as a clear amber-yellow liquid. The properties of B20 are shown in *Table 1*.

Engine

The engine used in this study was a S1100 LY-16 diesel engine and its specifications are shown in *Table 2*.

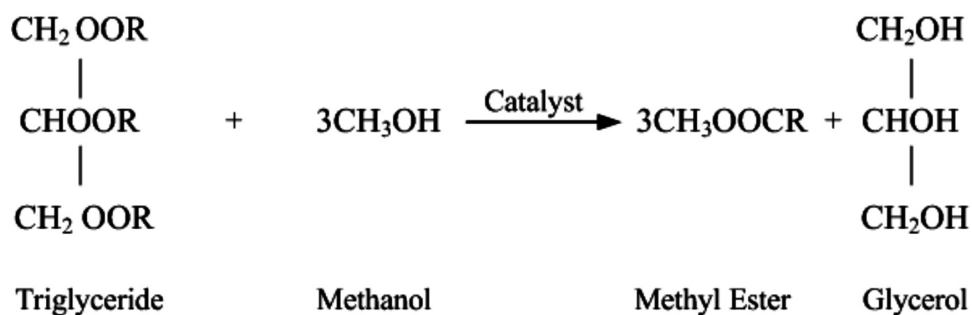


Figure 1. Principle of transesterification reaction with methanol.

Table 1. Properties of diesel oil, Jatropha oil and Jatropha biodiesel.^a

Property	Diesel	Jatropha oil	Jatropha biodiesel
Density (gm/cc at 30°C)	0.84	0.93	0.85
Kinematic viscosity (cSt at 30°C)	3.6	42	4.5
Cetane number	40–55	38–51	50
Flash point (°C)	45–80	110–240	170
Calorific value (MJ/kg)	42–46	38–42	38
Sulphur (%)	1.0–1.2	0.13	0
Carbon residue (%)	0.1	0.64	0.5

^a Hoa *et al.*

Table 2. S1100 LY-16 diesel engine specifications.

Type	Single-cylinder, four-stroke, horizontal
Cylinder bore (mm)	100
Piston stroke (mm)	115
Compression ratio	20
Fuel consumption (gal/hr)	0.55
Output power (kW)	11.03
Rated speed (r.p.m)	2200
Piston displacement (litre)	0.903

Experiment Method

A schematic diagram of the experimental setup is shown in *Figure 2*. Before the performance test, proper operation of the test engine was ensured. The performance characteristics of the engine using diesel and B20 were quantified by measuring fuel consumption and brake torque at various operating speeds. Before each measurement, steady operation of the engine was ensured. Rotational speed of the engine (N) was measured by a tachometer with the use

of reflective tape on the crankshaft. The speed was varied in 100 r.p.m increments from 1000 to 2000. Fuel consumption (m_f) was measured by recording the initial and instantaneous volume of the fuel. The fuel tank was attached to a graduated burette. The valve at the bottom of the tank was closed when fuel consumption rate was to be measured so that the fuel was consumed only from the burette. The time taken for the fuel to be consumed was recorded to measure the fuel consumption rate.

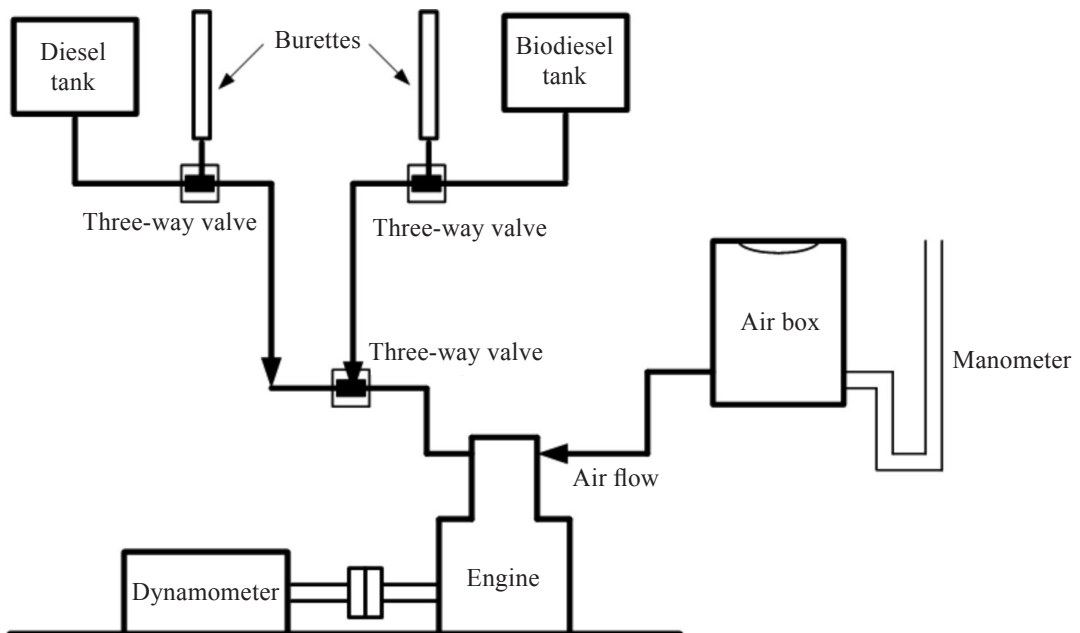


Figure 2. Experimental setup.

Engine torque measurements were performed with a dynamometer at speeds from 1000 to 2000 r.p.m. The engine was clamped to the floor. Then, the engine shaft was connected to the dynamometer rotor. Engine torque on the rotor was measured by balancing the stator with known weights (W) at known distances (D). Brake power (BP) was calculated from the measured engine torque (Pulkrabek 1988).

$$BP = \frac{\pi DWN}{60} \quad (1)$$

Torque and power were recorded for each speed increment to determine brake specific fuel consumption (bsfc), and brake thermal efficiency can then be computed if the calorific value of the fuel (CV) is known.

$$\text{Brake thermal efficiency} = \frac{BP}{m_v CV} \quad (2)$$

Theoretical Model

A theoretical model of the engine performance was constructed based on the theory of the engine operating cycles: intake, compression, combustion and expansion (Heywood 1988). An algorithm was written to calculate the theoretical brake power, specific fuel consumption and thermal efficiency for both diesel and B20 fuels (khovakh 1971). The flow chart for this algorithm is shown in *Figure 3*.

RESULTS AND DISCUSSION

Experimental Results

Figure 4 shows the variations in brake power at full load as a function of operating speed for both B20 and diesel. It was observed that brake power increased with speed for both diesel and B20. Moreover, the rate of brake power increment with speed was lower for speeds above 1500 r.p.m. This may be due to the fact that friction losses at higher speeds were relatively more dominant than at lower speeds. However, it must be noticed that the

brake power of the engine had not achieved its maximum value compared with typical diesel engines (Pulkrabek 1988). Most diesel engines have a maximum brake power at engine speeds of approximately 6000 r.p.m. to 7000 r.p.m. However, brake power measurements in this study were performed in the speed range of only 1000 r.p.m. to 2000 r.p.m. Therefore, in order to compare the maximum brake powers of engines with diesel and B20, it is suggested that more studies be performed to measure brake power at higher speeds of up to 6000 r.p.m. However, based on the existing results with some limitations, it can be concluded qualitatively that the engine running on B20 had almost equal available brake power to that of the diesel-run engine although brake power with diesel was slightly larger.

Figure 5 shows the variations in brake specific fuel consumptions at different engine speeds for both B20 and diesel. At all speeds, the brake specific fuel consumption for B20 was approximately 2% higher than that for diesel fuel. At speeds below 1200 r.p.m., the consumptions of both fuels decreased with speed. This decrement in fuel consumption with speed has also been reported in a study by Nematullah (2010) although the speed range in that study was different from this study. As speed increased, the consumptions of both fuels increased, as was also shown in the previous study (Nematullah 2010). However, at speeds above 1900 r.p.m., the rate of fuel consumption of B20 was higher than that of diesel. One of the possible reasons for this discrepancy could be experimental error due to incorrect timing between speed increment and load increment as this experiment was controlled manually. Engine speeds may have fluctuated whenever the load was increased or decreased.

Figure 6 shows engine brake thermal efficiency as a function of engine speed. The range of brake thermal efficiencies for both diesel and B20 was between 30 and 37. This result is comparable to the brake thermal

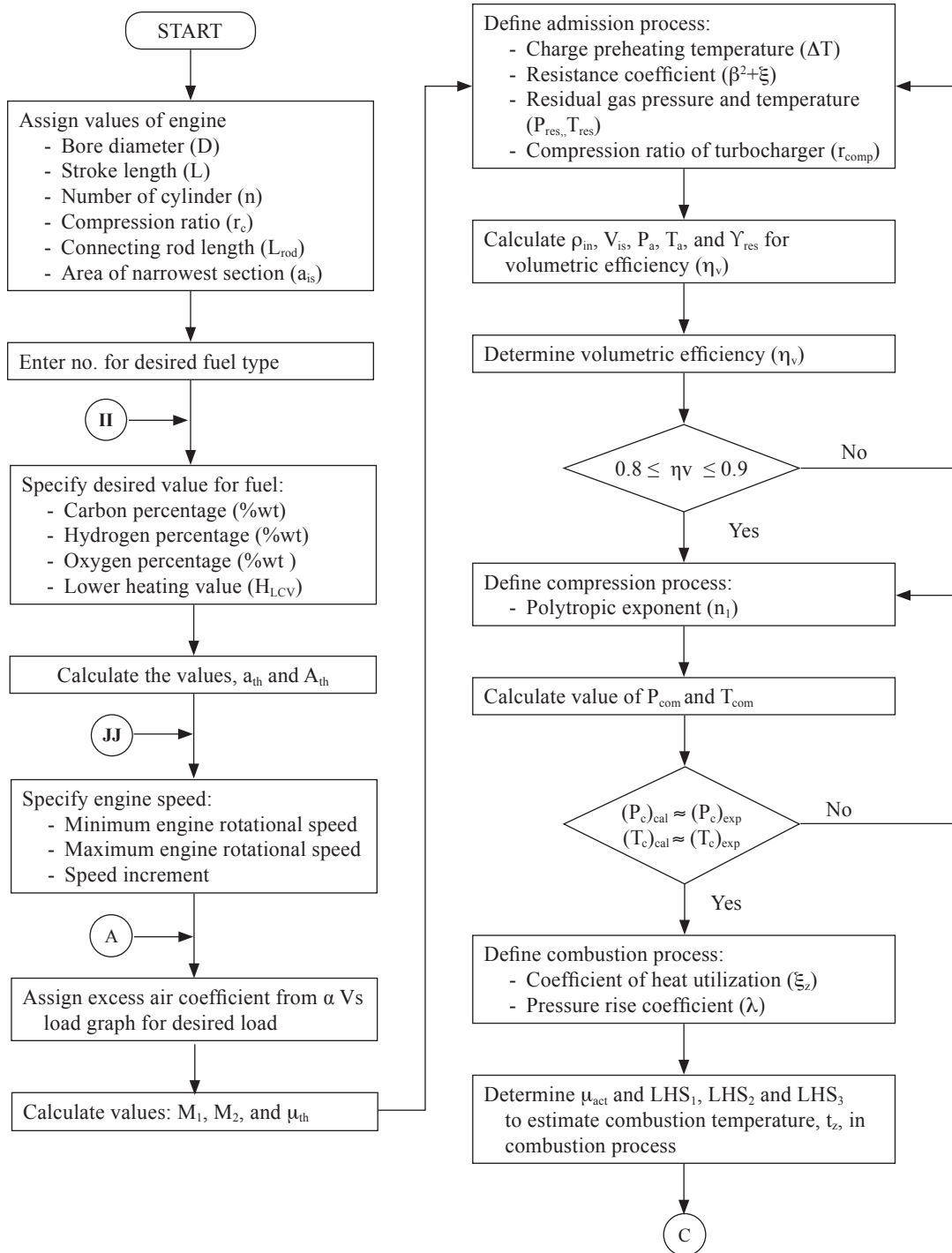


Figure 3. Flow chart for estimating theoretical performance by simulation.

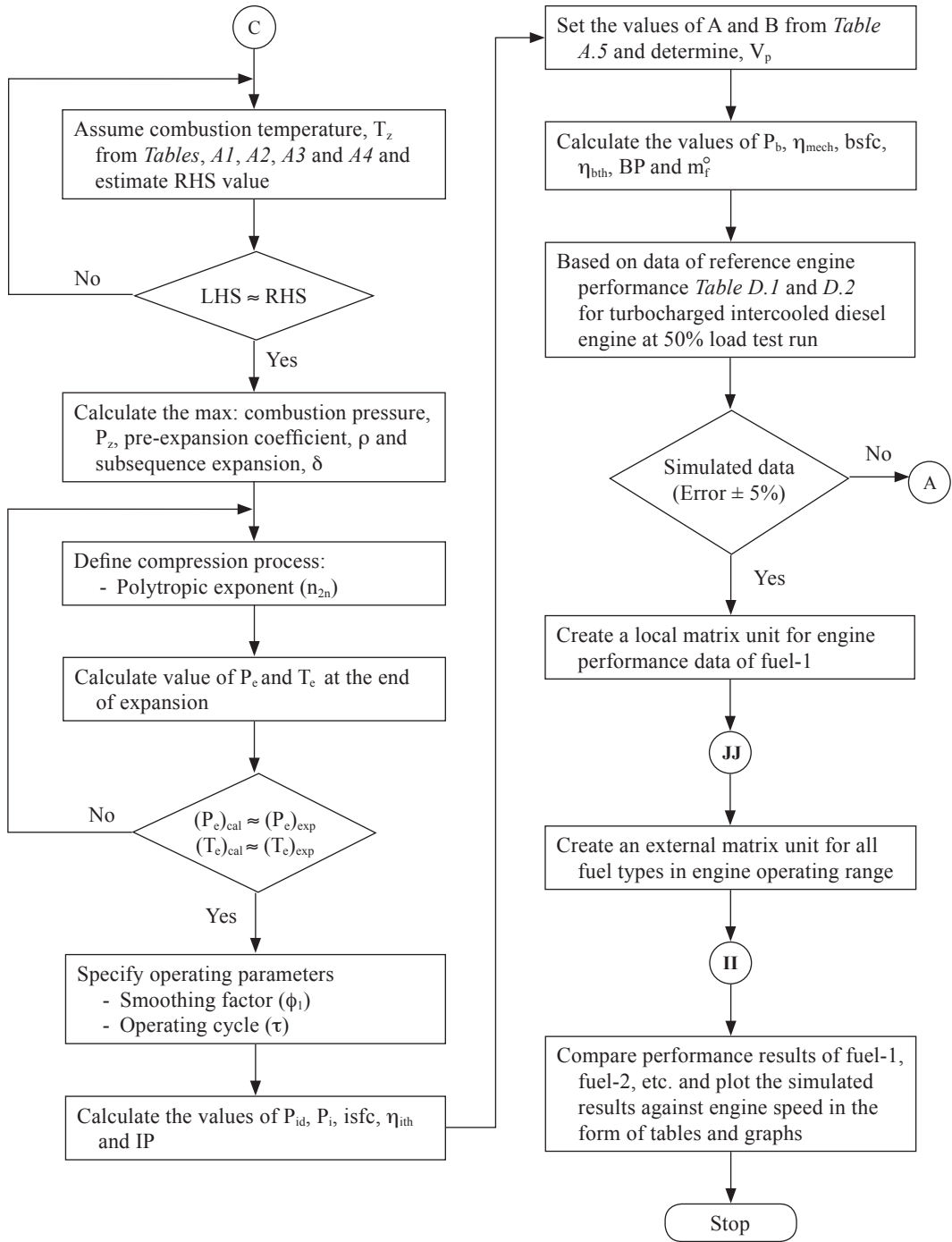


Figure 3 (Cont.). Flow chart for estimating theoretical performance by simulation.

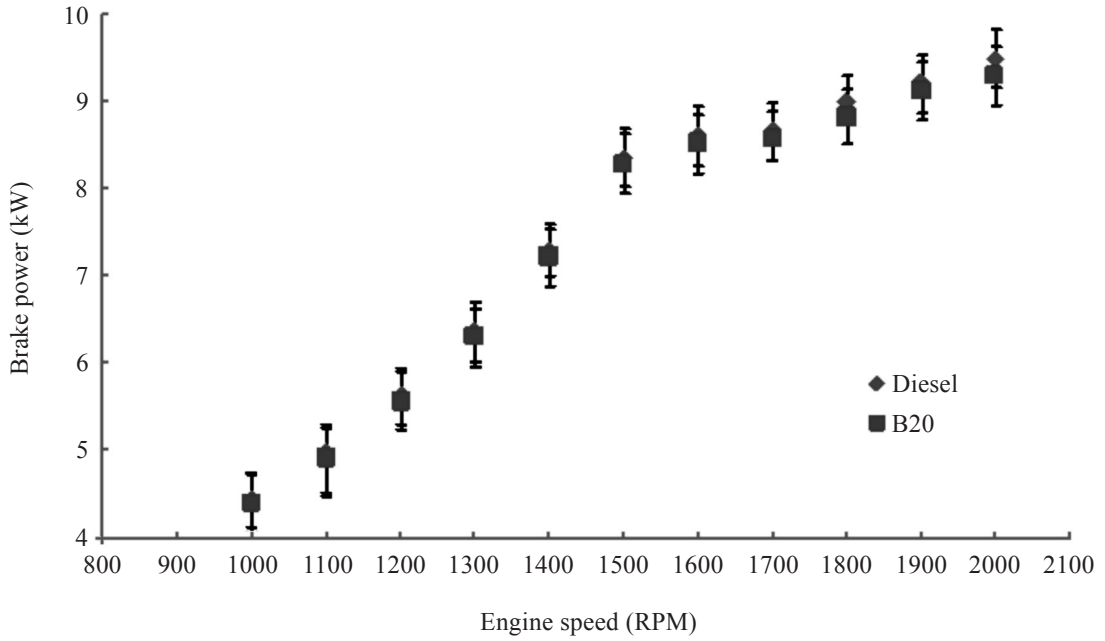


Figure 4. Comparison of engine brake power with different fuels.

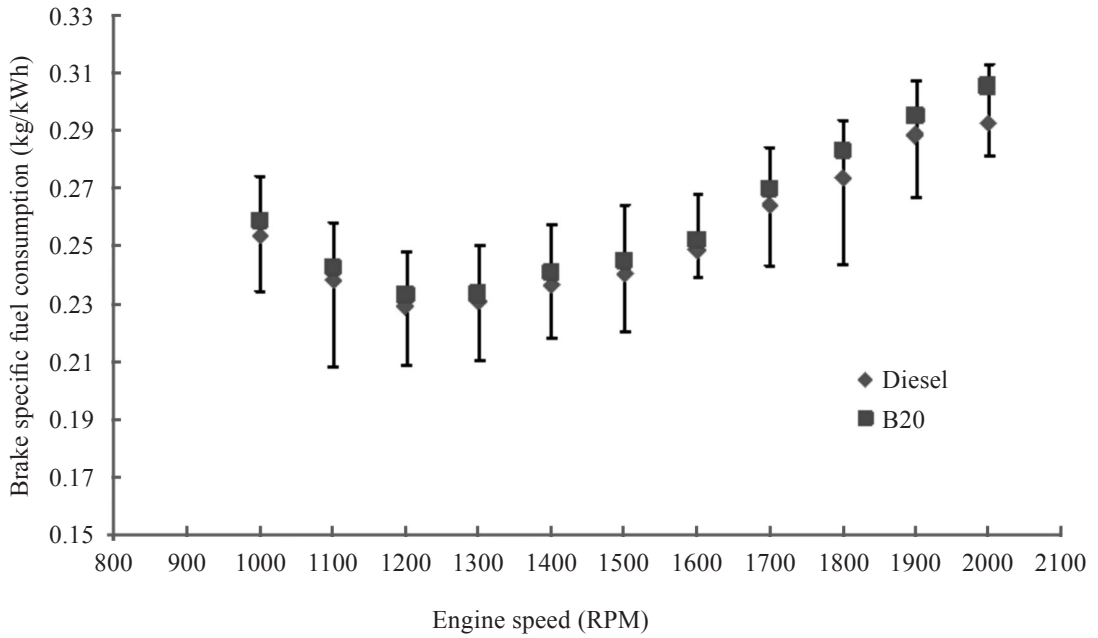


Figure 5. Comparison of engine brake specific fuel consumption with different fuels.

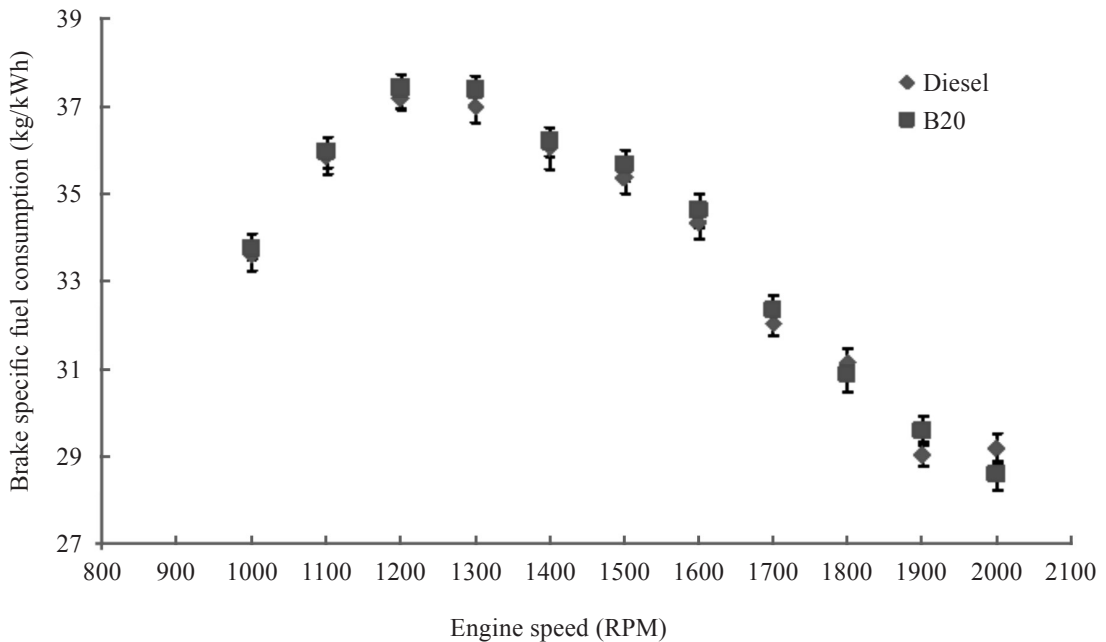


Figure 6. Comparison of engine brake thermal efficiency with different fuels.

efficiency range for B20 reported in literature (Nematullah 2010). It can also be seen that, as expected, the brake thermal efficiency was inversely proportional to the specific fuel consumption (Figure 5). It is also observed that there was no significant difference in the brake thermal efficiencies when using the conventional diesel fuel and B20 biodiesel both at low and high speeds. This result was expected because the calorific value of B20 (41.24 MJ/kg) was close to that of diesel (42.2 MJ/kg). Therefore, B20 can be used as a substitute for diesel fuel. Another advantage with B20 is that unlike other biodiesels such as B100, no combustion deposits on valve, piston crown, cylinder head and injector were observed after a long period of operation.

Simulation Results

Figure 7 shows the experimental and simulation brake powers for both diesel and B20 fuels. The experimental and simulation brake powers were similar in trend for both diesel and B20

fuels. For diesel, the maximum error between the experimental and simulation results was approximately 7% although the maximum error for B20 was around 1%. However, the simulation results also showed that brake power with diesel was slightly higher than that with B20, which is in agreement with the experimental results shown in Figure 4, suggesting again that B20 can be used as a substitute for diesel.

Similar trends between experimental and simulation results for brake specific fuel consumption and thermal efficiency were also observed as shown in Figure 8 and Figure 9. In Figure 8, the maximum error in brake specific fuel consumption between experiments and simulations was around 1% with both diesel and B20. The maximum error in thermal efficiency was also around 1% with both diesel and B20. Therefore, overall, the experimental results were in good agreement with the simulation results. The simulation results in Figure 8, which were in agreement with the experimental results,

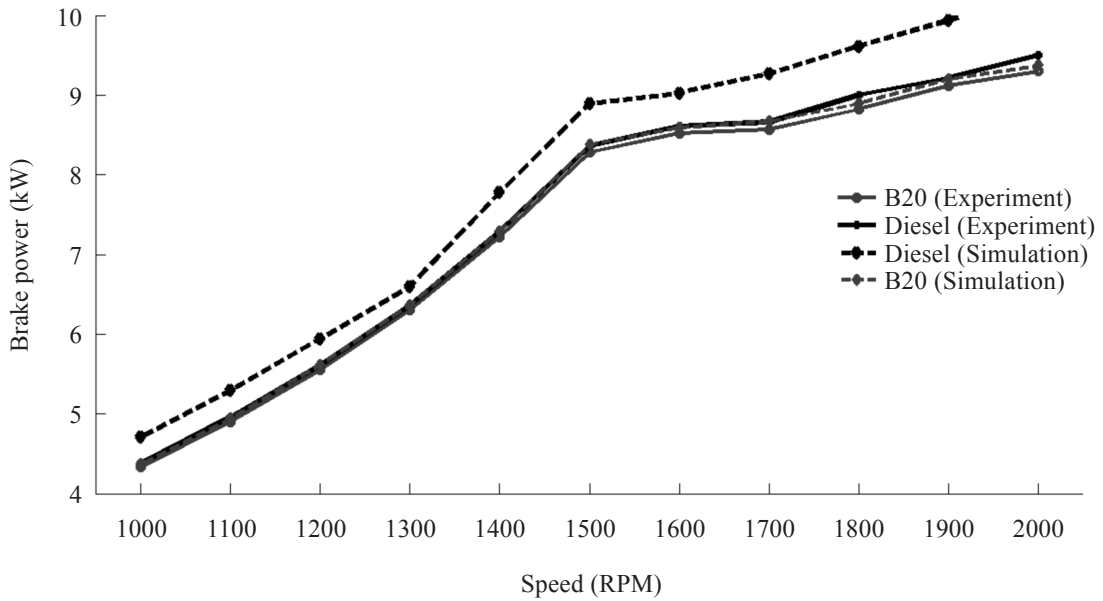


Figure 7. Comparison between experiments and simulations in engine brake power.

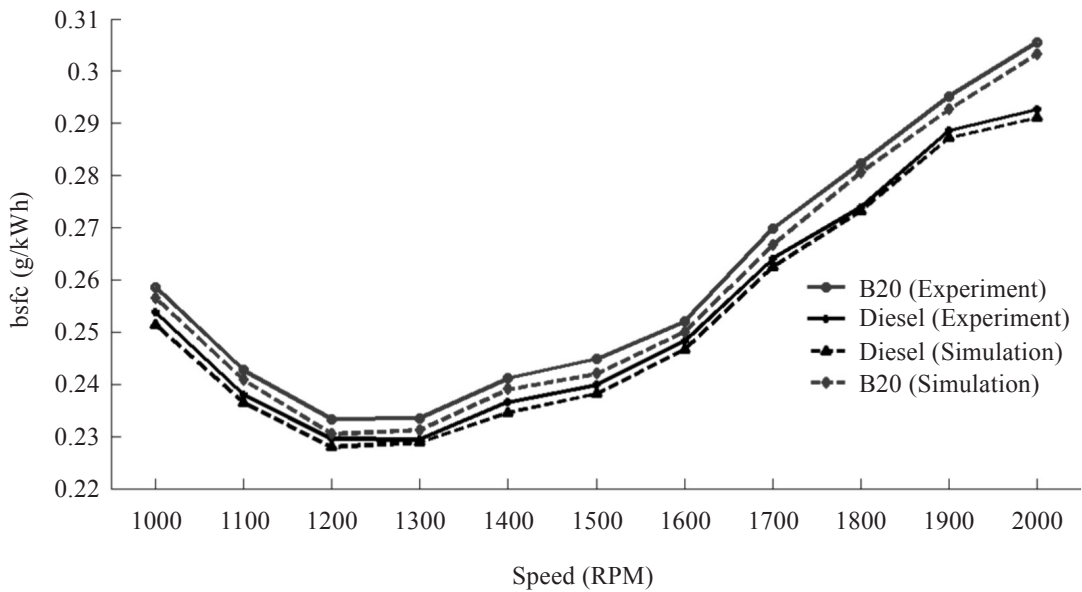


Figure 8. Comparison between experiment and simulation: specific fuel consumption.

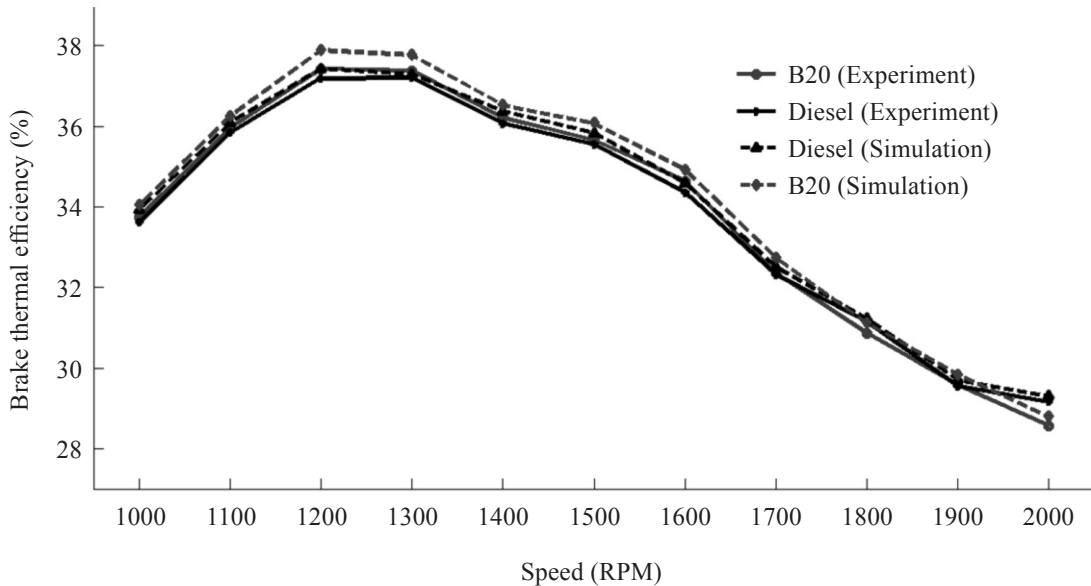


Figure 9. Comparison between experiments and simulations in brake thermal efficiency.

suggest that brake specific fuel consumption with B20 was slightly higher than that with diesel. The simulation results in *Figure 9* also suggest that there was no significant difference in brake thermal efficiency between using diesel and B20 supporting the experimental findings in *Figure 6*.

CONCLUSIONS

The performance of biodiesel blend B-20 was tested in a single-cylinder four-stroke indirect injection diesel engine. It was found, during the experiments, that the use of B-20 fuel did not require any additional modification to the engine and that it could operate smoothly with no notable problems. Based on the experimental analysis on brake power, specific fuel consumption and thermal efficiency, it can be concluded that B-20 can perform almost as efficiently as diesel fuel. This result is in line with the results reported in literature (Hoa 2012; Forson *et al.* 2004; Baitiang *et al.*

2008). Therefore, Jatropha oil-based diesel fuel has great potential to replace conventional diesel fuel. Apart from the experimental analyses, a theoretical model which can represent the performance of a compression ignition engine was also built and verified with the experimental findings for both diesel and B20 fuels. However, the experimental performance data were collected within limited engine speeds. In order to fully investigate the performance of B20 at higher engine speeds, more experimental studies should be done on engines with higher rated speeds.

Date of submission: August 2012

Date of acceptance: September 2012

REFERENCES

- BAITIANG, T *et al.* 2008, 'Effects of biodiesel and Jatropha oil on performance, black smoke and durability of single-cylinder diesel engine', *Journal of Metals, Materials and Minerals*, vol. 18, no. 2, pp. 181–185.

- Forson, FK *et al.* 2004, 'Performance of Jatropha oil blends in a diesel', *Renewable Energy*, vol. 29, pp. 1135–1145.
- Heywood, JB 1988, *Internal combustion engine fundamentals*, International Edition, McGraw Hill, London.
- Hoa, DT *et al.* 2012, 'The Potential Jatropha curcas for agriculture and forest diesel engine in Vietnam', *International Conference on Environment, Energy and Biotechnology*, IPCBEE 33, pp. 7–11.
- Khovakh, M 1971, *Motor vehicle engines*, MIR Publishers, Moscow.
- Kywe, TT & Oo, MM 2009, 'Production of biodiesel from Jatropha oil (*Jatropha Curcas*) in Pilot Plant', *World Academy of Science, Engineering and Technology*, no. 26, pp. 477–483.
- Nasim, MN *et al.* 2010, 'Simulation of CI engine powered by neat vegetable oil under variable fuel inlet temperature', *Indian Journal of Science and Technology*, vol. 3, no. 4, pp. 387–392.
- Pulkrabek, WW 1988, *Engineering fundamentals of the internal combustion engine*, Prentice Hall, New Jersey, pp. 35–68.

Developing a Generalized Combined Model for Gas-liquid Two-phase Flow Pressure Drop in Elbow Bends

N. Z. AUNG^{1*} AND T. YUWONO²

In this work, a generalized combined model was proposed for prediction of two-phase flow pressure drop in elbow bends. In this proposed model, restriction, frictional and elevational losses were considered separately. The frictional and static losses were approached by using Lockhart_Martinelli correlation. This model was tested to predict the pressure drop across the elbows with inside diameter of 0.036 m and R/D = 0.6, 2.5. The superficial liquid velocity was varied in the range of 0.3~1.1 m/s and volumetric gas quality was varied from 0.02~0.3. The results from this model had good predictions with a maximum error of $\pm 13\%$ for long elbow bends and showed great discrepancy with a peak error of -50% for short elbow bends. The model is reliably acceptable for the elbow bends with relative radius (R/D) greater than 2 at volumetric gas fractions less than 0.3.

Key words: Generalized combined model; two-phase flow; pressure drop; elbow bends

Multi-phase flows are widely encountered in several engineering and industrial facilities such as conventional steam power plants, evaporators and condensers, pressurized-water nuclear reactors, a wide variety of petroleum industries, chemicals and food processing industries. Piping systems in these steam power plants, chemical plants, refineries, oil and gas transportation grids are a very wide and complex. Pipes have to be laid out according to many geometrical and physical constraints. In these piping systems, elbows and bends, expanders and reducers, tee-junctions and control valves are a very common occurrence. In this point, the knowledge of two-phase flow pressure drop in piping components apart from straight pipes is very important for accurate and reliable piping design. It enables the designer to size the pump that is reliable and economic for the operation of the flow system.

On account of two different velocities, two different densities and very complicated flow phenomenon in elbow bends, theory for two-phase flow pressure drop in elbow bends is very rear to be found. Therefore, estimating two-phase flow pressure drop in elbow bends is numerically not an easy task. Even in a single phase flow, there is no exact solution for pressure drop in elbow bends because of the complicated flow phenomena. Nowadays, a few of researchers are trying to develop empirical formula for two-phase flow pressure drop in elbow bends based on experimental data. Benard (2006) developed a correlation for two-phase flow pressure drop in elbow by using his experimental data, but his correlation is limited only for R/D = 0.6539, $Re_{SL} = 280-9800$ and $Re_{SG} = 2000-30000$. Seungjin Kima (2008) calculated total losses coefficients K from experimental pressure drop for 45° and 90°

¹ Department of Mechanical Engineering, Mandalay Technology University, Myanmar

² Laboratory of Fluid Mechanics, Department of Mechanical Engineering, Institute Technology Sepuluh Nopember, Campus ITS, Sukolilo, Surabaya

* Corresponding author (e-mail: nay1572@gmail.com)

elbows. Unfortunately their calculation so far has not been satisfactory.

Thus, the objective of this work is to develop a general model that can be used for estimating two-phase flow pressure drops in a wide range of elbow dimensions.

SINGLE PHASE PRESSURE DROP IN ELBOW BENDS

For a single phase flow, the energy loss through a pipe fitting arising from internal friction, flow separation and secondary flow it is approximately proportional to the square of the flow velocity. Thus, prediction of pressure drop in various pipe fittings (including elbow bends) is not an easy work and most of data on flow through such things are obtained by carefully conducted experiments. In turn, correlating with experimental data, some acceptable formulas have been developed and commercially used to predict pressure drop in piping system designs. In this section, three methods for calculating pressure drop in bends are presented and one of them is proposed for two-phase flow. Generally, for single phase flow, pressure drop in elbow

bends is a combination of three components as shown below:

$$\Delta P = \Delta P_{res} + \Delta P_f + \Delta P_s \sin(\gamma) \quad (1)$$

If the elbow is horizontal, there is no static pressure losses, and so $\Delta P_s = 0$

$$\Delta P = \Delta P_{res} + \Delta P_f \quad (2)$$

$$\Delta P = \left(k_{res} + f \frac{\pi R}{2D} \right) \times \rho \frac{V_{avg}^2}{2} \quad (3)$$

$$\Delta P = K \times \rho \frac{V_{avg}^2}{2} \quad (4)$$

$$\left(\text{Where, } K = k_{res} + f \frac{\pi R}{2D} \right)$$

Total Losses Coefficient Method

In this method, total losses coefficient K is defined as combination of restricted loss and frictional loss. The relation of restriction coefficient (k_{res}) and relative radius (R/D) for various elbow bends is shown in *Figure 1*.

$$K = k_{res} + f \frac{\pi R}{2D} \quad (5)$$

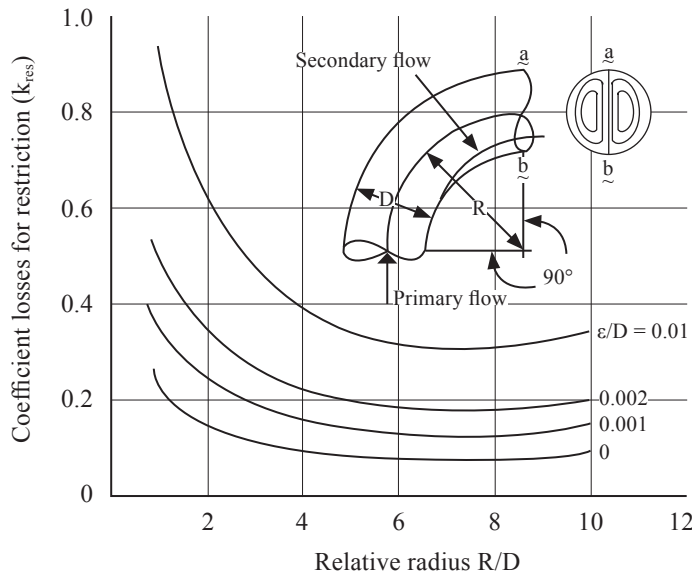


Figure 1. Coefficient losses (k_{res}) for restriction at various R/D .

Equivalent Length Method

In this method, total losses coefficient K is defined as in term of equivalent length.

$$K = f \frac{L_e}{D} \tag{6}$$

Total Losses Coefficient Method Based on Turbulent Friction Factor

In fully developed turbulent flow, total losses coefficient is twelve times the turbulent friction factor and it can be calculated by using Colebrook equation for friction factor.

$$K = 12 f_T \tag{6}$$

$$f_T = f(\text{Re}, \kappa/D) \tag{7}$$

$$\frac{1}{\sqrt{f_T}} = -4 \log \left(\frac{2\kappa}{D} + \frac{9.35}{\text{Re}\sqrt{f_T}} \right) + 3.48 \tag{8}$$

LOCKHART–MARTINELLI
CORRELATION FOR TWO-PHASE
FLOW PRESSURE DROP

The Lockhart–Martinelli (Lockhart & Martinelli 1949) correlation is perhaps the oldest available correlation for two-phase frictional pressure drop in horizontal pipes. It is widely used in the process industry. It is very simple to apply because it is independent of flow pattern. No liquid fraction information is needed to compute the frictional pressure gradient. It is calculated by multiplying the frictional pressure gradient for single-phase flow (either liquid or gas) by a two-phase flow multiplier Φ_L^2 or Φ_G^2 .

$$-\frac{dp}{dx} = \Phi_L^2 \left(-\frac{dp}{dx} \right)_{SL,f} = \Phi_G^2 \left(-\frac{dp}{dx} \right)_{SG,f} \tag{9}$$

$$\left(-\frac{dp}{dx} \right)_{SL,f} = 2 f_{SL} \rho_L U_{SL}^2 / D \tag{10}$$

$$\left(-\frac{dp}{dx} \right)_{SG,f} = 2 f_{SG} \rho_G U_{SG}^2 / D \tag{11}$$

Here, superficial velocities, U_{SL} and U_{SG} are expressed as:

$$U_{SL} = \frac{Q_L}{A} \tag{12}$$

$$U_{SG} = \frac{Q_G}{A} \tag{13}$$

The friction factor for each phase can be calculated by using Colebrook equation. The parameter X, known as the *Lockhart–Martinelli parameter* which is correlated to the two-phase multipliers will be introduced as,

$$X = \left[\frac{\left(-\frac{dp}{dx} \right)_{SL,f}}{\left(-\frac{dp}{dx} \right)_{SG,f}} \right]^{1/2} \tag{14}$$

$$\Phi_G^2 = 1 + CX + X^2 \tag{15}$$

$$\Phi_L^2 = 1 + \frac{C}{X} + \frac{1}{X^2} \tag{16}$$

Chisholm (1967) introduced a convenient expression for the two-phase multipliers with the following C values for different types of flow.

Table 1. C values in two-phase multiplier (Chisholm 1967).

Liquid	Gas	C
Turbulent	Turbulent	20
Laminar	Turbulent	12
Turbulent	Laminar	10
Laminar	Laminar	5

The gas fraction needed for the pressure gradient contribution due to gravity is also determined by a correlation developed by Lockhart and Martinelli:

$$\alpha_G = \left[1 + 0.28 \left(\frac{1-x}{x} \right)^{0.64} \left(\frac{\rho_G}{\rho_L} \right)^{0.36} \left(\frac{\mu_L}{\mu_G} \right)^{0.07} \right]^{-1} \quad (17)$$

Therefore, the static pressure losses are:

$$\frac{dp}{dx} = g \times [\rho_L \alpha_L + \rho_G (1 - \alpha_L)] \quad (18)$$

To be general, if there was any inclination angle γ from horizontal, it could be:

$$\frac{dp}{dx} = g \times [\rho_L \alpha_L + \rho_G (1 - \alpha_L)] \times \sin(\gamma) \quad (19)$$

DEVELOPING GENERALIZED COMBINED MODEL FOR GAS-LIQUID TWO-PHASE FLOW PRESSURE DROP IN ELBOW BEND

In this section, a generalized model was proposed for a two-phase flow pressure drop in elbow bends with reasonable considerations so that it could be used in a wide range of conditions. The **total losses coefficient method** was used in developing the model. The following equation could be written for the two-phase flow pressure drop in elbow bend by using *Equation 1*:

$$\Delta P_{EB} = \Delta P_{res, Two-phase} + \Delta P_{f, Two-phase} + \Delta P_{s, Two-phase} \sin(\gamma) \quad (20)$$

Here, first we will consider the two-phase frictional pressure drop, $\Delta P_{f, Two-phase}$ and static pressure drop, $\Delta P_{s, Two-phase}$. Basically, the two-phase flow pressure drop is strongly dependent on phase fraction and the flow pattern. However, in elbow bend it was very difficult to define the flow pattern because of interferences such as separation and secondary flow. Therefore, to solve this problem, *Lockhart_Martinelli Correlation* was chosen which does not depend on the flow pattern.

The second problem was how to solve the two-phase flow pressure drop because of elbow restriction. According to the momentum theory (ρVV), if the flowing fluids pass any restriction, fluids with higher densities would suffer from higher momentum losses than lower density fluids. Therefore, if we consider gas-liquid two-phase flow in any elbow bend, momentum losses contributed from liquid phase is nearly the same momentum losses for the whole mixture. As the gas phase density was very low compared with liquid phase, losses contributed from gas phase could be neglected in low gas concentration. But at high gas velocities or high gas concentrations, restriction losses for gas would be considerable as a factor that had to be accounted. Therefore, for low gas concentration it could be written as:

$$\Delta P_{res, Two-phase} = k_{res} \rho_L \frac{U_{SL}^2}{2} \quad (21)$$

$$\Delta P_{f, Two-phase} = \frac{dp}{dx} \times \frac{\pi R}{2} \quad (22)$$

$$\Delta P_{s, Two-phase} = \frac{dp}{dz} \times R \times \sin(\gamma) \quad (23)$$

By combining the above three expressions:

$$\Delta P_{EB} = k_{res} \rho_L \frac{U_{SL}^2}{2} + \left(\frac{dp}{dx} \times \frac{\pi R}{2} \right) + \left(\frac{dp}{dz} \times R \times \sin(\gamma) \right) \quad (24)$$

Then, we considered for the case in which the dispersed density became nearly the same with continuous phase density (*liquid-liquid flow, oil-water flow*). In such a case, the assumption that as homogeneous flow was very reasonable and the mixture possessed average properties of the phases involved. The mixture could be assumed as a single fluid with average properties. The restriction losses, frictional losses and static losses would be contributed from both fluids. Therefore for the two-phase flow in which $\rho_{DL} \approx \rho_L$ and $\mu_{DL} \approx \mu_L$, the pressure drop in elbow bends could be developed as follow:

$$\Delta P_{res, Two-phase} = k_{res} \rho_{mix} \frac{U_{mix}^2}{2} \quad (25)$$

$$\Delta P_{f, Two-phase} = f_{mix} \frac{\pi R}{2D} \frac{U_{mix}^2}{2} \quad (26)$$

$$\Delta P_{s, Two-phase} = \rho_{mix} \times g \times R \times \sin(\gamma) \quad (27)$$

By combining the above three expressions:

$$\Delta P_{EB} = k_{res} \rho_{mix} \frac{U_{mix}^2}{2} + f_{mix} \frac{\pi R}{2D} \frac{U_{mix}^2}{2} + \rho_{mix} g R \sin(\gamma) \quad (28)$$

$$U_{mix} = U_{SL} + U_{SDL} \quad (29)$$

$$U_{SDL} = \frac{Q_{DL}}{A} \quad (30)$$

$$\rho_{mix} = \rho_L (1 - \beta) + \rho_{DL} \beta \quad (31)$$

$$\mu_{mix} = \mu_L (1 - \beta) + \mu_{DL} \beta \quad (32)$$

$$Re_{mix} = \frac{\rho_{mix} D U_{mix}}{\mu_{mix}} \quad (33)$$

$$\beta = \frac{Q_{DL}}{Q_{DL} + Q_L} = \frac{U_{SDL}}{U_{mix}} \quad (34)$$

Here, f_{mix} could be calculated by using *Equation 8* and mixture Reynolds number.

AVAILABLE EXPERIMENTAL DATA

Aung (2009) and Sukmono (2009) performed experiments with gas-liquid two-phase flow through elbow bends to investigate gas-liquid two-phase flow pattern and pressure drop characteristics through a vertical to horizontal 90° elbows. The first conducted tests for elbow bend having (center bend radius to diameter ratio) $R/D = 2.5$ and the later for $R/D = 0.6$. For every elbow bend, forty different flow conditions were created by varying inlet superficial liquid velocity ($U_{SL} = 0.3 \sim 1.1$ m/s) and volumetric gas quality ($\beta = 0.05 \sim 0.2$). The test section had 2 m high vertical pipe and 1 m long horizontal pipe which was connected with selected elbow. All parts of test section were made of acrylic pipe. A water-filled manometer set was used to measure pressure gradients along test section. The detail of the experimental setup and measuring techniques could be seen in corresponding references. These measured data in experiments were used in validation of estimated data from proposed model.

PREDICTION WITH PROPOSED MODEL AND ERROR ANALYSIS

Table 1 and *2* summarize the properties of fluids used in experiments and restriction coefficients for elbow bends. These are required data for predictions with the proposed model. The flow diagram for tasks in prediction is shown in *Figure 2* and the prediction calculations would be served by using MATLAB as computational tool.

Table 1. Restriction coefficient for elbow bends.

Parameter	Long elbow	Short elbow
Relative radius (R/D)	2.5	0.6
Diameter [D (m)]	0.036	0.036
Radius of curvature [R (m)]	0.09	0.0216
Restriction coefficient for elbow bends (k_{res})	0.156	0.35

Table 2. Properties of fluids used in experiments and predictions.

Fluids	Water	Air
Density [$\rho(\text{kg/m}^3)$]	997	1.17
Viscosity [$\mu (\text{Ns/m}^2)$]	0.00089	0.0000181

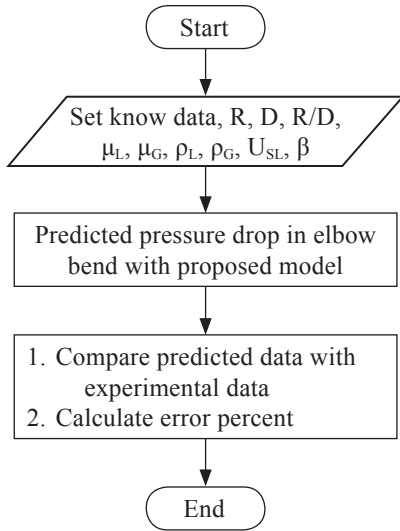


Figure 2. Flow diagram for tasks in prediction.

The validity of the developed model is defined based on definition that corresponds to the minimum root mean square (rms) error. The error (ϵ) from applying the model to each available data point is defined as:

$$\epsilon (\%) = \left| \frac{\text{Predicted} - \text{Experimental}}{\text{Experimental}} \right| \times 100 \quad (35)$$

For groups of data, the root mean square error, ϵ_{rms} , is defined as:

$$\epsilon_{rms} (\%) = \left[\frac{1}{N} \sum_{i=1}^N \epsilon_i^2 \right]^{1/2} \quad (36)$$

RESULT AND DISCUSSION

A typical photo of a two-phase flow phenomenon in elbow bend recorded in experiment is shown in *Figure 3*. It will not be dealt with here, but just for seeing how it behaves. The characteristics of pressure drop in elbow bend were related with observed flow behaviour in it. In general, the results showed that pressure drop characteristics in elbow bends had decreasing trends since elevational pressure drop was the most dominant component in vertical positioned elbow which decreased with increasing amount of gas. However, the frictional and restriction pressure drop become more dominant at high velocities.

Table 3 exhibits comparisons of experimental data and predicted data calculated from proposed method for every constant superficial liquid Reynolds number and *Figure 4* shows graphical presentation for $Re_{SL} = 13497$.

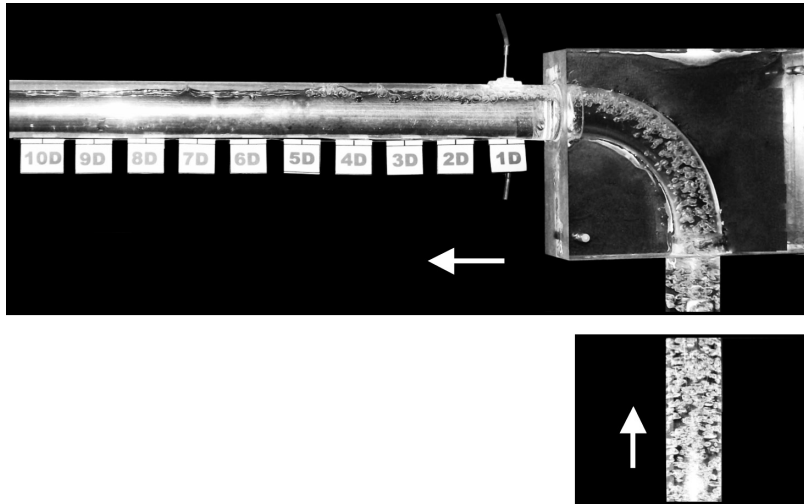


Figure 3. Visual observation of two-phase flow pattern across the elbow at $Re_{SL} = 13497$, $\alpha = 0.07$.

Generally, the proposed method could give estimated data which have the same trend with experimental data. It gives good predictions for long elbow bend (Nay's data) with root mean square error of 2.1%. For short elbow

(Yudi's data), there is a great difference between predicted data and experimental ones until it shows rms of as large as 46%. This discrepancy can be explained by the pressure drop due to restriction and friction. In real two-phase flow in

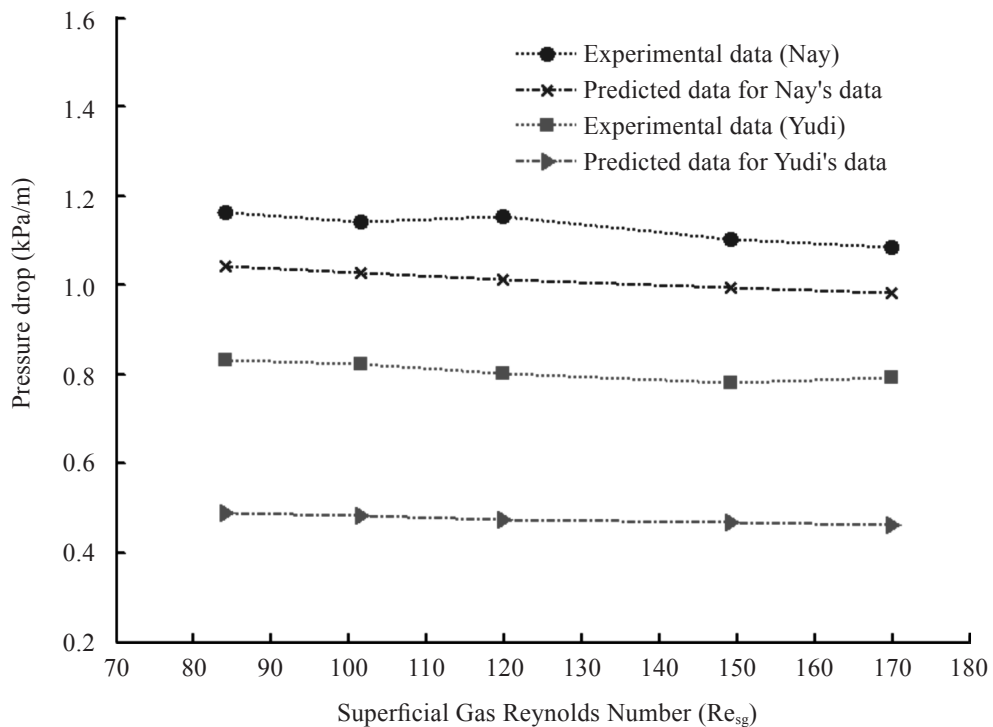


Figure 4. Pressure drop in elbow bends for $Re_{SL} = 13497$.

Table 3. Comparison of experimental data and predicted data.

U_{SL} (m/s)	β	Yudi's data		Nay's data	
		Experimental Pressure drop (N/m ²)	Predicted data (N/m ²)	Experimental Pressure drop (N/m ²)	Predicted data (N/m ²)
0.3	0.11	831.35	528.26	1162.72	1126.47
	0.13	821.57	522.03	1143.18	1112.84
	0.15	802.01	516.04	1152.95	1099.71
	0.18	782.45	507.33	1104.10	1080.64
	0.20	792.23	501.77	1084.55	1068.46
0.5	0.07	948.72	576.80	1221.30	1181.32
	0.09	899.81	569.74	1201.80	1165.83
	0.11	890.03	563.23	1172.50	1151.57
	0.13	880.25	557.06	1182.30	1138.03
	0.15	831.35	551.14	1123.60	1125.06
	0.18	802.01	542.58	1113.90	1106.29
	0.20	831.35	537.08	1104.10	1094.24
	0.7	0.05	1173.67	635.66	1240.90
	0.07	1173.67	628.03	1221.30	1216.47
	0.09	1144.33	621.14	1192.00	1201.35
	0.11	1124.77	614.71	1182.30	1187.23
	0.13	1075.86	608.55	1162.70	1173.72
	0.15	1026.96	602.80	1143.20	1161.09
	0.18	997.62	594.38	1104.10	1142.61
	0.20	1007.40	588.97	1094.30	1130.73
0.9	0.05	1359.50	703.07	1280.00	1278.32
	0.07	1369.28	695.63	1280.00	1261.95
	0.09	1427.96	688.85	1250.70	1247.03
	0.11	1330.16	682.54	1211.60	1233.17
	0.13	1261.69	676.56	1201.80	1220.01
	0.15	1232.35	670.84	1172.50	1207.45
	0.18	1203.01	662.59	1182.26	1189.30
	0.20	1212.79	657.27	1182.30	1177.60
1.1	0.05	1760.50	786.76	1348.40	1333.51
	0.07	1799.62	779.44	1348.40	1317.40
	0.09	1770.28	772.81	1289.70	1302.78
	0.11	1828.97	766.62	1299.50	1289.15
	0.13	1760.50	760.77	1309.30	1276.26
	0.15	1740.94	755.17	1280.00	1263.93
	0.18	1604.01	747.09	1250.70	1246.13
	0.20	1594.23	741.88	1280.00	1234.65

very short elbow, the turbulence is enhanced by gas bubbles that cause an increase in frictional and restricting pressure drop. Therefore, the experimental pressure drops greatly to overcome the predicted data.

The other observation is that at higher liquid velocities, the pressure drop in the short elbow is much higher than that in the long elbow bend. Thus, the higher the gas velocity, the bigger is the error for the proposed model. It is noteworthy that predictions by the proposed model is appropriate for long elbows while it is quite poor for short elbows. *Figures 5–6* depict the direct comparison of the whole predictive data to the experimental database for both elbows. It can be seen that this proposed method is weak in estimating pressure drop for $R/D = 0.6$ with maximum error greater than -50% . However, most of predicted data fall within the error limits of $\pm 13\%$ for $R/D = 2.5$.

CONCLUSION

From this work, a general combined model to predict two-phase flow pressure drop in elbow bends was developed. In the model, restriction pressure drop, frictional pressure drop and elevational pressure drop were considered separately. *Lockhart_Martinelli Correlaiton* was borrowed to predict the frictional and elevational pressure drop. It was tested to predict the experimental data for two types of elbow bends with $R/D = 0.6$ and $R/D = 2.5$. The results showed that the proposed model well predicted pressure drop for long elbow ($R/D = 2.5$) with maximum error of $\pm 13\%$ and ϵ_{rms} of 2.1% , meanwhile it had poor predictions for short elbow ($R/D = 0.6$) which gave a maximum error higher than -50% and ϵ_{rms} of 46% . However, it was appropriate for all experimental data. As discussed earlier, this model could be proposed for future studies on two phase flow in the long elbows with a

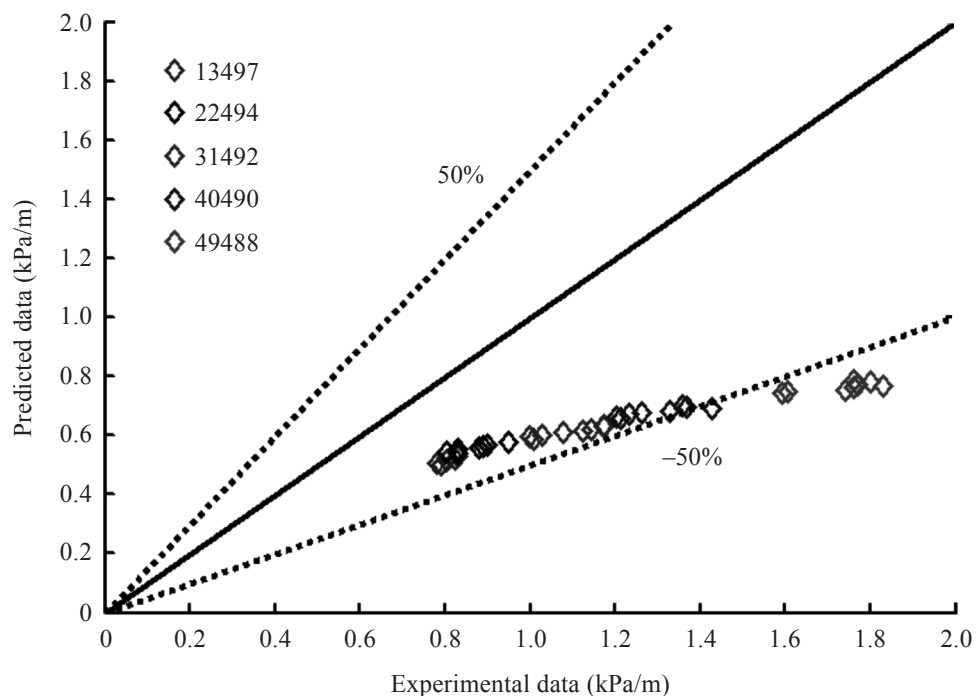


Figure 5. Experimental pressure drops against predicted pressure drops in elbow bend with $R/D = 0.6$.

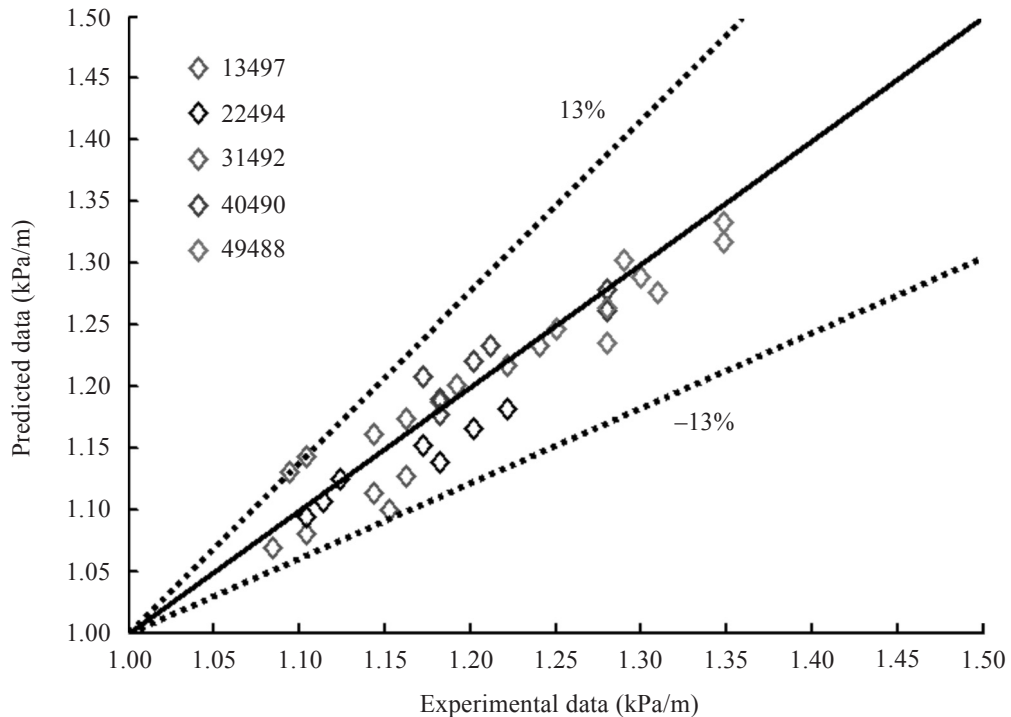


Figure 6. Experimental pressure drops against predicted pressure drops in elbow bend with $R/D = 2.5$.

relative radius greater than 2 and volumetric gas quality not higher than 0.3. But a higher value of k_{res} could be considered in the short elbow bends.

Date of submission: June 2012

Date of acceptance: October 2012

ACKNOWLEDGEMENT

The author would like to express his special thanks to his supervisor and advisor Prof. Dr. Triyogi Yuwono, DEA for his valuable advice, patience, understanding and educational challenges throughout the duration of this research and all the staff of the Fluid Mechanic Lab, Mesin, ITS for the facility support and valuable assistance.

REFERENCES

- Angeli, P 2006, 'Upward and downward inclination oil-water flow', *International Journal of Multiphase Flow*, vol. 32, pp. 413–435.
- Aung, NZ 2009, 'Experimental and numerical investigation of gas-liquid two phase flow characteristics after vertical to horizontal 90° elbow (case study for $R/D=2.5$)', Thesis, Department of Mechanical Engineering, Institute Technology Sepuluh Nopember.
- Benard, E 2006, 'Gas-liquid two phase flow through a vertical 90° elbow bend', *Experimental Thermal and Fluid Science*, vol. 31, pp. 761–769.
- Crowe, CT 2006, *Multiphase flow handbook*, Taylor & Francis Group, New York.
- Guo, B *et al.* 2005, *Offshore pipelines*, University of Louisiana at Lafayette.

- Kima, S 2007, 'Geometric Effects of 90-degree elbow in the development of interfacial structures in horizontal bubbly flow', *Nuclear Engineering and Design*, vol. 237, pp. 2105–2113.
- Levy, EK 2000, 'Gas–solid flow behavior in a horizontal pipe after a 90° vertical-to-horizontal elbow', *Powder Technology*, vol. 116, pp. 43–52.
- Sukmono, Y 2009, 'Experimental and numerical investigation of gas-liquid two phase flow characteristics after vertical to horizontal 90° elbow (case study for R/D=0.6)', Thesis, Department of Mechanical Engineering, Institute Technology Sepuluh Nopember.
- Wang, CC 2002, 'Influence of horizontal return bend on the two-phase flow pattern in small diameter tubes', *Experimental Thermal and Fluid Science*, vol. 28, pp. 145–152.

NOMENCLATURE

Notation

D	Diameter of the pipe (m)
dp/dx	Pressure gradient with vitiation of pipe length (Pa/m)
dp/dz	Pressure gradient with lavational variation (Pa/m)
f	Fanning friction factor
g	Acceleration due to gravity (m/s ²)
K	Total losses coefficient
k	Restriction coefficient
L	Length (m)
P	Toal pressure (kPa)
Q	Flow rate (m ³ /s)
R	Radius of curvature (m)
Re	Reynolds number
U	Superficial velocity respective phase (m/s)
V	Velocity of single phase flow (m/s)
x	Mass quality of gas

Symbols

α	Fraction of respective phase
β	Fraction of respective phase in homogenous flow
γ	Elbow inclination angle (degree)
ρ	Density (kg/m ³)
μ	Viscosity (N-s/m)
κ	Pipe surface roughness (m)

Subscript

EB	Elbow
f	Fractional
res	Reaction
s	Static
Two-phase	Two-phase flow
mix	Mixutre
L	Liquid
G	Gas
SDL	Superficial dispersed liquid
SG	Superficial gas
SL	Superficial liquid

Ethanol Production in Yeasts Isolated from Fermented Kitchen Waste

S. WONG¹, S. K. WONG^{1*} AND J. S. BUJANG¹

Microbial ethanol is a potential substitute for the non-renewable fossil fuel which is depleting. Yeasts have been long and extensively studied for ethanol production. The objectives of this study were to isolate yeasts from fermented kitchen waste and to determine their ethanol production performances. A number of fifteen yeasts were isolated from fermented kitchen waste. The yeasts were then grouped based on their ability to ferment different types of sugars. Three yeast isolates were selected for the analysis of ethanol production. Fermentation was carried out for 72 h in yeast extract peptone dextrose broth containing 18% glucose. Fourier transform infrared attenuated total reflection spectroscopy was used to monitor the ethanol production and glucose utilization. Isolate Y4 achieved the highest ethanol production at the level of 16%, while Y6 and Y8 demonstrated 12% and 11% ethanol yields, respectively. The isolates Y4, Y6 and Y8 were identified using universal fungal primers ITS1 and ITS4. The yeast isolates were closest to *Saccharomyces cerevisiae* (76%), *Paracoccidioides brasiliensis* (56%) and *Saccharomyces boulardii* (64%), respectively. This study showed that fermented kitchen waste could serve as a good source of yeasts for ethanol production.

Key words: Yeast; ethanol; fermentation; kitchen waste; FTIR-ATR; *Saccharomyces cerevisiae*; *Paracoccidioides brasiliensis*; *Saccharomyces boulardii*

Microbial ethanol is gaining worldwide acceptance to overcome problems associated with the depletion of fossil fuels and environmental pollution. The non-renewable energy sources have been depleting and it takes a few hundred million years for natural processes to recreate them. Therefore, the primary benefit of switching fuel source to microbial ethanol is that the biomass is renewable, and can potentially provide a sustainable supply over a long term. In addition, many estimate that the production and use of bioethanol could cause a reduction in net greenhouse gas emissions (Mabee & Saddler 2010).

Ethanol production is usually done by chemical synthesis of hydrocarbons. In recent years, there is a global emphasis in ethanol

production by fermentation process. Increased yield of ethanol production by microbial fermentation depends on the use of ideal microbial strain, appropriate fermentation substrate and suitable process technology. An ideal micro-organism used for ethanol production must have rapid fermentative potential, improved flocculating ability, appreciable osmotolerance, enhanced ethanol tolerance and good thermotolerance (Brooks 2008; Stewart *et al.* 1982; Yan & Tanaka 2006). To date, there is no microbial strain which meet these qualities (Brooks 2008).

Brooks (2008) reported various strains of indigenous yeasts capable of producing ethanol had been isolated from different local sources such as molasses (Yan & Tanaka 2006), sugar

¹ Department of Animal Science and Fishery, Faculty of Agriculture and Food Sciences, Universiti Putra Malaysia Bintulu Sarawak Campus

* Corresponding author (e-mail: wongsk@btu.upm.edu.my)

mill effluents, local fermented foods, and fermented pineapple juice and lignocellulosic agroindustrial residues (Okur & Saracoğlu 2006). In most of these studies, the preferred candidate for industrial production of ethanol has been *Saccharomyces cerevisiae* due to its ability to produce high concentration of ethanol and the ethanol is not contaminated by other products from the substrate (Yan & Tanaka 2006).

Thus the aims of this study were to isolate indigenous yeast strains from the fermented kitchen waste and to evaluate their potential in ethanol production.

MATERIALS AND METHODS

Fermentation mixture was prepared by mixing kitchen waste (vegetables and fruits) and brown sugar and water at a weight ratio of 3:1:10. Fermentation was carried out in a closed container at room temperature (26°C–28°C) under non-sterile condition. The seven-day-old product was subjected to 10-fold serial dilution then it was spread onto potato dextrose agar (PDA) containing 0.1% chloramphenicol. The PDA plates were incubated at 30°C for 24 h–48 h. The yeast isolates were characterized by their ability to ferment sugars in broth containing 1% yeast extract and 2% sugars (glucose, lactose, galactose, fructose, xylose, maltose or sucrose).

Ethanol fermentation was carried out in conical flask at 26°C–28°C for 72 h in yeast extract peptone dextrose broth (1% yeast extract, 2% peptone, 18% glucose) under sterile condition. Ethanol production and glucose utilization were monitored using Fourier transform infrared attenuated total reflection (FTIR-ATR) spectroscopy. The levels of ethanol and glucose in the samples were estimated based on the selected absorption wavenumber and absorbance value corresponding to those of the chemical standards. The isolates were

identified through molecular approach based on the internal transcribed spacer (ITS) sequence. The DNA of the yeasts was extracted by boiling in 2% SDS followed by ethanol precipitation. The ITS region was amplified using universal primers ITS1 and ITS4 (White *et al.* 1990). Nucleotide sequences of the PCR products were analyzed by automated DNA sequencing by First Base Laboratories.

RESULTS AND DISCUSSION

Fifteen yeasts were isolated from fermented kitchen waste. They were grouped into six groups based on their sugar fermentation profiles (Table 1). Group 6 was the only group which did not ferment glucose and any other tested sugars. The Y7, Y9, Y10 and Y14 were therefore regarded as yeast-like microorganisms based on their colony morphologies and they were excluded from the fermentation test where glucose was used as carbon source. Primary fermentation analysis on the yeast isolates from the other 5 groups detected different levels of ethanol. Yeasts from groups 1, 2 and 3 produced substantial amount of ethanol as shown by the FTIR spectrums. However, there was only <10% (v/v) of ethanol observed in the culture media of yeast isolates in Groups 4 and 5 (data not shown).

Subsequent time course studies of ethanol production were performed on isolates Y4, Y6 and Y8, respectively representing group 1, 2 and 3. It was observed that ethanol production peaked after 36 h of fermentation. Y4 recorded the highest ethanol production as high as 16% followed by 12% and 11% in Y6 and Y8, respectively (*Figure 1*). Elevated level of ethanol in Y4 could be explained by efficient glucose utilization to below 1% after 36 h fermentation (*Figure 1*). In contrast, glucose levels in Y6 and Y8 were 7% and 5%, respectively at 36 h and gradually decreased to 3% at 72 h. Ethanol has been reported to show inhibitory effects on yeast fermentation through

Table 1. Sugar fermentation test of the yeasts.

Yeasts	Sugars							Grouping
	Glu	Mal	Lac	Gal	Xyl	Suc	Fru	
Y1	+	-	-	+	-	+	+	4
Y2	+	-	-	+	-	+	+	4
Y3	+	-	-	+	-	+	+	4
Y4	+	+	-	+	-	+	+	1
Y5	+	-	-	-	-	-	-	5
Y6	+	+	-	-	-	+	+	2
Y7	-	-	-	-	-	-	-	6
Y8	+	-	-	-	-	-	+	3
Y9	-	-	-	-	-	-	-	6
Y10	-	-	-	-	-	-	-	6
Y11	+	-	-	-	-	-	-	5
Y12	+	-	-	+	-	+	+	4
Y13	+	-	-	-	-	-	+	3
Y14	-	-	-	-	-	-	-	6
Y15	+	-	-	-	-	-	-	5

Note: + : Positive fermentation; - : Negative fermentation; Glu: Glucose; Mal: Maltose; Lac: Lactose; Gal: Galactose; Xyl: Xylose; Suc: Sucrose; and Fru: Fructose.

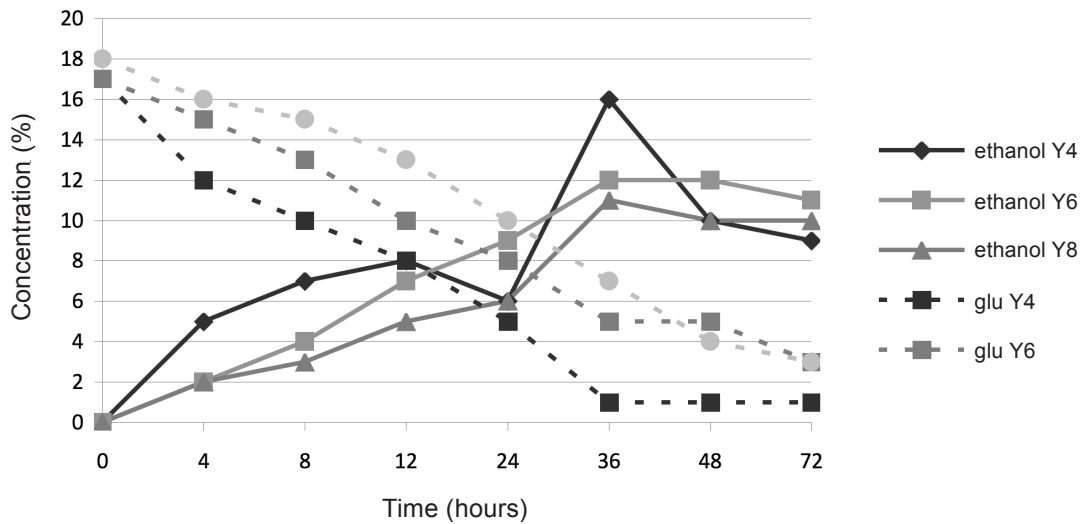


Figure 1. Time course study of ethanol fermentation in yeasts.

the alteration of membrane permeability and disruption of its function (Dombek & Ingram 1987). These lead to an increase in hydrogen ion influx which causes the decline in transport rates and eventually, there was no further glucose uptake for ethanol production.

FTIR spectroscopy offers rapid and convenient means in estimating the amounts of ethanol and glucose in fermentation mixture. There was no requirement for pre-analysis sample preparation and separation. The absorptions around 3000 cm^{-1} (likely a C-H stretch) (Coates 2000) and 1000 cm^{-1} (likely a C-O region) (Petibois *et al.* 1999) were used to quantitate the levels of ethanol and glucose

respectively (Figure 2). These 2 wavenumbers were found to exhibit positive linear relationship towards different concentrations of ethanol (0%–35%) and glucose (0%–18%) standard at respective R^2 values of 0.915 and 0.997.

Isolates Y4, Y6 and Y8 generated PCR products at different sizes at 620 b.p., 500 b.p. and 520 b.p., respectively (Figure 3). ITS has been regarded as highly variable region for fungi identification. However, in this study, attempts to identify the yeasts isolates based on the ITS sequences were not conclusive due to low similarity (<90%) between the sample sequences and the fungal DNA database. Isolates Y4, Y6 and Y8 were

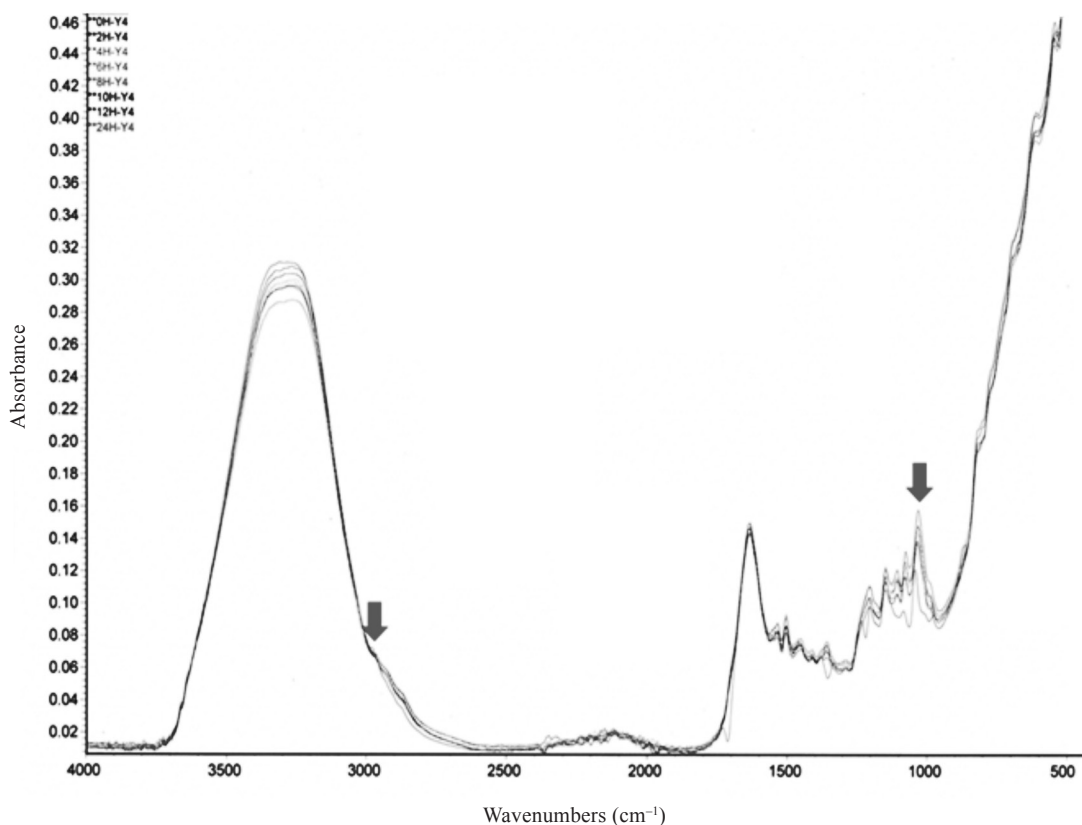


Figure 2. FTIR spectrum of yeast fermentation mixture: arrows indicate the absorption peaks used for quantitating ethanol (3000 cm^{-1}) and glucose (1000 cm^{-1}).

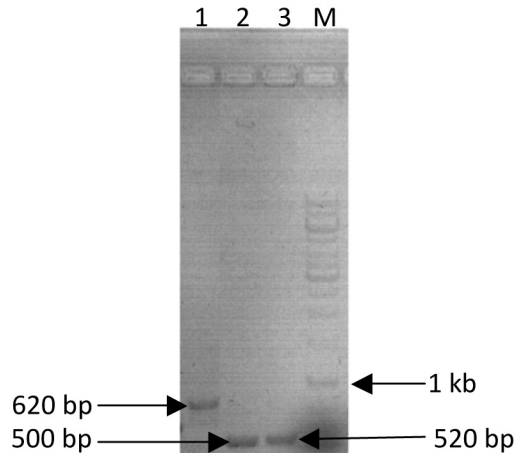


Figure 3. Amplified ITS regions of isolates Y4, Y6 and Y8
Lane 1: Y4; lane 2: Y6; lane 3: Y8;
M: VC 1kb DNA ladder (Vivantis).

found closest to *Saccharomyces cerevisiae* (76%), *Paracoccidioides brasiliensis* (56%) and *Saccharomyces boulardii* (64%) respectively based on the ITS sequences.

CONCLUSION

A number of three yeasts with promising ethanol production were isolated and partially identified from fermented kitchen waste. A rapid and simple FTIR based method has been developed to detect the ethanol and glucose levels during the fermentation process. The highest ethanol production was achieved in the yeast isolate Y4 which is believed to be closely related to *Saccharomyces cerevisiae*. Further analysis need to be carried out to verify the yeast species and its ethanol yield in a scale up of the fermentation process.

ACKNOWLEDGEMENTS

The authors thank Chiew C.H. for his help in conducting the experiments in this study.

Date of submission: January 2013

Date of acceptance: March 2013

REFERENCES

- Brooks, AA 2008, 'Ethanol production potential of local yeast strains isolated from ripe banana peels'. *African Journal of Biotechnology*, vol. 7, pp. 3749–3752.
- Coates, J 2000, 'Interpretation of infrared spectra, a practical approach', in *Encyclopedia of Analytical Chemistry*, ed RA Meyers, John Wiley & Sons Ltd, Chichester, pp. 10815–10837.
- Dombek, KM & Ingram, LO 1987, 'Ethanol production during batch fermentation with *Saccharomyces cerevisiae*: changes in glycolytic enzymes and internal pH', *Applied and Environmental Microbiology*, vol. 53, pp. 1286–1291.
- Mabee, WE & Saddler, JN 2010, 'Bioethanol from lignocellulosics: status and perspectives in Canada', *Bioresource Technology*, vol. 101, no. 13, pp. 4806–4813.
- Okur, TM. & Saracoğlu, NE 2006, 'Ethanol production from sunflower seed hull hydrolysate by *Pichia stipitis* under uncontrolled pH conditions in a bioreactor', *Turkish Journal Engineering Environmental Sciences*, vol. 30, pp. 317–322.
- Petibois, C, Rigalleau, V, Melin, AM, Perromat, A, Cazorla, G, Gin, H & Déléris, G. 1999, 'Determination of glucose in dried serum samples by Fourier-transform infrared spectroscopy', *Clinical Chemistry*, vol. 45, pp. 1530–1535.

- Stewart, GG, Panchal, CJ & Peacock, I 1982, 'Increased osmotolerance of genetically modified ethanol producing strains of *Saccharomyces* sp.. *Biotechnology Letters*, no. 4, pp. 639-644.
- White, TJ, Bruns, TD, Lee, S & Taylor, J 1990, 'Analysis of phylogenetic relationships by amplification and direct sequencing of ribosomal RNA genes, in *PCR Protocols: a Guide to Methods and Applications*, eds MA Innis *et al.*, Academic Press, New York, pp. 315–322.
- Yan, L & Tanaka, S 2006, 'Ethanol fermentation from biomass resources: current state and Prospects', *Applied Microbiological Biotechnology*, vol. 69, pp. 627–642.

Chemical Composition of Leaf and Seed Oils of *Dryobalanops aromatica* Gaertn. (Dipterocarpaceae)

A. S. KAMARIAH^{1*}, T. OZEK², B. DEMIRCI³ AND K. H. C. BASER^{2,3}

The essential oils of the leaves and seed of *Dryobalanops aromatica* Gaertn. obtained by hydro-distillation resulted in 0.07% and 1.89% yield, respectively. These oils were then examined by GC-MS. Eighty-three components (plus an unknown) were identified from the leaf oil, representing 92% of the oil. Oxygenated monocyclic monoterpenes (terpinen-4-ol 15%, α -terpineol 16%), bicyclic monoterpene (α -pinene 7%) and oxygenated bicyclic sesquiterpene (globulol 8%) were the major constituents. In the case of the seed oil, 31 components were identified, representing 100% of the oil, while acyclic monoterpene (myrcene 5%), monocyclic monoterpene (limonene 6%), bicyclic monoterpenes (α -pinene 41%, α -thujene and β -pinene 13% each, sabinene 6%), and bicyclic sesquiterpene (bicyclogermacrene 6%) made up the major components. The remaining constituents of each oil (54% and 10%, respectively) were found to be minor ($\leq 4\%$ each). The chemical compositions of both oils differed quantitatively but showed important qualitative similarities and differences. The results of this study serve as the first report of complete chemical profiles of both oils.

Key words: *Dryobalanops aromatica*; essential oils; leaf; seed; hydro-distillation; GC-MS; oxygenated monocyclic monoterpenes; α -terpineol; bicyclic monoterpene; oxygenated bicyclic sesquiterpene; acyclic monoterpene

Dryobalanops, locally known as *kapur*, is a genus of large and tall trees from the Family Dipterocarpaceae. The genus consists of seven species which are widely distributed in Sumatra, Peninsular Malaysia and Borneo (Corner 1981; Ashton 2004). The four species found in Brunei Darussalam are *Dryobalanops aromatica* Gaertn, *D. beccari* Dyeri, *D. lanceolata* Burck and *D. rappa* Becc.

D. aromatica (Figure 1), commonly known as the Bornean Camphor-Tree, and locally known as *kapur peringgi*, is a large and lofty tree, reaching up to 65 m in height and 7 m in

girth. The trunk is usually a straight, cylindrical and clear bole of 30 m–40 m. This species is a well-known and valuable timber tree. The timber has been described as being moderately hard, heavy and durable (Ashton 1964). It is used as an internal wood and resembles mahogany when given a good polish. It has a camphor odour, and the camphor in the wood was sought after and sold as medicine in the past (Burkill 1966). The camphor produced by the tree is less important today than its timber, but in the earlier days the reverse was the case. The species also produces camphoraceous oleo-resin.

¹ Biology Programme, Faculty of Science, Universiti Brunei Darussalam, Tungku Link Road, Bandar Seri Begawan BE 1410, Negara Brunei Darussalam

² Department of Pharmacognosy, Faculty of Pharmacy, Anadolu University, 26470 Eskisehir, Turkey

³ Badebio Ltd., Technopark of Anadolu University, 26470 Eskisehir, Turkey

* Corresponding author (e-mail: kamariah.salim@ubd.edu.bn)

The uses of the wood and camphor of *D. aromatica* in both eastern and European medicines have been well documented (Burkill 1966; Perry 1980; Siang 1983; Duke & Ayensu 1985). The camphor has also been used by the Malays and the Sumatran people in the ceremonial purification of dead bodies and their preservation until burial (Burkill 1966). A mixture of the volatile oils of *D. aromatica*, *Piper longum*, *Santalum album*, *Asarum sieboldi* and *Alpinia officinarum* is said to be effective in the treatment of acute anginal attack (Guo *et al.* 1983). The methanol extract of the wood is also shown to have antifungal properties (Hong & Abdul Razak 1983; Kim *et al.* 2005).

Chemical examination on the oleo-resin of *D. aromatica* shows that it consists of 35% terpenes (including pinene), 10% alcohols (including borneol), 20% sesquiterpenes and

35% resin (Burkill 1966, p. 881). The resin consists mainly of triterpenes (Cheung & Wong 1972) and the oxygenated derivatives of asiatic acid as minor constituents (Cheung & Tokes 1968). The camphor consists of borneol, camphor, camphene, sesquiterpenes and terpineol (Perry 1980, Duke & Ayensu 1985), while the wood extracts contain largely terpenes and fatty acids (Ali & Koh 1991). However, an earlier distillation attempt on the leaves in 1910 yielded little oil and no details were provided (Burkill 1966, p. 881). A later attempt at distilling the leaves and twigs showed that no oil or borneol was obtained (Eaton 1925). Since then, there has not been any study on the essential oils in the leaves of this plant. In addition, no published work can be traced with reference to the volatile oil of its seed. The lack of information and details on both the leaf and seed oils of *D. aromatica* prompted us to undertake this investigation.

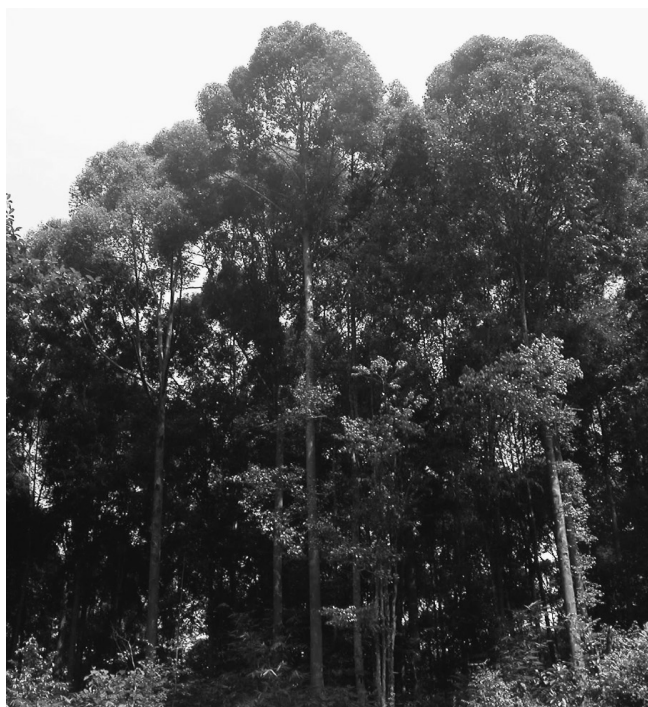


Figure 1. *Dryobalanops aromatica* Gaertn. (Bornean Camphor-Tree), a popular timber species today, was once well-known for its camphor.

Thus, the present study aims to identify and document fully for the first time the chemical constituents present in the essential oils obtained from the fresh leaves and seed of *D. aromatica*. This study may allow us to identify potential uses and better utilization of these plant parts which are usually discarded when the tree is harvested for its timber.

EXPERIMENTAL

Plant Material

Fresh leaves (Figure 2A) and seed (Figure 2B) of *D. aromatica* were collected from the Bukit Sawat forest in the Belait District of Brunei Darussalam. The species was identified by the author, Dr Kamariah Abu Salim and confirmed by Awang Ariffin Abdullah Kalat of the Brunei National Herbarium (BRUN), Sg. Liang. A voucher specimen bearing reference no. SN-B000340 was deposited at BRUN.

Isolation of Essential Oils

Immediately, after collection, the fresh leaves and seed were subjected to hydro-distillation in a Neo-Clevenger apparatus for 4 h. The

oils were collected in dark brown glass vials and stored at 4°C until further analysis. The percentage compositions of the oils were calculated based on the fresh weight of the respective plant parts.

Properties of Essential Oils

Oil density was determined by using a pycnometer, refractive index by a Shimadzu Bausch and Lomb Abbe refractometer, and optical rotation by an Onel Pol S-2 polarimeter.

Gas Chromatography-mass Spectrometry (GC-MS analysis)

GC-MS analysis of the oils was carried out on a Hewlett Packard GCD system. Separation was performed in an Innowax fused silica capillary (FSC) column (60 m × 0.25 mm id; 0.25 mm film thickness). Helium at a flow rate of 1 ml min⁻¹ was used as the carrier gas. The temperature of the GC oven was initially set at 60°C for 10 min, and then increased at a rate of 4°C min⁻¹ to 220°C. It was held isothermally at 220°C for 10 min, programmed to 240°C at a rate of 1°C min⁻¹, and finally maintained at

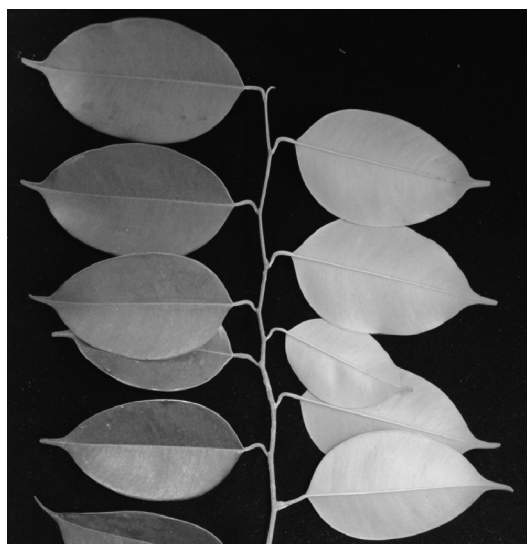


Figure 2. *Dryobalanops aromatica* Gaertn (A) fresh leaves and (B) fresh fruit.

240°C for 20 min. Split injection was conducted at a flow rate of 50 ml min⁻¹ with a split ratio of 50:1. The temperature of the injector was set at 250°C and the ionization energy was 70 eV. The mass range was from 35 to 425 m/z.

Determination of Essential Oil Composition

Chemical identification of the different components of the oils was based on their retention times and comparison of their mass spectra with those of the Wiley GC-MS Library and a home-made library (Baser Library of Essential Oil Constituents). The relative percentage composition of the volatile compounds was calculated from the Total Ion Chromatogramme (TIC), assuming that the relative response factor was equal to 1.

RESULTS AND DISCUSSION

Yields and General Considerations

The yields and physico-chemical properties of the leaf and seed oils of *D. aromatica* are shown in *Table 1*.

Although the density, refractive index and optical rotation of both oils appear to show very little difference, the oil yield of the seed was significantly (twenty-nine times) higher than that of the leaves. Thus, the seeds are a better source of oil than the leaves. However, the higher oil yield from the seed may not necessarily prove to be of significant importance for commercial exploitation because the trees only flower and fruit once in every 3–4 years. In addition, the conservation

status of the species must be considered and given a priority in any attempt to exploit the seed for commercialization of the oil. It may be better for the discarded seed (when present) during timber extraction to be collected for propagation and re-planting purposes.

The low percentage of oil yield from the leaves seems to be in agreement with earlier work carried out when negligible (Burkill 1966, p. 881) or no yield at all was obtained (Eaton 1925). Thus, any commercial exploitation of discarded leaves for the oil during timber harvest needs to take into account this low yield, available resources and the cost of production.

Chemical Composition

The identified compounds in the oils of *D. aromatica* leaves and seed, their relative amounts and their retention indices (Kovats's Indices for Polar Column) are shown in *Table 2*.

The leaf oil contains 84 compounds representing 92 % of the total oil. α -terpineol (16%), terpinen-4-ol (15%), globulol (8%) and α -pinene (7%) were the major constituents. The seed oil contains 31 compounds representing 100% of the total oil, with the major constituents being α -pinene (41%), α -thujene and β -pinene (13% each), sabinene, limonene and bicyclogermacrene (6% each), and myrcene (5%). These compounds are probably the most significant volatile compounds that characterize the overall scent of the two oils. They are also common ingredients in perfumes, food products, cosmetics and medicines.

Table 1. Physico-chemical properties of leaf and seed oils from *Dryobalanops aromatica* Gaertn.

Properties	Leaf oil	Seed oil
Yield [% (w/w) by fresh weight]	0.065	1.893
Colour	Clear, golden yellow	Clear, colourless
Density (d_{20})	0.893	0.853
Refractive index (n_D^{20})	1.476	1.467
Optical rotation (α_D^{20})	-10.103	-11.056

Table 2. Percentage composition and retention index (RI) of the compounds identified in the essential oils of fresh leaves and seed of *Dryobalanops aromatica* Gaertn., in order of their elution in a FSC column; tr = trace (< 0.1 %).

Peak no.	Compound	Peak area (%)		RI
		Leaves	Seed	
1	α -Pinene	6.9	40.8	1032
2	α -Thujene	2.0	12.9	1035
3	Camphene	0.1	0.3	1076
4	β -Pinene	2.3	12.7	1118
5	Sabinene	0.2	6.4	1132
6	Myrcene	1.1	4.9	1174
7	α -Terpinene	0.3	0.3	1188
8	Limonene	3.0	6.0	1203
9	1, 8-Cineole	–	0.2	1213
10	β -Phellandrene	0.3	0.7	1218
11	γ -Terpinene	1.1	0.9	1255
12	(<i>E</i>)- β -Ocimene	0.1	0.2	1266
13	<i>p</i> -Cymene	0.8	0.2	1280
14	Terpinolene	0.8	0.8	1290
15	6-Methyl-5-hepten-2-one	tr	–	1348
16	Hexanol	0.4	–	1360
17	(<i>Z</i>)-3-Hexenol	0.3	-	1391
18	α -Fenchone	0.1	–	1406
19	(<i>E</i>)-2-Hexenol	tr	–	1412
20	α - <i>p</i> -dimethylstyrene	0.2	–	1452
21	Fenchyl acetate	tr	–	1482
22	Bicycloelemene	–	0.1	1495
23	α -Copaene	0.3	0.1	1497
24	Camphor	0.6	–	1532
25	Isopinocampnone	0.1	–	1562
26	(<i>E</i>)- <i>p</i> -menth-2-en-1-ol	0.1	tr	1571
27	Fenchyl alcohol	0.2	–	1591
28	(<i>E</i>)- β -Bergamotene	0.1	–	1594
29	α -Guaiene	0.2	tr	1597
30	Terpinen-4-ol	15.0	–	1611
31	β -Caryophyllene	3.6	4.3	1612
32	Aromadendrene	0.2	0.1	1628
33	(<i>Z</i>)- <i>p</i> -menth-2-en-1-ol	0.1	–	1638
34	Alloaromadendrene	0.2	tr	1661
35	<i>p</i> -Mentha -1, 5-dien-8-ol	0.1	–	1678
36	α - Humulene	3.1	0.7	1687
37	<i>p</i> -Mentha-1, 8-dien-4-ol	tr	–	1700
38	γ -Muuroolene	0.2	–	1704
39	α -Terpineol	15.8	0.2	1707
40	Ledene	1.0	0.1	0.1
41	Borneol	0.6	-	1719
42	Verbenone	0.3	–	1725

Table 2 (Cont.). Percentage composition and retention index (RI) of the compounds identified in the essential oils of fresh leaves and seed of *Dryobalanops aromatica* Gaertn., in order of their elution in a FSC column; tr = trace (< 0.1 %).

43	Germacrene D	0.2	0.3	1726
44	Carvenone	0.1	–	1737
45	(<i>E</i>)- <i>p</i> -menth-2-en-1, 8-diol	0.2	–	1740
46	α -Muurolene	0.3	–	1740
47	α -Selinene	0.1	–	1740
48	Piperitone	0.1	–	1748
49	Bicyclogermacrene	1.7	5.9	1755
50	(<i>E,E</i>)- α -Farnesene	0.1	–	1758
51	δ -Cadinene	0.2	–	1776
52	γ -Cadinene	0.1	–	1776
53	(<i>Z</i>)- <i>p</i> -menth-2-en-1, 8-diol	0.1	–	1797
54	Myrtenol	0.1	–	1804
55	<i>p</i> -Mentha-1, 3-dien-7-al	0.1	–	1811
56	(<i>E</i>)-Carveol	0.1	–	1845
57	(<i>Z</i>)-Calamenene	0.1	–	1853
58	<i>p</i> -Cymen-8-ol	0.6	–	1864
59	Hexanoic acid	0.1	–	1871
60	α -Calacorene-1	0.2	–	1941
61	Palustrol	0.7	–	1953
62	(<i>E</i>)-12-Norcaryophyll-5-en-2-one	0.1	–	1984
63	Caryophylleene oxide	0.6	–	2008
64	Epiglobulol	0.5	–	2033
65	Humulen epoxide - I	0.1	–	2045
66	(<i>E</i>)-Nerolidol	0.1	–	2050
67	Ledol	0.6	–	2057
68	Humulen epoxide-II	0.4	–	2071
69	Unknown-I	4.0	–	2077
70	Cubenol	0.1	–	2080
71	1-Epi-cubenol	0.2	–	2088
72	Globulol	8.2	0.2	2098
73	Viridiflorol	3.8	0.1	2104
74	Spathulenol	1.0	0.1	2144
75	Neointermedeol	0.3	–	2153
76	β -Bisabolol	0.9	–	2170
77	T-Cadinol	0.4	–	2187
78	T-Muurolol	0.5	–	2209
79	δ -Cadinol	0.3	–	2219
80	Isospathulenol	0.1	–	2228
81	(<i>E</i>)- α -bergamotol	0.9	tr	2247
82	α -Cadinol	0.8	–	2255
83	Selin-11-en-4- α -ol	0.2	tr	2273
84	Caryophylla-2(12), 6(13)-dien-5- α -ol	0.2	–	2324
85	Caryophylla-2(12), 6-dien-5- β -ol	0.1	–	2392
86	Hexadecanoic acid	0.6	–	2931

α -thujene, β -pinene, limonene, γ -terpinene, β -caryophyllene, α -humulene, ledene, bicyclogermacrene, viridiflorol, spathulenol and an unknown compound were also present but in quantities $\leq 4\%$ each in the leaves, whilst only β -caryophyllene was present in similar quantity in the seed of the plants. The earlier attempt (Eaton 1925) at distillation of the leaves of this species reported that no borneol was obtained, but this study showed its presence in the leaf oil although in a low quantity (0.6%). Compounds such as camphene, terpineol and pinene which have been reported to be present in the camphor and oleo-resin of the plant (Perry 1980; Duke & Ayensu 1985) were also found in this study.

The essential oils from the seed and leaves of *D. aromatica* showed important similarities because out of the 85 identified compounds, 29 (1–8, 10–14, 23, 26, 29, 31, 32, 34, 36, 39, 40, 43, 49, 72–74, 81 and 83, see Table 2) were common in both leaves and seed although in different quantities. However, some specific compounds allowed for the differentiation of the two essential oils. Indeed, 55 compounds (15–21, 24, 25, 27, 28, 30, 33, 35, 37, 38, 41, 42, 44–48, 50–71, 75–80, 82, and 84–86) including an unknown were found only in the leaves and not in the seed, while 2 compounds (9 and 22) were found only in the seed and not in the leaves. This pattern of findings has been similarly obtained in many studies of plant species involving different organs (Rehder *et al.* 2006; Ghasempour *et al.* 2007; Bhuiyan *et al.* 2009; Chowdhury *et al.* 2009). Thus, common volatile compounds were found to be non-uniformly distributed in different organs of *D. aromatic*, whilst the different volatile compounds accumulated could be the result of various metabolic processes in the specific cells or vessels of these organs.

Chemical Classification

Table 3 shows the identified volatile compounds listed by chemical class, which to some

degree reflects their biosynthetic origin. Out of the 85 identified compounds, 5 were fatty acids and their derivatives, 79 isoprenoids and 1 benzenoid. The presence of fatty acids and isoprenoids, in particular terpenes and sesquiterpenes, had been recorded in the oleo-resin, camphor, resin and wood extract of this species (Burkill 1966; Cheung & Wong 1972; Perry 1980; Duke & Ayensu 1985; Ali & Koh 1991). In this study, the fatty acids and their derivatives were found in the leaf oil only, and were represented by C6 compounds, mainly acids and alcohols, which made up 1.4% of the oil. In plants, fatty acids are synthesized in chloroplasts from acetyl-CoA and malonyl-CoA in repetitive reactions that result in longer molecules (Cseke *et al.* 2006). The alcohols which give the characteristic 'green' note or odour of the leaves are biosynthesised from α -linolenic and linoleic acids *via* their respective hydroperoxides (Stone *et al.* 1975; Hatanaka *et al.* 1987; Hatanaka 1993).

The isoprenoids in both leaf and seed oils were mainly monoterpenes and sesquiterpenes, and their derivatives. The amount of monoterpenes and their derivatives was higher in the seed oil (87.5%) than in the leaf oil (53.4%). However, the sesquiterpenoid fractions were higher in the leaf oil (33%) than in the seed oil (12%). Previous work on the oleo-resin of this plant recorded the presence of 20% sesquiterpenes, an amount which lies in between the contents of leaf and seed oils in this study. In the leaf oil, oxygenated monocyclic monoterpenes (32%) and oxygenated bicyclic sesquiterpenes (20%) dominated whilst bicyclic monoterpenes (73%) and bicyclic sesquiterpenes (11%) formed the major isoprenoids in the seed. Most isoprenoids can be traced back to geranyl- or farnesyl- pyrophosphates (Croteau & Karp 1991). The isoprenoids are synthesized in cytosol from acetyl-CoA *via* the mevalonic pathway as well as in plastids from pyruvic acid and glyceraldehydes-3-phosphate *via* 1-deoxy-D-xylulose-5-phosphate (DOXP) and

2-C-methyl-D-erythritol-4-phosphate (MEP) (Eisenreich *et al.* 1998; Kuzuyama 2002; Dubey *et al.* 2003; Eisenreich *et al.* 2004).

The irregular terpene, 6-methyl-5-heptene-2-one, occurred in a negligible amount. Similarly, the only benzenoid, α -*p*-dimethylstyrene, was also present in a very small quantity.

CONCLUSION

This study provides the complete chemical profiles of the essential oils obtained from the fresh leaves and seed of *D. aromatica*. The essential oils of both leaves and seed of *D. aromatica* were particularly rich in monoterpenes. Sesquiterpenes were present in both oils in lower amounts whilst fatty acids and benzenoid were present in minute

Table 3. Classes of volatile compounds identified from fresh leaves and seed of *D. aromatica* Gaertn.; tr = trace (< 0.1 %)

Class of compounds	Peak area (%)	
	Leaves	Seed
Fatty acids and derivatives		
Acids (59 & 86)	0.7	–
Alcohol (16, 17, 19)	0.7	–
Total %	1.4	–
Isoprenoids		
Irregular terpene (15)	tr	–
Monoterpenes and derivatives		
Acyclic monoterpenes (6, 12)	1.2	5.1
Monocyclic monoterpenes (7, 8, 10, 11, 13, 14)	6.3	8.9
Oxygenated monocyclic monoterpenes (9, 26, 30, 33, 35, 37, 39, 44, 45, 48, 53, 55, 56, 58)	32.4	0.4
Bicyclic monoterpenes (1, 2, 3, 4, 5)	11.5	73.1
Oxygenated bicyclic monoterpenes (18, 21, 24, 25, 27, 41, 42, 54)	2.0	–
Total %	53.4	87.5
Sesquiterpenes and derivatives		
Acyclic sesquiterpenes (50)	0.1	–
Oxygenated acyclic sesquiterpenes (66)	0.1	–
Monocyclic sesquiterpenes (36, 43)	3.3	1.0
Oxygenated monocyclic sesquiterpenes (65, 68, 76)	1.4	–
Bicyclic sesquiterpenes (22, 23, 28, 29, 31, 32, 34, 38, 40, 46, 47, 49, 51, 52, 57, 60)	8.5	10.6
Oxygenated bicyclic sesquiterpenes (61, 62, 63, 64, 67, 70, 71, 72, 73, 74, 75, 77, 78, 79, 80, 81, 82, 83, 84, 85)	19.6	0.4
Total %	33.0	12.0
Benzenoid		
(20)	0.2	–
Unknown		
(69)	4.0	–

concentrations in the leaf oil only. The study concluded that *D. aromatica* was a good source of aromatic oil which contained important chemical components well-known in the flavour, fragrance, food, cosmetics and pharmaceutical industries. However, the commercial extraction of either the essential oil or favoured component(s) of these oils might not be viable due to the low yield of the leaf oil, and the infrequent fruiting and seed production pattern of the species.

ACKNOWLEDGEMENTS

The authors would like to thank the staff members of the Brunei National Herbarium of the Forestry Department for their assistance in collecting the plant materials, Dr David S. Edwards for valuable comments on the original manuscript and Mr M. Sugumaran for the photographs.

Date of submission: July 2012

Date of acceptance: February 2013

REFERENCES

- Ali, RM & Koh, MP 1991, 'Quantification of some components of the extractives of *Dryobalanops aromatica* obtained from different sources', *Journal of Tropical Forest Science*, vol. 3, no. 4, pp. 367–371.
- Ashton, PS 1964, *A manual of the dipterocarp trees of Brunei State*, Oxford University Press.
- Ashton, PS 2004, Dipterocarpaceae' in *tree flora of Sabah and Sarawak*, vol. 5, eds E Soepadmo, LG Saw & RCK Chung, Forest Research Institute Malaysia (FRIM), Sabah Forestry Department, Malaysia and Sarawak Forestry Department, Malaysia.
- Bhuiyan, MNI, Begum, J & Sultana, M 2009, 'Chemical composition of leaf and seed essential oil of *Coriandrum sativum* L. from Bangladesh', *Bangladesh Journal of Pharmacology*, vol. 4, pp. 150–153.
- Burkill, IH 1996, *A Dictionary of the economic products of Malay Peninsula*, Ministry of Agriculture and Co-operatives, Kuala Lumpur, Malaysia.
- Cheung, HT & Tokes, L 1968, 'Oxygenated derivatives of Asiatic acid from *Dryobalanops aromatica*', *Tetrahedron Letters*, vol. 41, pp. 4363–4366.
- Cheung, HT & Wong, CS 1972, 'Structures of triterpenes from *Dryobalanops aromatica*', *Phytochemistry*, vol. 11, pp. 1771–1780.
- Chowdhury, JU, Mobarok, MH, Bhuiyan, MN & Nandi, NC 2009, 'Constituents of essential oils from leaves and seeds of *Foeniculum vulgare* Mill. cultivated in Bangladesh', *Bangladesh Journal of Botany*, vol. 38, no. 2, pp. 181–183.
- Corner, EJH 1981, *Wayside trees of Malaya*, Malayan Nature Society, Kuala Lumpur, Malaysia.
- Croteau, R & Karp, F 1991, 'Origin of natural Odorants', in *Perfumes: art, science and technology*, eds PM Miller & D Lamparsky, Elsevier Applied Science, London and New York.
- Cseke, LJ, Kirakosyan, A, Kaufman, PB, Warber, SL, Duke, JA & Briemann, HL 2006, *Natural products from plants*, 2nd edn., CRC Press Taylor and Francis Group, U.S.A.
- Dubey, VS, Bhalla, R & Luthra, R 2003, 'An overview of the non-mevalonate pathway for terpenoid in plant', *Journal of Biosciences*, vol. 28, no. 5, pp. 637–647.
- Duke, JA & Ayensu, ES 1985, *Medicinal plants of China*, vol. 1, Reference Publications, Inc., Michigan, U.S.A..
- Eaton, J 1925, 'Annual Report of the chemical division for 1924', *The Malayan Agricultural Journal*, vol. 13, no. 7, pp. 179–188.
- Eisenreich, W, Schwarz, M, Cartayrade, A, Arigoïn, D, Zenk, MH & Bacher, A 1998, 'The deoxyxylulose phosphate pathway of terpenoid biosynthesis in plants and microorganisms', *Chemistry & Biology*, vol. 5, no. 9, pp. 221–233.
- Eisenreich, W, Bacher, A, Arigoïn, D & Rohdich, F 2004, 'Biosynthesis of isoprenoids via the non-mevalonate pathway', *Cellular & Molecular Life Sciences*, vol. 61, no. 12, pp. 1401–1426.
- Ghasempour, HR, Shirinpour, E & Heidari, H 2007, 'The constituents of essential oils of *Ferulago angulata* (Schlecht.) Boiss at two different habitats, Nevakoh and Shahoo, Zagross Mountain, Western Iran', *Iranian Journal of Science and Technology*, Transaction A, vol. 31, no. A3, pp. 309–312.

- Guo, SK, Chen, KJ, Weng, WL, Zhang, WQ & Yu, YQ 1983, 'Immediate effect of Kuan-xiong aerosol in the treatment of anginal attacks', *Planta Medica*, vol. 47, no. 2, p. 116.
- Hatanaka, A 1993, 'The Biogenesis of green odour by green leaves', *Phytochemistry*, vol. 34, no. 5, pp. 1201–1218.
- Hatanaka, A, Kajiwara, T & Sekiya, J 1987, 'Biosynthetic pathway for C6-aldehydes formation from linolenic acid in green leaves', *Chemistry and Physics of Lipids*, vol. 44, no. 2–4, pp. 341–361.
- Hong, LT & Abdul Razak, MA 1983, 'Antifungal properties of methanol extractive from some tropical hardwoods', *The Malaysian Forester*, vol. 46, no.1, pp. 138–139.
- Kim, YJ, Hwang, GB & Seu, YB 2005, 'Antifungal activity of Borneolum (Borneo-camphor) from *Dryobalanops aromatica* against *Malassezia furfur*', *Journal of Microbiology and Biotechnology*, vol. 33, pp. 236–239.
- Kuzuyama, T 2002, 'Mevalonate and nonmevalonate pathways for the biosynthesis of isoprene units', *Bioscience Biotechnology & Biochemistry*, vol. 66, no. 8, pp. 1619–1627.
- Perry, LM 1980, *Medicinal Plants of East and Southeast Asia: attributed properties and uses*. MIT Press, Cambridge, Massachusetts and London, England.
- Rehder, VLG, Sartoratto, A & Rodrigues, MVN 2006, 'Essential oils composition from leaves, inflorescences and seeds of *Mikania laevigata* Schutz Bip. ex Baker and *Mikania glomerata* Sprengel', *Revista Brasileira De Plantas Medicas*, vol. 8, pp. 116–118.
- Siang, ST 1983, 'Use of combined traditional Chinese and Western medicine in the management of burns', *Panminerva Medica*, vol. 25, no. 3, pp. 197–202.
- Stone, EJ, Hall, RM & Kazeniac, SJ 1975, 'Formation of aldehydes and alcohols in tomato from U-14C-labelled linoleic and linolenic acids', *Journal of Food Science*, vol. 40, pp. 1138–1141.

Evaluation of Mixture Viscosity Models in the Prediction of Two-phase Flow Pressure Drops

N. Z. AUNG^{1*} AND T. YUWONO²

Nine existing mixture viscosity models were tested for predicting a two-phase pressure drop for oil-water flow and refrigerant (R.134a) flow. The predicted data calculated by using these mixture viscosity models were compared with experimental data. Predicted data from using one group of mixture viscosity models had a good agreement with the experimental data for oil-water two-phase flow. Another group of viscosity models was preferable for gas-liquid flow, but these models gave underestimated values with an error of about 50%. A new and more reliable mixture viscosity model was proposed for use in the prediction of pressure drop in gas-liquid two-phase flow.

Key words: Mixture viscosity model; prediction; oil-water, gas-liquid two-phase flow; pressure drop; refrigerant R.134a

Over the years, studies on two-phase (gas-liquid, liquid-liquid) flows have accelerated because understanding the two-phase flow phenomenon becomes more and more important and necessary in scientific and industrial applications. In many works of research, the characteristics of two-phase flow have been investigated by using theoretical and experimental approaches. Numerous theoretical models and empirical correlations have also been developed for predicting two-phase pressure drop. However, no general model reliably predicts the two-phase flow pressure drop because of the complexity of phase interaction, motion and deformation of the interface between phases, as well as non-linearity characteristics. Therefore, by trial and error, many researchers are developing new models and testing these for predicting two-phase flow pressure drop in attempts to improve the accuracy of prediction.

The homogenous model is one of the oldest models and provides the simplest technique

for analyzing two-phase (or multiphase) flows. The homogeneous model considers two-phase flow as a single-phase flow having average fluid properties which depend upon mixture quality. Here, many averaging methods have been used to find the mixture properties (*especially mixture viscosity*) which strongly influence two-phase flow pressure drop. In a literature review, it was found that many of the mixture viscosity models were developed for use in a homogeneous two-phase flow model. Using different mixture viscosity models will result in different predictions. Although mixture viscosity models (or mixture viscosity correlations) have been extensively developed in the past, little attention has been paid to the comparison of these various models. Somchai Wongwises (2008) examined the applicability of several widely used viscosity models to pressure drop prediction in air-water flow through a 0.53 mm diameter micro channel. Awad (2008) examined the error of existing viscosity models in predicting pressure drop for various refrigerants (R12, R22, R740,

¹ Department of Mechanical Engineering, Mandalay Technology University, Myanmar

² Laboratory of Fluid Mechanics, Department of Mechanical Engineering, Institute Technology Sepuluh Nopember, Campus ITS, Sukolilo, Surabaya

* Corresponding author (e-mail: nay1572@gmail.com)

R717, etc.) in micro and mini channels, and he proposed new definitions for two-phase mixture viscosity by using an analog between thermal conductivity. The prediction of pressure drop using the homogeneous model is reasonably accurate only for bubble and mist flows because the entrained phase travels at nearly the same velocity as the continuous phase. Besides, if the density ratio (ρ_L/ρ_G) approaches 1 (i.e. nearly equal densities), the homogeneous model is also applicable for predicting pressure drop.

Previous work has studied viscosity models only for air-water two-phase flow and refrigerant two-phase flow in micro and mini channels. In pipeline-conveying systems, one of the most common but least understood phenomenon is the mixing behaviour of two immiscible liquids, especially oil and water. Accurate prediction of the viscosity of an oil-water mixture is essentially needed for the calculation of frictional pressure drop for pipeline design purposes. In addition, the reliability level of some existing mixture viscosity models should be examined, and these should be categorized in their use for liquid-liquid flow and gas-liquid flow. Some attempts have been made to compare reliabilities of mixture viscosity models for some types of refrigerants but not for R134a.

Therefore, the objective of this work is to investigate the influence of mixture viscosity models in the prediction of pressure drop for both liquid-liquid two-phase flow (oil-water) and gas-liquid two-phase flow (refrigerant, R134a) in micro-, mini- and large-diameter circular pipes.

HOMOGENEOUS TWO-PHASE FLOW MODEL

In the homogeneous model, the fluids are characterized by a fluid that effectively has suitably averaged properties of the two phases in the pipe. This is also known as the *No-Slip Model*. It is assumed that there is no velocity difference between the phases and so the two fluids flow at the same velocity.

By assuming no heat and mass transfer for the homogeneous model, the pressure gradient can be written as the sum of three pressure gradient components, namely, due to friction, gravity and acceleration:

$$-\left(\frac{dp}{dz}\right)_{total} = 2f_h \rho_h \frac{U_m^2}{2} + \rho_h g \sin(\theta) + \frac{d}{dx} \left[\rho_G \frac{U_{SG}^2}{\alpha_G} + \rho_L \frac{U_{SL}^2}{\alpha_L} \right] \quad (1)$$

Normally, the contribution of momentum pressure drop is very small. To simplify the theory in analytical predictions, momentum pressure drop in *Equation 1* will be ignored, and, for horizontal flow, pressure drop by elevation difference is zero. The void fraction based on the homogeneous model (α_h) can be expressed as follows:

$$\alpha_h = \beta_G = \frac{Q_G}{Q_G + Q_L} = \frac{U_{SG}}{U_m} \quad (2)$$

The homogeneous void fraction can also be expressed in terms of mass quality (x):

$$\alpha_h = \frac{1}{1 + \left(\frac{1-x}{x}\right) \left(\frac{\rho_G}{\rho_L}\right)} \quad (3)$$

For the homogeneous model, the homogeneous density of two-phase flow (ρ_h) can be expressed as:

$$\rho_h = \alpha_G \rho_G + \alpha_L \rho_L \quad (4)$$

or it can be expressed in terms of mass quality (x):

$$\rho_h = \left(\frac{x}{\rho_G} + \frac{1-x}{\rho_L} \right) \quad (5)$$

The mixture viscosity is defined as:

$$U_m = U_{SG} + U_{SL} \quad (6)$$

In the above equations, the required basic parameters can be calculated as follows:

$$x = \frac{G_G}{G_{tot}} \quad (7)$$

$$U_{SG} = \frac{G_G}{\rho_G} \quad (8)$$

$$U_{SL} = \frac{G_{tot} - G_G}{\rho_L} \quad (9)$$

The Reynolds number based on the homogeneous model can be expressed as:

$$Re_h = \frac{D \rho_h U_m}{\mu_h} = \frac{G_{tot} D}{\mu_h} \quad (10)$$

The required Fanning friction factor can then be calculated from Blasius correlation:

$$\left. \begin{aligned} f &= \frac{16}{Re} & Re \leq 2300 \\ f &= \frac{0.079}{Re} & Re > 2300 \end{aligned} \right\} \quad (11)$$

where, μ_h in Equation 10 is two-phase mixture viscosity. Several two-phase viscosity models proposed by different researchers are given in Equations 12–20, shown below:

Owen's model (1961) $\mu_h = \mu_L$ (12)

McAdams *et al.*'s model (1942) $\frac{1}{\mu_h} = \frac{x}{\mu_G} + \frac{(1-x)}{\mu_L}$ (13)

Lin *et al.*'s model (1991) $\mu_h = \frac{\mu_L \mu_G}{\mu_G + x^{1.4} (\mu_L - \mu_G)}$ (14)

Cicchitti *et al.*'s model (1960) $\mu_h = x\mu_G + (1-x)\mu_L$ (15)

$$\text{Dukler } et al.'s \text{ model (1964)} \quad \mu_h = \beta_G \mu_G + (1 - \beta_G) \mu_L \quad (16)$$

$$\text{Beattie and Whalley's model (1982)} \quad \mu_h = \beta_G \mu_G + (1 - \beta_G)(1 + 2.5\beta_G) \mu_L \quad (17)$$

$$\text{Fourar and Bories model (1995)} \quad \mu_h = \rho_h \left(\sqrt{xv_G} + \sqrt{(1-x)v_L} \right) \quad (18)$$

$$\text{Davidson } et al.'s \text{ model (1943)} \quad \mu_h = \mu_L \left[1 - x \left(\frac{\rho_L}{\rho_G} - 1 \right) \right] \quad (19)$$

$$\text{García } et al.'s \text{ model (2003)} \quad \mu_h = \mu_L \left(\frac{\rho_h}{\rho_L} \right) \quad (20)$$

INVESTIGATION PROCEDURE

Predicted two-phase pressure drops were calculated by using the homogeneous two-phase flow model with variation of the mixture viscosity models from *Equations 13 to 20*. For oil-water two-phase flow, the experimental data were obtained from Angeli (2006). For refrigerant (R134a) two-phase flow, data on experimental pressure drop were obtained from Kattan (1996) and Thome (2006). Details on the experimental setup and strategies of measurements are given in (Angeli 2006), (Kattan 1996) and (Thome 2006). The required fluid properties were taken from the experiments and shown in *Tables 1, 2 and 3*.

To determine the effect of the mixture viscosity models, only frictional pressure drops from the experimental data were used to compare with the predicted data. Good agreement between the experimental data and predicted data when using the well-known viscosity models was defined by having a low root mean square (rms) error.

The error (ϵ) from applying a model to each available data point is defined as:

$$\epsilon (\%) = \left| \frac{\text{Predicted} - \text{Experimental}}{\text{Experimental}} \right| \times 100 \quad (21)$$

For groups of data, the root mean square error, ϵ_{rms} , is defined as:

$$\epsilon_{rms} = \left[\frac{1}{N} \sum_{k=1}^N \epsilon_k^2 \right]^{1/2} \quad (22)$$

Table 1. Properties of oil and water at T = 25°C.

Liquid	Oil Exxsol D140 (Exxon Chemicals)	Water
Density (kg/m ³)	828	998
Viscosity (N.s/m ²)	0.0055	0.000993

Table 2. Properties of refrigerant R134a at $T_{sat} = 4^{\circ}\text{C}$

Fluid	Refrigerant, R134a (Liquid)	Refrigerant, R134a (Vapour)
Density (kg/m^3)	1282	16.7
Viscosity (N.s/m^2)	0.000254	0.000011

Table 3. Properties of refrigerant R134a at $T_{sat} = 30^{\circ}\text{C}$

Fluid	Refrigerant, R134a (Liquid)	Refrigerant, R134a (Vapour)
Density (kg/m^3)	1188	37.5
Viscosity (N.s/m^2)	0.000181	0.0000119

RESULTS AND DISCUSSION

Oil-water Two-phase Flow

Comparisons of the predicted frictional pressure gradients and published experimental data are shown in *Figure 1* and *Figure 2*. The experimental data taken from Angeli (2006) frictional pressure gradients for a mixture velocity of 1.5 m/s and volumetric oil concentration between 10% and 90%. According to his definition, the mixture viscosity models can be classified into two groups. The first group [Group I] satisfies the following conditions:

$$\left. \begin{array}{l} \text{if } x = 0 \quad \mu_h = \mu_L \\ \text{if } x = 0 \quad \mu_h = \mu_G \end{array} \right\}$$

Group I includes *Equations 13–18*.

The second group [Group II] includes *Equations 12, 19 and 20* which do not satisfy the above conditions.

The results of this work show that Group II mixture viscosity models gave fair predictions which had the same trends as the experimental data. In Group II, García *et al.*'s model (2003) had a good agreement with the experimental data. Group I mixture viscosity models has

different trends compared with the experimental data, i.e. Group I's predictions gave increasing values while the experimental data showed decreasing values with an increase in oil concentration.

Predictions by Group I models were theoretically correct. When the volumetric oil concentration becomes higher, the mixture viscosity will increase and that will raise the pressure gradient. However, the experimental data on pressure gradient decreased with an increase in oil concentration. Angeli (2006) said that the reason of the decreasing pressure gradient is because of high *in situ* water fraction at an upward inclination. Therefore the mixture viscosity is still close to water viscosity even when oil concentration becomes high. This is noteworthy for oil-water two-phase flows.

For liquid-liquid two-phase flow, García *et al.*'s model (2003) was the most appropriate one (*especially for upward inclined flow*). Unfortunately comparison of the predicted data and experimental friction pressure drops in horizontal oil-water flow could not be reported in this work. However, it is reasonable to say that the frictional drops in inclined flow and horizontal flow are not so different.

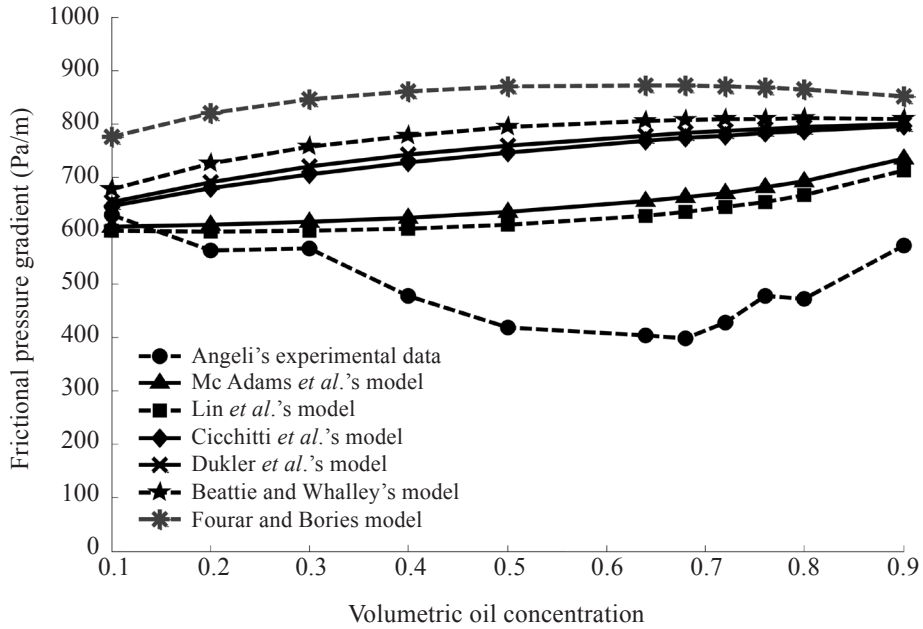


Figure 1. Predicted and experimental frictional pressure gradients for oil-water two-phase flow at $U_m = 1.5$ m/s, $+10^\circ$ inclination (Angeli 2006).

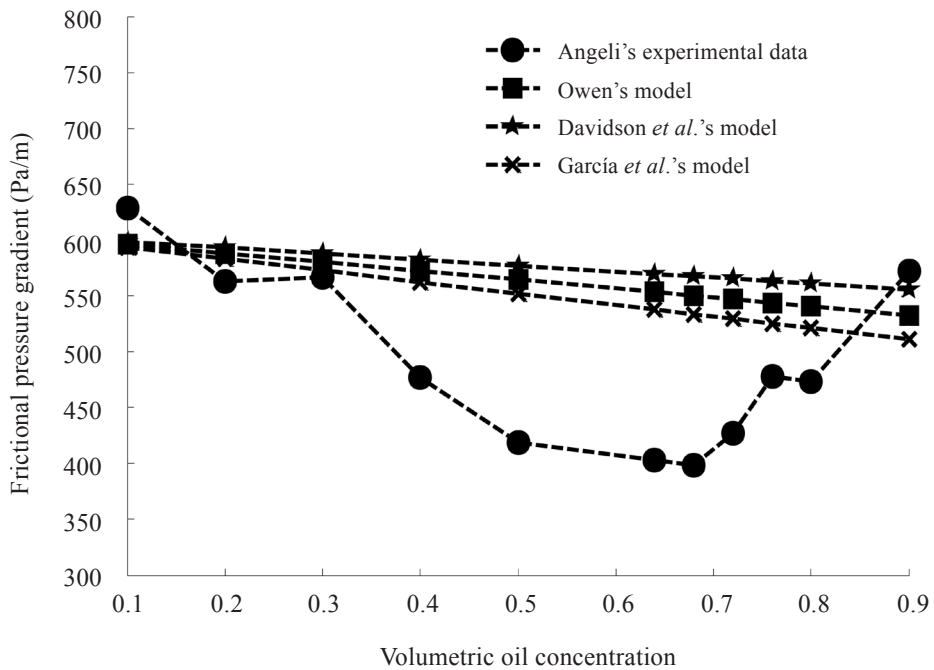


Figure 2. Predicted and experimental frictional pressure gradients for oil-water two-phase flow at $U_m = 1.5$ m/s, $+10^\circ$ inclination (Angeli 2006).

The ϵ_{rms} values of each model are shown in Table 4 in order of increasing error. It can be seen that for liquid-liquid flows with nearly the same densities (i.e. $\rho_L/\rho_G \approx 1$), Group II mixture viscosity models made good predictions. From Group I, Lin *et al.*'s model gave the smallest value of ϵ_{rms} .

From this study, it is shown that for liquid-liquid two-phase flows, making the assumption that the viscosity of the continuous phase is the same as the mixture viscosity can be considered reasonable until the medium range of dispersed phases' concentration.

Refrigerant (R134a) Flow

For refrigerant (R134a) two-phase flow, the experimental data from Kattan's work (1996) were obtained by performing experiments in 10.92 mm and 12 mm diameter circular horizontal pipes. In this study, comparisons were made with the experimental data for $D = 10.92$ mm and $G_{tot} = 300$ kg.s⁻¹.m⁻² with variations in vapour quality. The comparisons are shown in *Figure 3* and *Figure 4*. For gas-liquid flow, most of the mixture viscosity models gave underestimated values. All the mixture viscosity models in Group I had nearly the same predictions and ϵ_{rms} around 50%. For gas-liquid flow, Cicchitti *et al.*'s model (1960) and Fourar and Bories model (1995) gave

relatively better predictions although they had very high errors in their predictions for oil-water flow.

It can be observed that Davidson *et al.*'s model (1943) was not very suitable for predicting gas-liquid two-phase flow because it had a very high error term. From this definition, it can be seen that Davidson *et al.*'s model (1943) was suitable for two-fluid flow where $\rho_L/\rho_G \approx 1$. García *et al.*'s model (2003) gave very low predictions with an error of 66.64%. Therefore, Group II viscosity models (except Owen's model (1975)) are less preferable for pressure drop prediction in gas-liquid two-phase flows.

From this study, it is shown that it is convenient to use Owen's viscosity model (1961) in both liquid-liquid flow and gas-liquid flow because of it gives fair predictions for both types of flow. The ϵ_{rms} values from each viscosity model in predicting gas-liquid two-phase flow are shown in *Table 5*.

DEFINING A NEW MIXTURE VISCOSITY MODEL FOR GAS-LIQUID FLOW

In previous mixture viscosity models, the homogeneous viscosity decreases with increasing gas concentration. This gives a high error in estimation. Actually, at low gas concentrations, the viscosity of the gas has no

Table 4. ϵ_{rms} from each mixture viscosity model for oil-water flow.

No.	Mixture viscosity model	ϵ_{rms} (%)
1	García <i>et al.</i> 's model	20.3271
2	Owen's model	22.8621
3	Davidson <i>et al.</i> 's model	25.6263
4	Lin <i>et al.</i> 's model	37.8751
5	McAdams <i>et al.</i> 's model	42.7214
6	Cicchitti <i>et al.</i> 's model	63.0710
7	Dukler <i>et al.</i> 's model	64.9552
8	Beattie and Whalley's model	70.1044
9	Fourar and Bories' model	83.8308

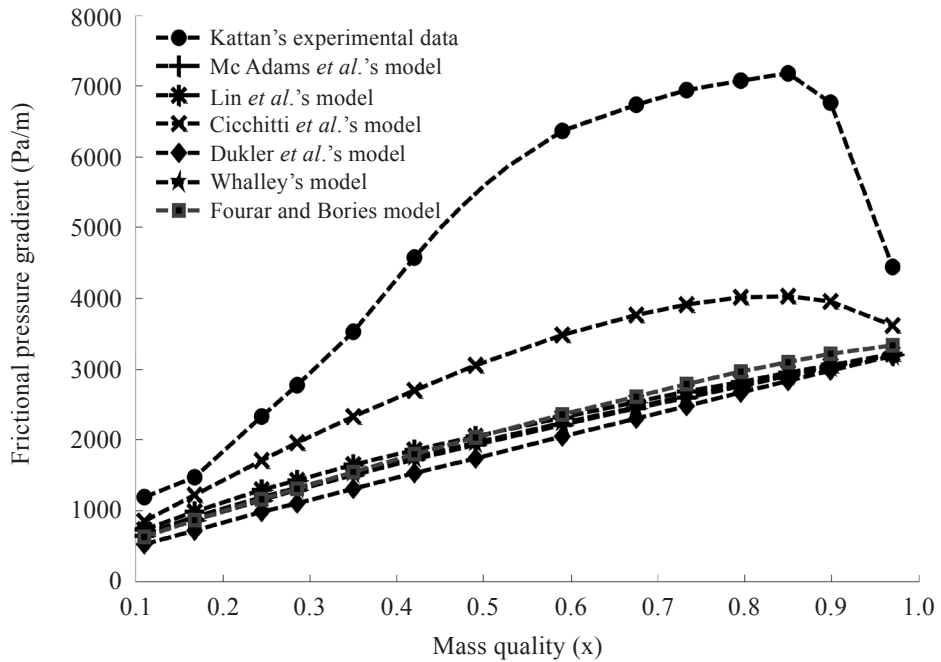


Figure 3. Predicted and experimental frictional pressure gradients for R134a two-phase flow $G_{tot} = 300 \text{ kg}\cdot\text{s}^{-1}\cdot\text{m}^{-2}$, $D = 10.92 \text{ mm}$ (Kattan 1996).

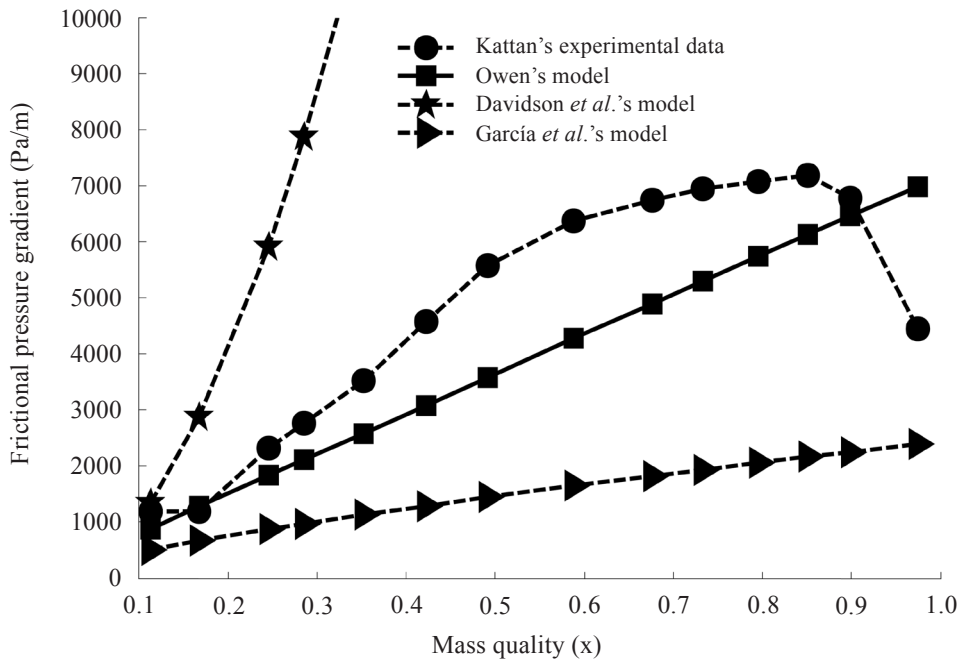


Figure 4. Predicted and experimental frictional pressure gradients for R134a two-phase flow $G_{tot} = 300 \text{ kg}\cdot\text{s}^{-1}\cdot\text{m}^{-2}$, $D = 10.92 \text{ mm}$ (Kattan 1996).

significant contribution and the viscosity of the liquid is still dominant in the mixture. Thus, Owen’s viscosity model ($\mu_h = \mu_L$) is an acceptable model for gas-liquid flow.

In fact, the homogenous flow model can reasonably be used for only bubbly flow and mist flow. Therefore, in bubbly flow, the effect of the turbulent characteristics induced by the bubbles should not be neglected. Kashinsky (1992) proved that laminar bubbly flow has turbulent characteristics and the wall shear stress becomes (1.5~3 times) higher than in single phase flow, depending on bubble size. Therefore, it is reasonable to define the new mixture viscosity model by including turbulent viscosity even if the flow is laminar.

$$\mu_h = \mu_L + \mu_T \tag{23}$$

Sato *et al.* (1975) introduced bubble-induced turbulent viscosity as follows:

$$\mu_T = C_{\mu} \rho_L \frac{k^2}{e} + C_{\mu b} \rho_L \alpha_G d_B \left| U_G - U_L \right| \tag{24}$$

By assuming homogeneous ($U_G = U_L$) flow, the second term of *Equation 24* is zero. Therefore,

$$\mu_h = \mu_L + C_{\mu} \rho_L \frac{k^2}{e} \tag{25}$$

According to the experimental data of Kashinsky (1992), $\tau_{W (two\ phase)} = (1.5 \sim 3) \times \tau_{W (single\ phase)}$ depending on bubble size; therefore, it is reasonable to make definitions that

$$\mu_h = (1.1 \sim 2) \mu_L \tag{26}$$

which is higher than Owen’s viscosity model by including turbulent viscosity from 10% to 100% . The proposed mixture viscosity model was tested to predict the data of Kattan (1996). A comparison of the data is shown in *Figure 5*, while ϵ_{rms} values are given in *Table 6*.

Table 6. ϵ_{rms} from each mixture viscosity model for refrigerant R.134a flow.

No.	Mixture viscosity model	ϵ_{rms} (%)
1	Owen’s model	28.294
2	Definition 1 ($\mu_h = 1.1 \mu_L$)	27.577
3	Definition 2 ($\mu_h = 1.3 \mu_L$)	26.572
4	Definition 3 ($\mu_h = 1.5 \mu_L$)	26.096
5	Definition 4 ($\mu_h = 1.7 \mu_L$)	26.024
6	Definition 5 ($\mu_h = 2 \mu_L$)	26.472

It can be seen that definition 4 from *Equation 26* gave the lowest ϵ_{rms} . However, *Equation 26* should be used in a limited range of gas concentrations because when the gas concentration becomes high, the viscosity of gas will be significantly involved in the mixture viscosity. Therefore, by choosing definition 4, it is desirable to define the new mixture viscosity model as follows:

$$\left. \begin{aligned} \mu_h &= 1.7\mu_L & (0 < x < 0.6) \\ \mu_h &= 1.7 [x\mu_G + (1 - x) \mu_L] & (x > 0.6) \end{aligned} \right\} \tag{27}$$

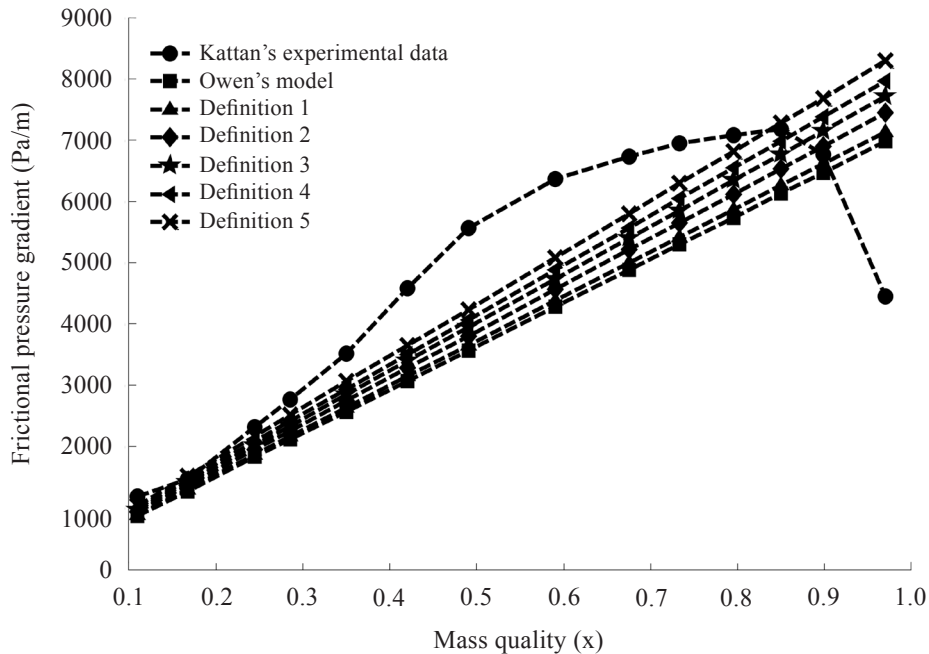


Figure 5. Predicted and experimental frictional pressure gradients for R134a two-phase flow $G_{tot} = 300 \text{ kg}\cdot\text{s}^{-1}\cdot\text{m}^{-2}$, $D = 10.92 \text{ mm}$ (Kattan 1996).

Figure 6 to Figure 8 show the comparison of the experimental data and predicted data using Owen's mixture viscosity model and the present viscosity model (Equation 27). The experimental data were taken from Kattan (1996) and Thome (2006). The data of Thome (2006) were obtained from conducting experiments for the refrigerant R134a at $T_{\text{sat}} = 30^\circ\text{C}$ in a micro channel with a diameter of 0.509 mm. It can be seen that the present mixture viscosity model gave the best predictions with the lowest ϵ_{rms} . This proves that defining the new viscosity model by taking into account turbulent viscosity is very reasonable and appropriate for gas-liquid flow. A comparison of the mixture viscosity results from some of the models are shown in Figure 6 to Figure 8. Figure 9 shows the trend of the ratio of mixture viscosity to liquid viscosity for each model according to mass quality. It can be seen that Owen's model behaved like a datum line, showing values above the datum line to be higher than liquid viscosity and those below the datum line lower than liquid viscosity.

CONCLUSION

A reliable and accurate prediction of mixture viscosity is crucial in the evaluation of pressure drop for piping system design. An underestimation can lead to an insufficiently powered design, while an overestimation can result in a higher cost for an over-powered design. Further impacts include breakdowns in operation and effects on operating costs. Thus, this study investigated the effectiveness of existing mixture viscosity models in two-phase flow pressure drop prediction. Frictional pressure drops of oil-water flow and refrigerant (R134a) two-phase flow in micro, mini and large diameter pipes were predicted by using the homogeneous model with variation of the mixture viscosity model. From the results of this study, the following conclusions were made:

- Of the two groups of mixture viscosity models, Group II is suitable for use in pressure drop predictions for liquid-liquid flow (i.e. $\rho_L/\rho_G \cong 1$). In this group, García

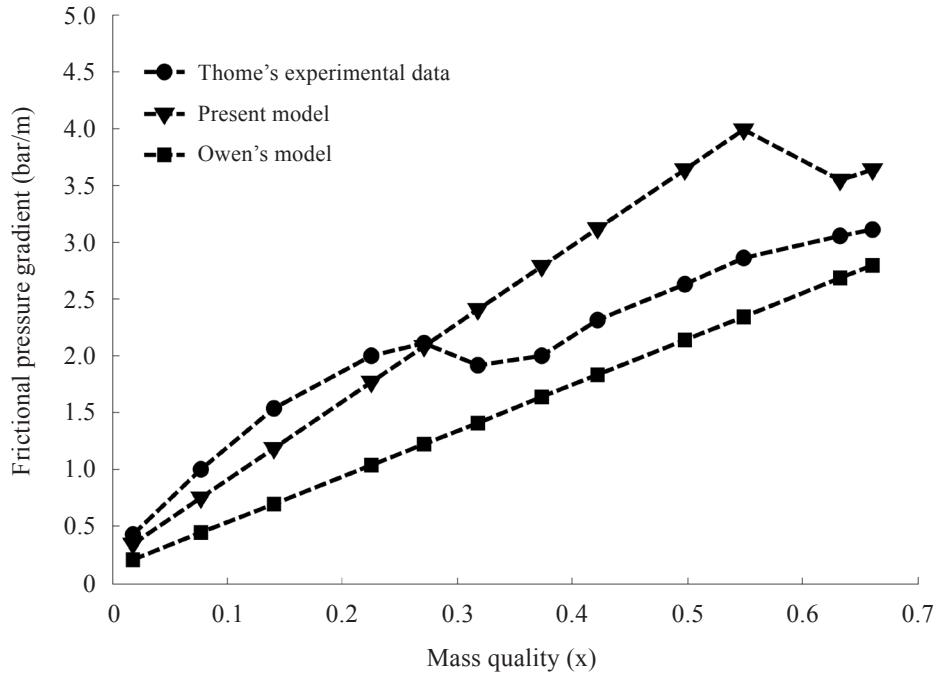


Figure 6. Predicted and experimental frictional pressure gradients for R134a two-phase flow $G_{tot} = 300 \text{ kg}\cdot\text{s}^{-1}\cdot\text{m}^{-2}$, $D = 10.92 \text{ mm}$ (Kattan 1996).

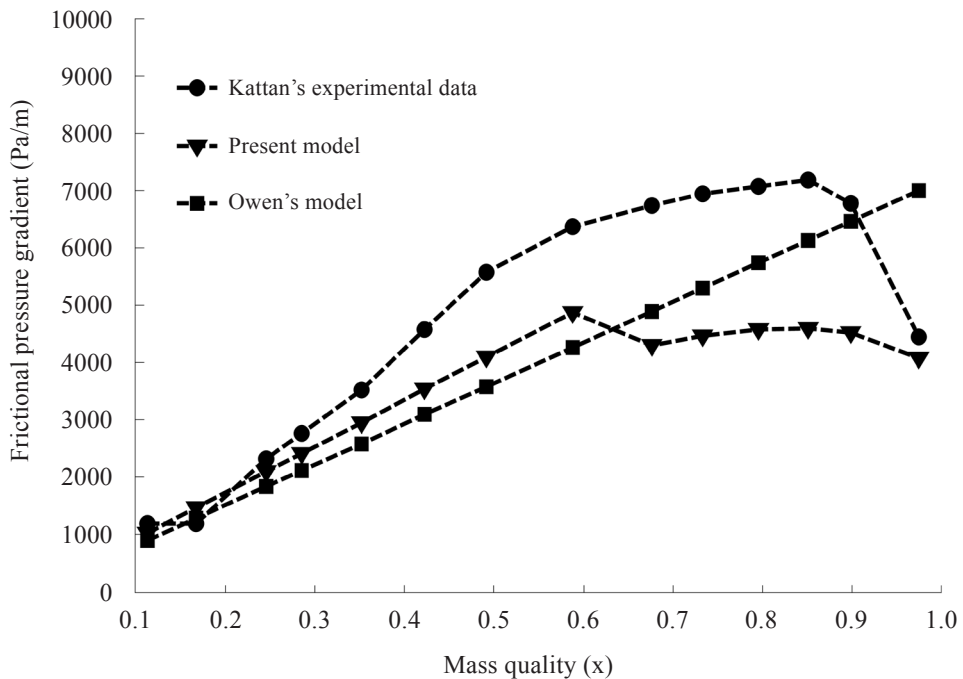


Figure 7. Predicted and experimental frictional pressure gradients for R134a two-phase flow $G_{tot} = 700 \text{ kg}\cdot\text{s}^{-1}\cdot\text{m}^{-2}$, $D = 0.509 \text{ mm}$ (Thome 2006).

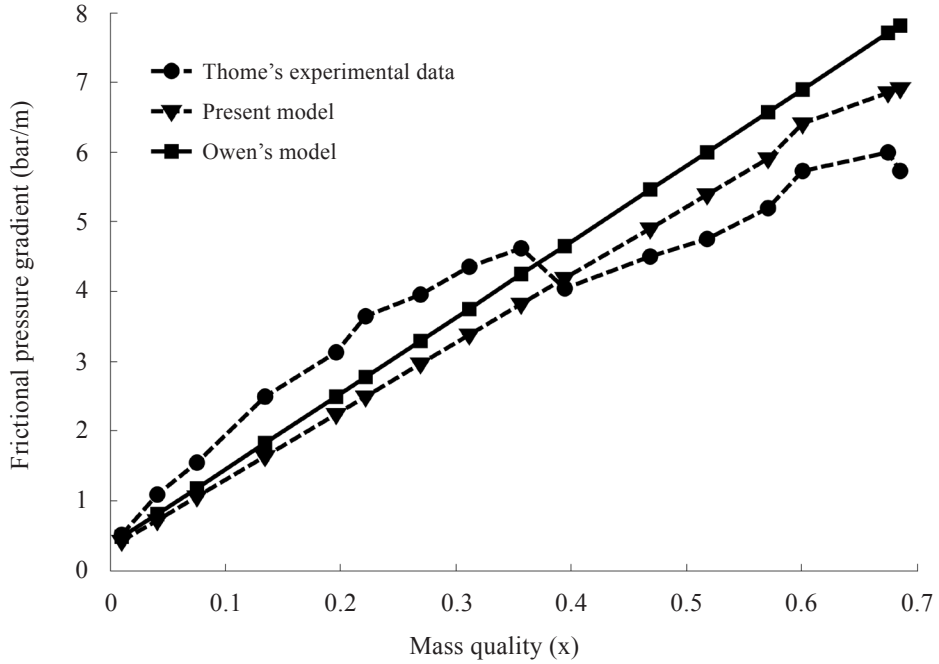


Figure 8. Predicted and experimental frictional pressure gradients for R134a two-phase flow $G_{tot} = 1000 \text{ kg}\cdot\text{s}^{-1}\cdot\text{m}^{-2}$, $D = 0.509 \text{ mm}$ (Thome 2006).

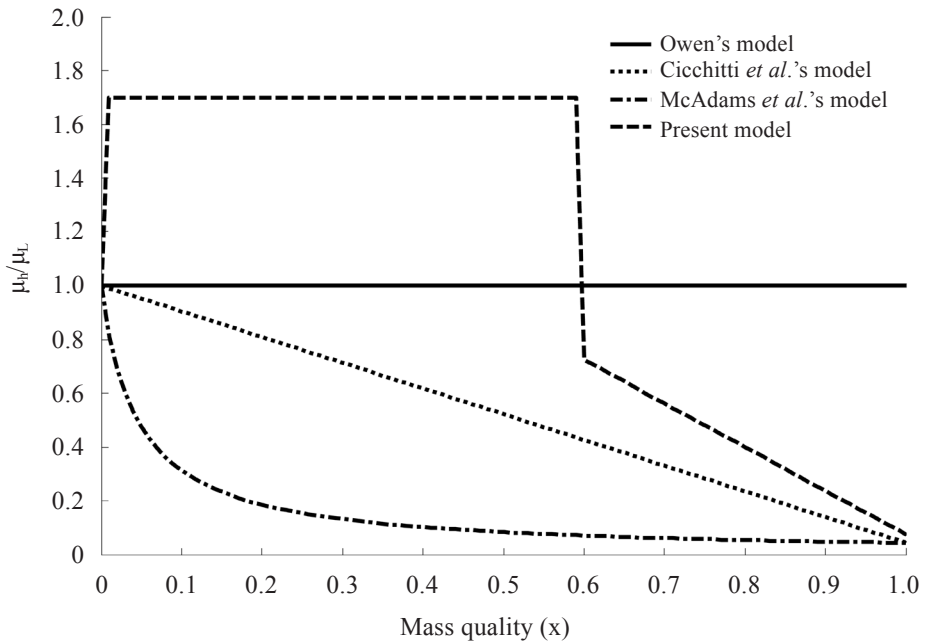


Figure 9. Comparison of mixture viscosity results from various viscosity models.

et al.'s model gives the best predictions in oil-water two-phase flow, but it has a very high error term in gas-liquid two-phase flow.

- Most of mixture viscosity models give underestimated values in predicting gas-liquid two-phase pressure drop. Except for Owen's model, Group II mixture viscosity models are not appropriate for pressure drop prediction in gas-liquid two-phase flow.
- Owen's viscosity model gives fair predictions in both liquid-liquid flow and gas-liquid flow.
- Most of existing mixture viscosity models assume that the mixture viscosity will decrease with increasing gas concentration. That is why these viscosity models give underestimated predictions. At low gas concentrations, the viscosity of gas will not contribute significantly to the mixture viscosity. Moreover, gas bubbles will create turbulent viscosity that will increase the mixture viscosity.
- The present mixture viscosity model is defined by including turbulent viscosity. It shows the best predictions in gas-liquid two-phase flow.
- The present mixture viscosity model can be strongly recommended for giving the best predictions for gas-liquid (which have nearly the same physical properties as R134a) two-phase flow at low gas concentrations.

ACKNOWLEDGEMENT

The author would like to express special thanks to his supervisor and advisor, Prof Ir. Triyogi Yuwono, DEA, for his valuable advice, patience, understanding and intellectual challenges throughout the duration of this research, and to all the members of the Fluid Mechanics Laboratory, Mesin, ITS for their support in providing facilities and great help.

Date of submission: October 2012

Date of acceptance: February 2013

REFERENCES

- Angeli, P 2006, 'Upward and downward inclination oil-water flows', *International Journal of Multiphase Flow*, vol. 32, pp. 413–435.
- Awad, MM 2008, 'Effective property models for homogeneous two-phase flows', *Experimental Thermal and Fluid Science*, vol. 33, pp. 106–113.
- Beattie, DRH & Whalley, PB 1982, 'Simple two-phase frictional pressure drop calculation method', *Int. J. Multiphase Flow*, vol. 8, no. 1, pp. 83–87.
- Cicchitti, A, Lombaradi, C, Silversti, M, Soldaini, G & Zavattarlli, R 1960, 'Two-phase cooling experiments – pressure drop heat transfer burnout measurements', *Energia Nucleare*, vol. 7, no. 6, pp. 407–425.
- Davidson, WF, Hardie, PH, Humphreys, CGR, Markson, AA, Mumford, AR & Ravese, T 1943, 'Studies of heat transmission through boiler tubing at pressures from 500–3300 Lbs.', *Trans. ASME*, vol. 65, no. 6, pp. 553–591.
- Dukler, AE, Moye, W & Cleveland, RG 1964, 'Frictional pressure drop in two-phase flow. Part A: a comparison of existing correlations for pressure loss and holdup, and Part B: an approach through similarity analysis', *AIChE J.*, vol. 10, no. 1, pp. 38–51.
- Fourar, M & Bories, S 1995, 'Experimental study of air-water two-phase flow through a fracture (narrow channel)', *Int. J. Multiphase Flow*, vol. 21, no. 4, pp. 621–637.
- García, F, García, R, Padrino, JC, Mata, C, Trallero, JL & Joseph, DD, 2003, 'Power law composite power law friction factor correlations for laminar turbulent gas-liquid flow in horizontal pipelines', *Int. J. Multiphase Flow*, vol. 29, no. 10, pp. 1605–1624.
- Kashinsky, ON 1992, 'Experimental study of "laminar" bubbly flows in a vertical pipe', *Experiments in Fluids*, vol. 14, pp. 308–314.
- Kattan, N 1996, 'Contribution to the heat transfer analysis of substitute refrigerants in evaporator tubes with smooth or enhanced tube surfaces', PhD thesis, No 1498, Swiss Federal Institute of Technology, Lausanne, Switzerland.

- Lin, S, Kwok, CCK, Li, RY, Chen, ZH & Chen, ZY 1991, 'Local frictional pressure drop during vaporization for R-12 through capillary tubes', *Int. J. Multiphase Flow*, vol. 17, no. 1, pp. 95–102.
- McAdams, WH, Woods, WK & Heroman, LC 1942, 'Vaporization inside horizontal tubes II-benzene-oil mixtures', *Trans. ASME*, vol. 64, no. 3, pp. 193–200.
- Owen, WL 1961, 'Two-phase pressure gradient', in *ASME Int. Develop. Heat Transf. Part II*, pp. 363–368.
- Sato, Y & Sekoguchi, K 1975, 'Liquid velocity distribution in two-phase bubbly flow', *Int. J. Multiphase Flow*, vol. 2, pp. 79–95.
- Thome, JR 2006, 'Adiabatic two-phase frictional pressure drops in micro-channels', *Experimental Thermal and Fluid Science*, vol. 31, pp. 673–685.
- Wongwises, S, 2008, 'An inspection of viscosity model for homogeneous two-phase flow pressure drop prediction in a horizontal circular micro-channel', *International Communications in Heat and Mass Transfer*, vol. 35, pp. 833–838.

NOMENCLATURE

Notations

C_μ	Constant in turbulent model
D	Pipe diameter (m)
d	Bubble diameter (m)
e	Turbulent dissipation rate (m^3/s)
f	Fanning friction factor
G	Mass flux (kg/m^2s)
k	Turbulent kinetic energy (m^2/s)
P	Pressure (N/m^2)
Q	Flow rate (m^3/s)
Re	Reynolds number
U	Velocity (m/s)
x	mass quality
Z	Pipe length along horizontal axis (m)

Greek Letters

α	Phase fraction
μ	Absolute viscosity (Ns/m^2)
ν	Dynamic viscosity (m^2/s)

β	Phase concentration
ϵ	Relative error
ρ	Density (kg/m^3)
θ	Inclination angle (degree)
τ	Shear stress (N/m^2)

Subscripts

B	bubble
f	friction
G	gas
h	homogeneous
L	liquid
m	mixture
SG	superficial gas
SL	superficial liquid
tot	total
T	turbulent
W	wall

Utilization of Agricultural Wastes in the Manufacture of Composite Boards

P. M. MACATANGAY¹, E. C. MAGUNDAYAO¹ AND C. A. M. ROSALES¹

Development of useful composite materials out of agricultural waste has become a desirable option in recycling. This led to the production of composite boards being used in the construction industry. In this paper, three types of available agricultural wastes in the province of Batangas — peanut shells, corn husks and banana sheath — were independently utilized in the production of composite boards. The raw materials were either air or sun dried, then crushed (for peanut shells) and extracted (for banana sheath and corn husks) before mixing with the binder. Urea formaldehyde (UF) was used as binder for peanut shells and banana sheaths while cleaned used plastic bags were chopped and mixed with corn husks before subjecting to hot compress machine. For each mat, the following proportions were used: 1000 gm banana fibres, 500 gm of UF mixed with 250 gm of water; 720 gm of crushed peanut shells, 133 gm UF with 12% resin content; 40% corn husks, 60% plastic strips by weight. The physical and mechanical characteristics like modulus of rupture (MOR), internal bond, face screw head test (FSHT) or Nail Head Pull through (NHPT), water absorption and thickness swelling were determined for each board and the results were compared to the values set by the Philippine National Standards (PNS). Based on statistical results, the corn husk-plastic composite boards conformed to all parameters in the PNS; the density, thickness swelling, IBS, and NHPT/FSHT of peanut shell-resin composite boards conformed to the PNS; and the thickness swelling, density, MOR and NHPT/FSHT of the banana sheath-UF composite boards conformed to the PNS.

Key words: agricultural wastes; composite boards; peanut shells; corn husks; banana sheath; urea formaldehyde

Growing concern for waste minimization led the construction industry to consider the use of agricultural waste in the production of building materials. The Philippines, being an agricultural country produces considerable amount of agricultural waste. As of 1999, generation of 40 million metric tons of agricultural wastes was documented by the Department of Energy (Baconguis 2008). This includes wastes from sugarcane, coconut, corn, rice and logs. If such waste is not be utilized, it will cover a large area of landfill.

Thus, the idea of using agricultural wastes as a renewable resource became an optimistic option to minimize this waste. Different types of agricultural waste are viable for a wide variety of products including paper, textiles, other fibre-based materials and wood-based panels such as fibreboards and particleboards (Magundayao *et al.* 2006; Macatangay 2010).

Composite panels made from agricultural materials are in the same product category as wood-based composite panels and include

¹ Faculty of the Department of Civil and Environmental and Sanitary Engineering, Batangas State University, Governor Pablo Borbon Main Campus II, Batangas City, Philippines 4200

* Corresponding author (e-mail: pauline_mac_2000@yahoo.com; c.magi@yahoo.com; cristinaamor@yahoo.com)

low-density insulating board, medium-density fibreboard, hardboard, and particleboard. More so, composite panel binders may be synthetic thermosetting resins or modified naturally-occurring resins like tannin or lignin, starches, thermoplastics, and inorganics (Rowell 1996).

Strength properties as well as other characteristics suited for their intended uses or application for various construction materials are prescribed by the Philippine National Standard (PNS). These are approved by the Bureau of Product Standards. PNS requirements for particle boards are shown in *Table 1*.

In Batangas State University, the Department of Civil Engineering conducted independent studies on the utilization of agricultural wastes available in the province. These studies focused on the use of corn husks, peanut shells and banana sheath as main components of composite boards.

Corn Husk

As of 2008, approximately 2,490,000 hectares of land in the Philippines were utilized for corn production area (Philippines Agriculture 2003–2009). Farmers typically leave husks and stalks behind in the fields as waste materials. According to Ohio State University, approximately 50 percent of the weight of the total corn plant is residue, consisting of stalk, leaf, cob and husk. In fact, 10% of dry matter residue came from corn husk (Myers 2009).

Corn husk is 80%–87% cellulose material. Its tensile properties show that corn fibre has

the unique advantage of moderate strength but with higher toughness, low modulus and higher elongation (Reddya & Yang 2005) which makes it comparable to existing fibres used for the production of fibreboard.

Peanuts Shell

Peanuts are very popular in the Philippines but not much attention is given to this crop for research and development. Almost 35,000 metric tons are harvested each year (Palomar 1998). The shells, which are biodegradable and absorbent, can be utilized as animal food filler, absorbents, or carriers for pesticides or fertilizers, although they are often simply landfilled (Bieak & George 2003; “Hulls” AgTech 2002).

Dried, ground peanut hulls were found to contain 34.56% lignin, 39.42% cellulose, 73.98% acid detergent fibre and 86.16% neutral detergent fibre (Childs & Abajian 2006). This characteristic is comparable to wood which is composed of fibres of cellulose (40%–50%) and hemicellulose (15%–25%) held together by lignin (15%–30%), 60% crude fibre, 7% protein and 3% ash (University of Minnesota Extension N.D.).

Banana Sheath

As of 2004, 5.9 million farm households were depending on banana as their source of income. Banana is still the leading fruit crop in terms of area, volume and value of production. The national average yield is 9.4 tons per hectare while corporate plantations produce 40 tons

Table 1. Particleboard properties set by the Philippine National Standards (1987).

Type	MOR (Min- (kg/cm ²))	IB (Min- (kg/cm ²))	FSHT/Density NHPT (kg) (g/cc)	WA (Max-%)	TS (Max-%)	
200	180	5	30–50	0.4–0.8	30	20
150	140	3	30–50	0.4–0.8	30	20
100	80	2	30–50	0.4–0.8	30	20

per hectare. It is a widely grown fruit in the country, planted as a component of farming system or as a main crop in large plantations in Mindanao. It is an important source of income for small farmers who constitute 80% of the banana growers (Rivera 2004).

Banana has different plant parts that could be good sources of various industrial products, aside from its fruit, its main product. The plant's *psuedostem* or trunk contains fibre that can be manufactured into rope, sack and mat. Pablo (1975) cited in his study that banana stalk is a potential source of material for the production of boards.

OBJECTIVES

This study aims to present the characteristics of composite boards produced using agricultural waste. Specifically, the study aims to:

- Present the individual characteristics of composite boards in terms of their (a) physical characteristics, and (b) mechanical properties
- Compare the properties of the agricultural waste composite boards with those prescribed by the Philippine National Standard (PNS).

MATERIALS AND METHODS

Each of the materials was collected from the locality: corn husks were gathered from Alitagtag, Batangas; peanut shells from peanut butter manufacturing industry in Batangas City; banana stalks were harvested from a small scale banana plantation in Batangas. These materials were sorted cleaned and dried.

Different binding agents were used in the composite boards. Corn husk fibreboard used waste plastics as binding agent while for the peanut shell particle board and banana sheath fibreboard, urea formaldehyde (UF) was used.

Banana fibres were extracted from the trunks which were soaked in water for a week, by pounding using a wooden mallet. The fibres were air dried for one full day. A set of comblike row of pins were used to separate the fibres. For five minutes the fibres were oven dried at 100°C then cut into 5 cm long pieces before mixing with UF and shaped into 300 mm by 300 mm mat. For each mat 1000 gm of fibres were used with 500 gm of powder UF mixed with 250 gm of water.

Peanut shells were sun dried until they became brittle and crushed using an electric food processor. Mats were formed from a mixture of 720 grams of crushed peanut shells and 133 grams of UF with 12% resin content.

Corn husks were sun dried for three days at approximately 30°C – 35°C temperature and then cut into about 5 mm wide and 40 mm long pieces and mixed with dry plastic strips of the same size. A 40% – 60% proportion by weight was considered in forming the 30 cm × 30 cm × 1.2 cm boards.

The moulded mats were separately placed in the Type VH2-749 Kitagawa hot press machine for about 20 minutes at a temperature of 150°C to achieve a thickness of 12 mm. Before testing, the boards were set aside for approximately three days then cut into 5 cm × 5 cm specimen sizes. A 5-ton Shimadzu Type RH10 Universal Testing Machine was used to test the modulus of rupture, internal bond strength and nail head pull through of the specimens.

Figure 5 shows the process of production of the composite boards. This process was recommended and implemented by Forest Products Research and Development Institute (FPRDI), an agency under the Department of Science and Technology (DOST) in Los



Figure 1. The hot compress machine used to form the boards.



Figure 4. Test for screw holding capacity.



Figure 2. Test for internal bond strength.



Figure 3. Test for modulus of rupture.

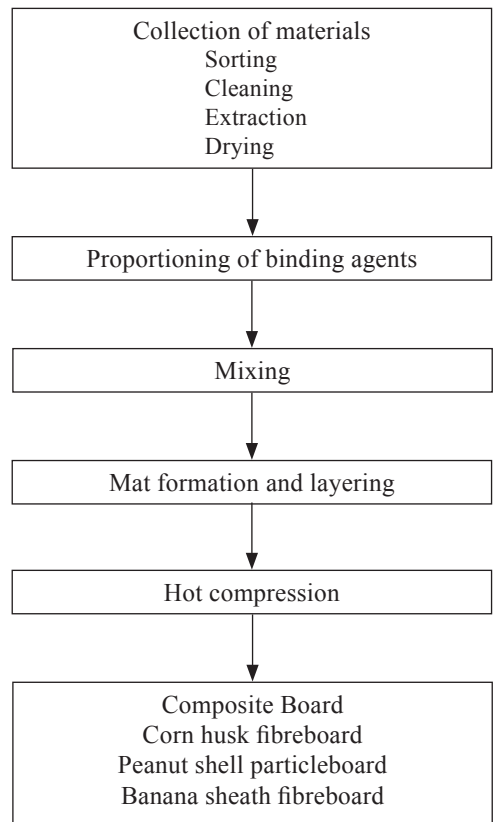


Figure 5. Composite boards production process.

Baños, Laguna, Philippines for the production of composite boards. This is also where the production and test procedures were done for the three boards.

Each board utilized different proportions of binding agents. *Table 2* shows the proportioning of materials and the binding agent used.

Property Testing and Analysis

To determine the different characteristics of the specimens produced, the following tests and analyses were conducted. Test procedures were patterned from the Philippine National Standards for Composite Boards (PNS 26). Tests performed are shown below.

Physical properties. The process determines the length, width, thickness, mass and density of the boards. The physical properties were determined using a caliper and an analytical balance.

Modulus of rupture (MOR). The MOR test was performed in order to determine the strength against bending using the Universal Testing Machine (UTM). The specimen’s dimensions were taken and then, force was applied using the UTM. The reading from the UTM determined the load capacity of the board.

The MOR, or bending strength, was then obtained using the formula:

$$MOR (kg/cm^2) = \frac{3P \times S}{2W \times T \times H^2} \tag{1}$$

where,
P = Ultimate load (kg); *S* = Length or span (cm); *W* = Width (cm); *T* = Thickness (cm).

Internal bond strength (IB). Internal Bond is a mechanical property of materials referring to the tensile strength perpendicular to the plane of the board. IB measured the quality of the particle-to-particle bonding.

The IB Test was computed using the formula:

$$IB (kg/cm^2) = \frac{P}{A} \tag{2}$$

where,
P = Load (kg); *A* = Area of test piece; = Length × Width.

Face screw head test (FSHT) / Nail head pull through (NPHT). The FSHT or NHPT determines the capacity of the board to hold a screw. This test was done by fastening two screws from the surface on both sides until it reached the bottom of the board and then subjected to a pulling force from the UTM. The screws were drawn vertically from the sample.

Table 2. Percentage of binding agent per type of board.

Agricultural waste	Binding agent	Percentage (By desired density)
Corn husk	Waste plastics	60% Plastics
Peanut shell	UF	12% resin content
Banana sheath	UF	47 % UF

The UTM showed the force required to do that. The purpose of using the screw was for its mechanical ability, the ability to pass through a surface just by turning it, making it much better to use than a nail.

The FSHT was determined using the formula:

$$\text{FSHT (kg)} = \frac{P_1 + P_2}{2} \quad (3)$$

where:

P_1 = Load on one side (kg); P_2 = Load on the opposite side (kg).

Thickness swelling (TS) and water absorption (WA). TS and WA measure the amount of water absorbed by the boards after 24 hours of soaking. The weight and thickness of each specimen were measured before submerging them in water. After soaking, the specimens were then measured again to determine the amount of water absorbed.

TS was determined using the formula:

$$\text{TS (\%)} = \frac{T_f - T_i}{T_i} \times 100 \quad (4)$$

where,

T_f = Final thickness; T_i = Initial thickness.

WA was determined using the formula:

$$\text{WA (\%)} = \frac{W_f - W_i}{W_i} \times 100 \quad (5)$$

where

W_f = Final weight; W_i = Initial weight.

For the comparison of the parameters MOR, IB, FSHT/NPHT, thickness swelling and water absorption; the statistical tool used was one tailed *t*-test, considering average value equivalence or non-equivalence to standard value, upper and lower bound tailed *t*-test were considered depending on the value of the PNS.

RESULTS AND DISCUSSION

The observed physical properties of the three different boards did not vary significantly. Both the banana sheath and corn husks boards had smooth surfaces while the peanut shell board was slightly rough; all boards reveal the colour of the materials used and were compact with plane surfaces.

For the banana sheath and peanut shell boards, the colour of the raw materials were evident since the binding agent used was colourless. The differing colours of the plastic strips in the cornhusk board dominate although the husk strips are also observed.

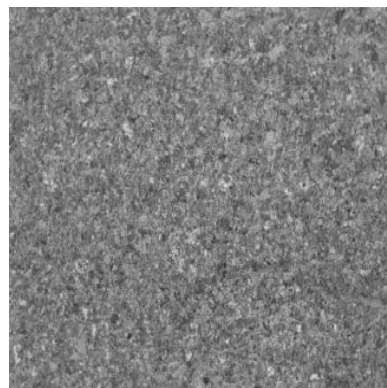
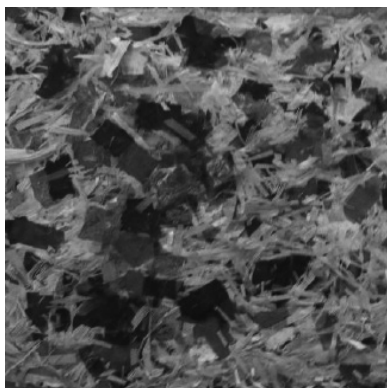


Figure 6. Samples of the composite boards: (Left) corn husks board, and (Right) peanut shells board.

The mechanical properties of the boards are shown in *Table 3* indicating the values obtained from the tests as compared with the PNS specifications for Type 100 particle board and the statistical comparison in graphical form can be seen in Figures.

Banana Sheath Fibreboard

For the average density of 0.6451 g/cc, a 0 *p*-value for the upper bound tailed *t*-test was obtained indicating the probability of achieving a value greater than 0.4 g/cc and a *p*-value of 1.000 for the upper bound tailed *t*-test was obtained indicating a value not greater than 0.8 g/cc. The statistical results for the density indicated conformance to the PNS in terms of density. The banana sheath board after being soaked in water for 24 hours, obtained an average of 44.66% water absorption which was greater than the maximum amount set by the PNS as depicted on the *p*-value of 0.016 for the upper bound tailed *t*-test, an indication of non-conformance to PNS. A

consistent average value of 14.29% thickness swelling was obtained, which was below 20%, the maximum set by the PNS for Type 100. In terms of strength, the board resisted an average 55.33 kg of load in the NHPT having a *p*-value of 0.022 for the upper bound tailed *t*-test indicating a non-probable equivalence to 30 kg and greater than 30 kg, and a *p*-value of 0.216 for upper bound tailed *t*-test indicating probable non-equivalence to 50 kg and not greater than 50 kg. In general, the NHPT for the banana sheath fibreboard conformed to the PNS. The MOR obtained an average value of 213.6 kg/cm², which conformed to the PNS (minimum of 80 kg/cm²) as reflected by 0.019 of *p*-value for upper bound tailed *t*-test. However, in the IB test, the banana sheath fibreboard obtained 1.0367 kg/cm² less than to the standard minimum value of 2 kg/cm². Based on the statistical results, a probable non-equivalence to 2 kg/cm² or not greater than the said value was concluded as depicted by the *p*-value of 0.996 upper bound tailed *t*-test indicated a non-conformance to PNS.

Table 3. The physical properties of the composite boards.

Physical properties	Banana sheath	Peanut board	Corn husk	PNS
Surface texture	Smooth	Slightly rough	Smooth	–
Material integrity	Compact with plane surface	Compact with plane surface	Compact with plane surface	–
Colour	Light brown	Light brown	Multicoloured due to plastic used	–
Proportion	57/43 UF	12% UF resin content	40% corn / 60% plastic husk by weight	–

Table 4. The mechanical properties of the composite boards.

Mechanical properties	Banana sheath	Peanut board	Corn husk	Standard for type 100
Density (g/cc)	0.6451	0.6565	0.6867	0.4 – 0.8
Water absorption (%)	44.66	72.05	29.29	30 (max)
Thickness swelling (%)	14.29	13.474	5.597	20 (max)
NHPT/ FSHT (kg)	55.33	30.83	26.33	30 (min)
Internal bond (kg/cm ²)	1.0367	2.396	2.22	2 (min)
Modulus of rupture (kg/cm ²)	213.6	46.57	162.1	80 (min)

Peanut Shell Fibreboard

The average density of the peanut shell board samples that were subjected to the different tests was 0.0.6565 g/cc with a p -value of 0 for the upper bound tailed t -test for the lower standard value of 0.4 g/cc and p -value of 0 for the lower bound tailed t -test . The statistical results indicates the probability of the average density within the PNS 0.4–0.8 g/cc. The average water absorption obtained was 72.05% with a p -value of 0.002 for the upper bound tailed t -test indicating a probability of the value greater than 30%, an indication of non-conformance to PNS. The thickness swelling obtained was

13.474% with a p -value of 0.011 for the lower bound tailed t -test . The thickness swelling for the peanut shell fibreboard conformed to PNS. The WA of the board was quite high as compared to the standard maximum value of 30%; in contrast with the TS result where the maximum value was 20%. Meanwhile, the NHPT/FSHT, IB and MOR results obtained 30.83 kg, 2.396 kg/cm², and 46.57 kg/cm², respectively. The statistical results for the NHPT indicates a p -value of 0.444 for the upper bound tailed t -test in comparison with the lower limit standard and a p -value of 0.033 for the lower bound tailed t -test in comparison

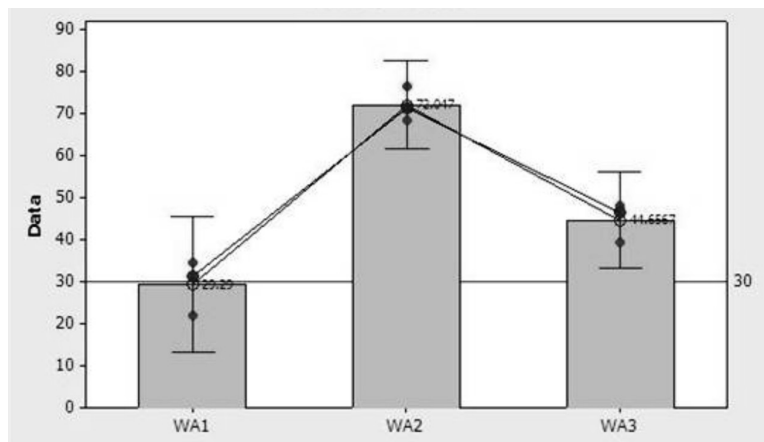


Figure 7. Statistical confidence interval for water absorption (%).

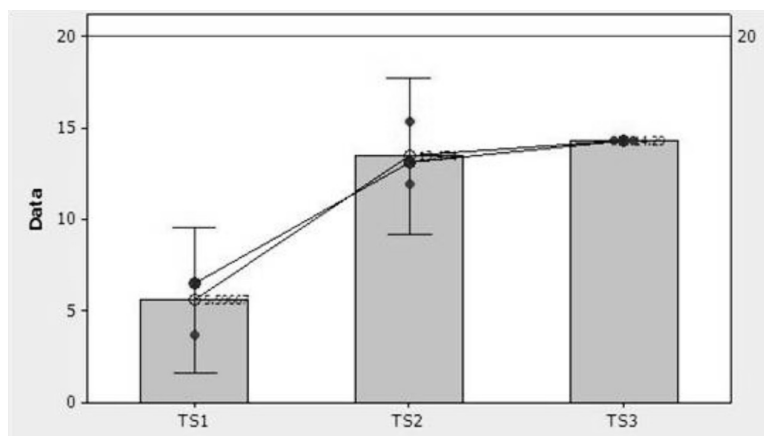


Figure 8. Statistical confidence interval for thickness swelling results (%).

Nomenclature:

Subscripts

- 1 – Corn husk – Plastic composite boards
- 2 – Peanut shell – Resin composite boards
- 3 – Banana – UF composite boards
- WA – water absorption (%)
- TS – thickness swelling (%)
- D – density (g/cc)
- IBS – Internal bond strength (kg/cm²)
- MOR – Modulus of rupture (kg/cm²)
- FSH – Face Screw Head Test or Nail Head Pull Through (kg)

with the upper limit standard. The IB statistical evaluation obtained a p -value of 0.305 to check for equivalence of the average value to that of the minimum value of the standard. This indicated a probable equivalence to 2 kg/cm². The MOR indicates a p -value of 0.004 for the lower bound tailed t -test indicated a probability of lesser value with the standard or non conformance to PNS for type 100 boards.

Corn Husks Fibreboard

The corn husks board samples tested had an average density of 0.6867 g/cc with a p -value of 0 for the upper bound tailed t -test for the comparison with the lower limit standard and a p -value of 0 for the lower bound tailed t -test for the comparison with the upper limit standard. The density of the corn husks board conformed to the PNS. As for the WA, an average value

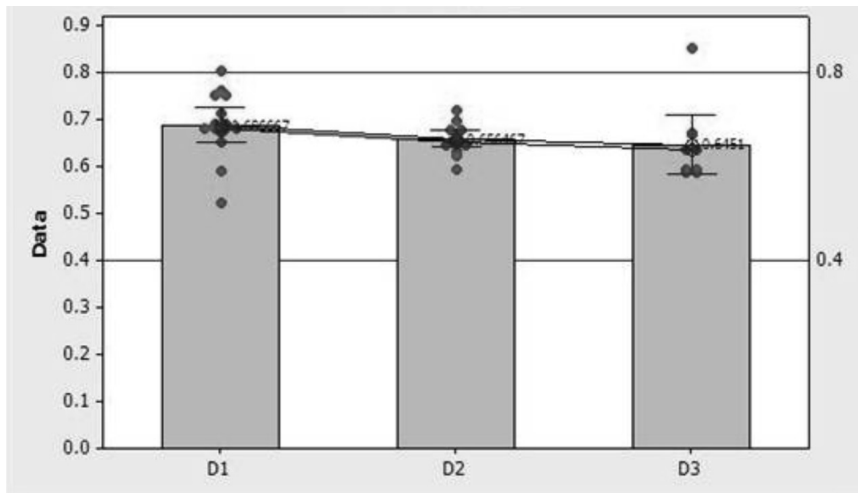


Figure 9. Statistical confidence interval for density (g/cc).

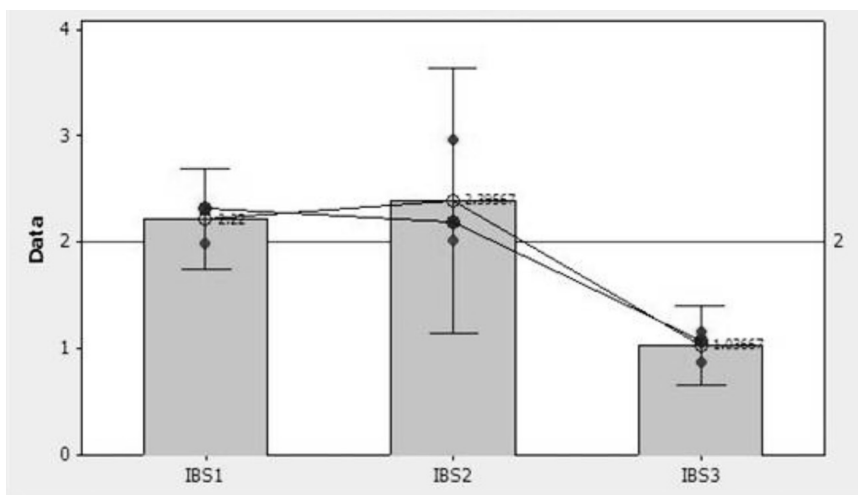


Figure 10. Statistical confidence interval for internal bond strength (kg/cm²).

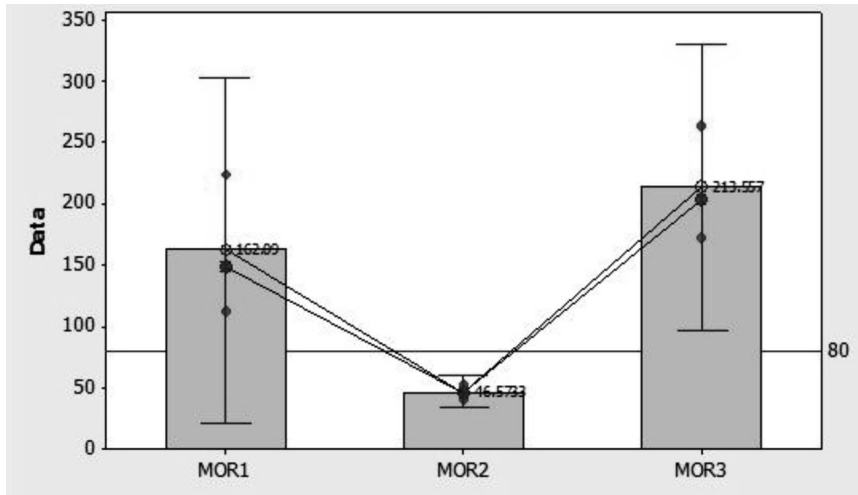


Figure 11. Statistical confidence interval for modulus of rupture (kg/cm^2).

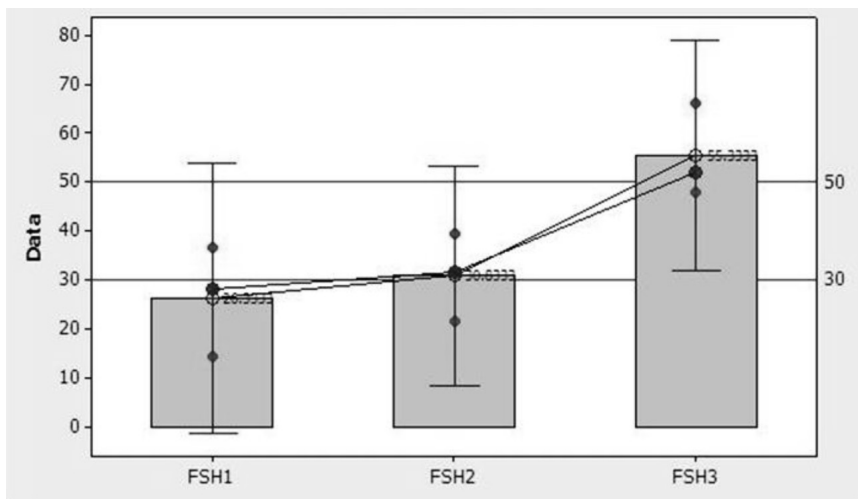


Figure 12. Statistical confidence interval for face screw head test or nail head pull through (kg).

of 29.29% was obtained with a p -value of 0.868 based on the statistical comparison being equivalent or not equivalent to the standard indicated probable equivalent to 30% maximum value, conforming to the PNS. On the case of thickness swelling, an average value of 5.597% was obtained with a p -value of 0.002 for the lower bound tailed t -test by comparison with

the maximum value of 20%. FSHT/NHPT was 26.33 kg, IB was $2.22 \text{ kg}/\text{cm}^2$, and the MOR was $162.1 \text{ kg}/\text{cm}^2$. A p -value of 0.312 was obtained for FSHT/NHPT for the one tailed t -test for the evaluation of the equivalence of the average value with that of the lower limit standard, 0.184 was obtained for IB for the one tailed t -test for the evaluation of the equivalence

of the average value with that of the minimum standard, and 0.129 for MOR for the one tailed *t*-test for the evaluation of the equivalence of the average value with that of the minimum standard.

The banana sheath board was very strong against rupture followed by the cornhusk board while the peanut board passed the standard value for the test with only a slight margin. However, with respect to internal bond, the peanut shell board is stronger than the other two. The banana sheath and peanut shell boards had almost the same resistance against nail head and face screw pull through. The corn husks board, when soaked in water did not swell as much as the other two boards, its water absorption falling within the range for Type 100. Only the corn husk-plastic composite boards conformed to standards for all parameters. The peanut shell-resin composite boards conformed in density, thickness swelling, IB, and NHPT/FSHT; while, the banana sheath-UF composite boards conformed in thickness swelling, density, MOR and NHPT/FSHT.

CONCLUSIONS

Based on the results of the tests conducted, the following conclusions were drawn:

1. Agricultural wastes such as banana sheath, peanut shells and corn husks could be used as alternative materials in the production of particleboard.
2. The boards produced from these materials could be used as Type 100 particleboard.
3. The boards' relatively high water absorption could limit their use to dry condition applications such as shelves, cabinets, partition walls or office tabletops and the like. However, the tested boards were bare in contrast to the commercially-used boards which were already laminated when put into service.

RECOMMENDATIONS

From the stated conclusions, the researchers proposed the following recommendations:

1. Commercial production of any or all of these boards could be pursued in conjunction with other government thrusts or programme such as waste minimization.
2. Appropriate binder in line with the objectives of using agricultural waste for material production could be considered for the commercial production of the boards: face screw holding capacity for corn husk board could also be enhanced by better binder.
3. Production process could be standardized to address the strength-deficiencies of the boards. Reducing the individual fibre length of the banana sheath could also increase the internal bond strength of banana sheath board.
4. Pursuing the commercial feasibility or production of the boards could be turned over by Batangas State University to the industry in order to effect the benefits possible from the use of the subject agricultural wastes.

Date of submission: October 2012

Date of acceptance: February 2013

REFERENCES

- Baconguis, SR 2008, 'Charcoal briquettes: fueling viable micro-financed and community-based livelihood enterprise', *4th National Biotechnology Week Institute of Small-Scale Industries (ISSI)*, University of the Philippines, Diliman, Quezon City, Philippines, viewed September 2009, <<http://emb.gov.ph/nswmc/alt/bio/Charcoal%20Briquettes.PDF>>.
- Bieak, N & George, BR 2003, Utilization of peanut shell fibres in non-woven erosion control materials, <http://www.india.org/subscrip/inj03_4/p60-65-george.pdf>.

- Childs, E & Abajian, A 2006, 'Physico-chemical characterization of peanut hull as a potential fibre additive', *Journal of Food Science*, vol. 41, no. 5, pp. 1235–1236.
- "Hulls" AgTech 2002, <<http://www.goldenpeanut.com/hulls.htm>>.
- Macatangay, PM 2010, 'Sugar cane bagasse as an alternative raw material in the production of fibre-cement board', in *Network of Calabarzon Educational Institutions Research Forum*, Batangas City, Philippines.
- Magundayao, EC, Mercado, LG & Paral, CC 2006, 'Utilization of banana sheath as raw material in the production of fibreboard', undergraduate thesis, Batangas State University, Batangas City, Philippines.
- Myers, DK 2009, 'Extension agronomist emeritus, forages, harvesting corn residue', viewed September 2009, <<http://ohioline.osu.edu/agfact/0003.html>>.
- Pablo, AA, Ella, AB, Perez, EB, Casal, EU 1975, 'Manufacture of particleboard using mixtures of banana stalk (saba, musa, compress blanco) and kaatoan bangkal (*Athocephalos chinenses* (Rich) Ex. Walp.) wood particles', *Forpride Digest*, vol. 4, pp. 36–44.
- Palomar, MK 1998, 'Peanut in the Philippine food system: a macro study', <<http://www.lanra.uga.edu/peanut/download/report1.pdf>>.
- Philippine Agriculture Stats, (nd), 'Usage implies agreement with terms', <http://www.nationmaster.com/red/country/rp-philippines/agr-agriculture&b_cite=1>.
- Reddya, N & Yang, Y 2005, 'Properties and potential applications of natural cellulose fibres from cornhusks', *Green chem.*, Royal Society of Chemistry vol. 7, pp. 190–195, <http://www.rsc.org/delivery/_ArticleLinking/DisplayArticleForFree.cfm?doi=b415102j&JournalCode=GC>.
- Rivera, RA (2004), 'Banana production and marketing', <http://hvcc.da.gov.ph/pdf/banana_phil_prodn_market.pdf>.
- Rowell, RM 1996, 'Paper and composites from agro-based resources', eds RM Rowell, RA Young, & Rowell, J, in *Properties of composite panels*, JA Youngquist *et al.*, Chap 9, CRC Press.
- University of Minnesota (nd), 'Lesson 1: tree growth and wood material at university of minnesota extension', <http://en.wikipedia.org/wiki/Wood#cite_note-3>.

CONTRIBUTIONS TO THE JOURNAL

Contributions from academics, policy makers, research personnel and managers in public institutions as well as those in private organizations and industry are welcome. However, it is required that manuscripts submitted to the Journal should not have been published and will not be simultaneously submitted or published elsewhere. Research papers must also be factual and original.

Contributions to the Journal will normally include original research work, papers on science and technology policy, and technical notes and communications. As the Journal is a prime source in information on science and technology for development, contributions that fall within the following areas are particularly welcome:

- Science and technology policy
- Original research work; and
- Technical notes and communications.

MANUSCRIPT PREPARATION

Manuscripts should be prepared in Microsoft Word 6.0 and above. Two copies of the manuscripts on A4-size paper and a soft copy on cd should be provided. The manuscript should not exceed 5000 words and specialist terminology and footnotes should be avoided. Each paper should be provided with an abstract of about 150 words, reporting concisely on the purpose and result of the paper. All papers will be published in English. The names(s) of the authors(s) should only appear on the title page which will be detached from the paper before the referees comments are invited.

Mathematical analysis and statistical data should be placed in appendices whenever possible. Numbered tables, figures and illustrations should have their intended position in the printed text clearly indicated. Photographs in black and white should be printed on glossy paper or scanned into text at the intended position. For illustrations, the original and one copy should be provided, if the illustration is not scanned into the text. Similarly, line drawings should either be provided in soft copy or be in a form suitable for reproduction, in Indian ink, with lettering, etc., completed.

References, or citing, should follow the Harvard author-date system. The in-text reference should contain: the author's or editor's family name (or organization responsible); year of publication; page number if appropriate and where available. The bibliography at the end of the article should be arranged alphabetically. Authors are responsible for checking and accuracy of all references.

The Editor-in-Chief reserves the right to adjust the style to certain standards of uniformity. All articles should be directed to:

Emeritus Prof Md Ikram Mohd Said
Editor-in-Chief

School of Chemical Sciences and Food Technology
Faculty of Science and Technology, Universiti Kebangsaan Malaysia
43600 UKM Bangi, Selangor D.E.
(e-mail:kiamco65@gmail.com; kiam@ukm.my)

Manuscripts are accepted for publication on the understanding that the copyright is assigned to the Journal. The completed copyright transfer form should be submitted together with the manuscript to the Editor. We regret that manuscripts without the copyright transfer form will not be considered for publication.

TRANSFER OF COPYRIGHT AGREEMENT

The author(s) agree that upon acceptance for publication, copyright (including the right to authorise photocopying and reproduction in all media, whether separately or as a part of a journal issue or otherwise) in any manuscript submitted, including its modifications thereafter, is transferred to the *ASEAN Journal on Science and Technology for Development*.

The author(s) agree that the Editors (including its Editorial Advisory Committee and its Board Members) of the *ASEAN Journal on Science and Technology for Development* will have worldwide rights, perpetually, to the manuscript (and the final published article with all its amendments), including the right to distribute the article in whatever form deemed appropriate in the information dissemination process (including the use of internet and WWW). This transfer includes the right to adapt the manuscript/article for use in computer systems and programme, including reproduction in machine readable form and incorporation in retrieval systems.

The author(s) retain the rights to:

- i. Any intellectual property rights to any process of procedure described in the manuscript.
- ii. Photocopy or make copies of the published article for their own personal use or use by colleagues, including for classroom teaching purposes, provided the copies are not offered for sale and are not distributed in a systematic way outside their employing institution; and
- iii. Compile the article into their own collection of printed works.

The author(s) should however, include an indication that the copyright ownership of article rests with the *ASEAN Journal on Science and Technology for Development*, and provide a full citation of the Journal source.

Warranties and Copyright Transfer

The author(s) warrant that the article is the author's original work that has not been published elsewhere. The author(s) warrant that the article contains no material that infringes the rights of other or are of a libelous nature. The author(s) warrant that if excerpts from copyrighted works are included, permission of the relevant copyright owners have been obtained and due acknowledgement given in the article.

If the article is prepared jointly with other author(s), the signing author has informed the co-authors of this copyright transfer and has obtained their permission to sign on their behalf. If copyright is held by the employer, the employer or an authorised representative of the employer must sign. If this assignment is signed by the author, it is taken that the author has the authorisation of the employer and that the terms and conditions of this transfer are with the acceptance of the employer.

Signature of copyright owner(s) : _____
(Please indicate if signing on YES/NO (Delete as appropriate)
behalf of all co-authors)

Full name (Please print) : _____

Name and designation if : _____
employer representative

Company or institution : _____

Date : _____

PLEASE RETURN AN **ORIGINAL** COPY OF THIS COMPLETED FORM, together with the relevant manuscript to the Editor-in-Chief. We regret that manuscripts without the copyright transfer form will not be considered for publication.

ASEAN JOURNAL ON SCIENCE AND TECHNOLOGY FOR DEVELOPMENT
(*ASEAN J. Sc. Technol. Dev.*)

SUBSCRIPTION FORM

The annual subscription rates for four issues per volume are as follows:

ASEAN countries: USD20.00

Outside ASEAN: USD60.00

Note that the above rate does not include the air mail charge. The air mail charge will be available individually for each subscriber upon request.

Please use the following form, to be returned together with the bank draft or send separately if you pay through bank:

I wish to subscribe to the ASEAN Journal on Science and Technology for Development.	
Name of Subscriber: _____	
Name of Contact Person: _____	
Telephone No.: _____	Fax No.: _____
E-mail Address: _____	
Mailing Address: _____	
Cheque/Bank Draft No.: _____	Amount: _____
Signature: _____	
Date: _____	

All subscription correspondence should be addressed to:

Emeritus Prof Md Ikram Mohd Said
Editor-in-Chief
School of Chemical Sciences and Food Technology
Faculty of Science and Technology, Universiti Kebangsaan Malaysia
43600 UKM Bangi, Selangor D.E.
Tel: +603 8921 5445
Fax: +603 8921 5410

Or

You can send information through e-mail:

(e-mail:kiamco65@gmail.com; kiam@ukm.my)

ADVERTISEMENTS

- (a) Scientific conferences/Seminars/Training courses
- (b) Books/Publications
- (c) Scientific instruments/Company/Industrial products
- (d) Technologies for licensing/research collaboration
- (e) Vacancies and appointments
- (f) General publicity on science and technology matters of interest to the scientific community.

The terms and conditions for advertising are as follows:

- (a) All advertisements will be in black and white.
- (b) The advertisement will be interspersed within the various pages of the Journal and will be charged at a flat rate of USD1000 per B5-sized page for two (2) issues or USD1800 for four (2) issues on a running basis.
- (c) Acceptance of advertisements will be on a first-come-first-served basis.
- (d) All advertisers will receive two (2) copies of each issue of the Journal free of charge for the duration of the advertisement.
- (e) Requests for advertisements should be accompanied with the following information:
 - Name of Advertiser
 - Contact Person
 - Tel. No., Fax No. and e-mail of contact person
 - Mailing address
 - Bank draft/cheque number of relevant amount made payable to the ASEAN Journal on Science and Technology for Development.

The Advertiser shall provide the copy in print ready form, in electronic copy using a common publishing software, together with a hard copy sample of the expected final print form. Advertisements will be published on an “as-is” basis using the material submitted by the Advertiser. No proofs will be given.

The Editor reserves the right to accept or reject requests for advertisements to ensure that the scholarly intent of the Journal is upheld.

All advertising and business correspondences should be addressed to:

Emeritus Prof Md Ikram Mohd Said

Editor-in-Chief

School of Chemical Sciences and Food Technology
Faculty of Science and Technology, Universiti Kebangsaan Malaysia
43600 UKM Bangi, Selangor D.E.
Tel: +603 8921 5445
Fax: +603 8921 5410
(e-mail:kiamco65@gmail.com; kiam@ukm.my)



ASEAN JOURNAL ON SCIENCE & TECHNOLOGY FOR DEVELOPMENT

Contents

ASEAN J. Sc. Technol. Dev.
Volume 29(2), 2012

Performance of Jatropha Oil-based Biodiesel Fuel in a Single-cylinder Four-Stroke Diesel Engine	77
<i>H. H. Win</i>	
Developing a Generalized Combined Model for Gas-liquid Two-phase Flow Pressure Drop in Elbow Bends	88
<i>N. Z. Aung and T. Yuwono</i>	
Ethanol Production in Yeasts Isolated from Fermented Kitchen Waste	99
<i>S. Wong, S. K. Wong and J. S. Bujang</i>	
Chemical Composition of Leaf and Seed Oils of <i>Dryobalanops aromatica</i> Gaertn. (Dipterocarpaceae)	105
<i>A. S. Kamariah, T. Ozek, B. Demirci and K. H. C. Baser</i>	
Evaluation of Mixture Viscosity Models in the Prediction of Two-phase Flow Pressure Drops	115
<i>N. Z. Aung and T. Yuwono</i>	
Utilization of Agricultural Wastes in the Manufacture of Composite Boards	129
<i>P. M. Macatangay, E. C. Magundayao and C. A. M. Rosales</i>	